The Dissertation Committee for Charles Kevin Terry certifies that this is the approved version of the following dissertation:

HUMAN MOTOR UNIT SYNCHRONY AND ITS RELATION TO FORCE STEADINESS

Committee:

Lisa Griffin, Co-Supervisor

H. Grady Rylander, Co-Supervisor

Jonathan B. Dingwell

Andrew J. Fuglevand

Mia K. Markey

Waneen W. Spirduso

HUMAN MOTOR UNIT SYNCHRONY AND ITS RELATION TO FORCE STEADINESS

by

Charles Kevin Terry, B.S.; M.E.; M.S.

Dissertation

Presented to the Faculty of the Graduate School of

The University of Texas at Austin

in Partial Fulfillment

of the Requirements

for the Degree of

Doctor of Philosophy

The University of Texas at Austin

August 2007

Acknowledgements

I am deeply grateful to everyone who helped me get to this point, including my family, friends, and instructors. To my supervisor, Lisa Griffin, for tolerating my unmitigated honesty and directness. To my committee, for reading and reviewing a dissertation that is, at times, unavoidably dense. To my classmates, for not teasing me too much about my age. And, most importantly, to the people who nobly pretended that having needles stuck in their hands for several hours while immobilized and without being paid was no big deal.

HUMAN MOTOR UNIT SYNCHRONY AND ITS RELATION TO FORCE STEADINESS

Publication No._____

Charles Kevin Terry, Ph.D.

The University of Texas at Austin, 2007

Co-Supervisor: Lisa Griffin

Co-Supervisor: H. Grady Rylander

Motor unit synchronization is phenomenon driven by a common input that results in the near-simultaneous firing of two or more motor units, which is referred to as short-term synchronization. The relationship between motor unit synchronization and force steadiness is still unclear, even after numerous experiments and simulations. Our main hypothesis was that the decreased force tetanus brought on by motor unit synchronization would be correlated to reduced steadiness at very low hand muscle forces. To determine if this correlation existed, young, healthy adults performed a submaximal, isometric pinch at four forces to determine if motor unit synchronization increased with a progressive decrease in force steadiness driven by reduced force levels. However, before performing synchronization analyses, we had to establish the best technique for measuring motor unit coherence, which quantifies the strength and frequency of a periodic common input.

We used a pool of simulated spike trains with various firing rates, coefficients of variation (CV), common input frequencies and trial durations to explore the effects of

data segmentation and spike train properties on coherence. We found that tapered segments overlapped by at least 50% maximized coherence measurements, regardless of taper type and that increasing common input frequency CV from 0.15-0.50 made coherence measurements unusable, even at high synchronization levels.

During an isometric pinch at 2, 4, 8, and 12% of maximum digit force, we recorded thumb and index finger forces and EMG from the first dorsal interosseous (FDI) and adductor pollicis (AdP) muscles. As expected, the force CV dropped as each digit force increased. Pooled coherence revealed a dominant peak for the 2-10 Hz, but power for both digits' forces was limited to the 0-2 Hz bandwidth. There was a weak correlation for thumb force CV and coherence for within-AdP pairs, but no significant correlations were found for within-FDI pair coherence and finger force CV. Therefore, motor unit synchronization was not a strong driver of force steadiness for this protocol.

To ensure that inherent firing rate nonstationarity of spike train data did not affect coherence measurements, we produced a new set of spike train pairs with firing rates and variances that approximated those for physiological motor units, which varied from 0-25%. Stationarity level was not significantly correlated to peak coherence (max R^2 = 0.082). Therefore, coherence measurements of spike train data with characteristics similar to those of the simulated trains were not significantly affected by nonstationarity.

The establishment of the best method for computing coherence, the lack of a strong correlation between force steadiness and motor unit synchronization for submaximal isometric forces, and the knowledge that spike train nonstationarity has no significant effect on coherence measurements are all important discoveries needed for progress in the areas of basic neuromuscular function, motor unit synchronization, and pathological force unsteadiness.

Table of Contents

List of Tables

List of Figures

Chapter 1: Introduction

SPECIFIC AIMS

The origin and prevalence of muscle force unsteadiness affects many aspects of daily living for both healthy people and those with neuromuscular pathologies that make force steadiness difficult to maintain, such as Parkinson's disease (PD) and essential tremor (ET). For healthy individuals, force unsteadiness presents itself during normal tasks in several forms. The most common form of unsteadiness is non-pathological tremor, which can be either load-dependent (mechanical) or load-independent (neurogenic) and generally produce force oscillations in the 8-12 Hz bandwidth (Sutton and Sykes, 1967; Elble and Randall 1976; Vaillancourt et al., 2002, Christakos et al., 2006). Force steadiness is also dependent upon visual and proprioceptive feedback, but produces force variability that is primarily a mixture of low (<2 Hz) frequency oscillatory and steady-state variations. Determining the sources of these common types of force unsteadiness could lead to a better understanding of pathological force unsteadiness and more effective treatment of those diseases.

One common example of non-pathological force steadiness is its degradation with decreasing force once force falls below about 10% of maximum (Galganski et al. 1993, Keen et al. 1994, Laidlaw et al. 2000, Semmler et al. 2000). One possible mechanism that could account for reduced force steadiness is an increase in the prevalence of synchronized motor unit activity, which reduces force tetanus by aligning some of the motor unit twitch forces. Should this alignment occur at a sufficient rate, the resulting force fluctuations could be large enough to cause a notable increase in force unsteadiness.

Synchronized firing of two motor units is revealed by using cross-correlation to measure short-term synchronization, which is the above-chance firing of two motor units

at a given time interval (Sears and Stagg, 1976). Although there have been investigations into the relationship between force steadiness and short-term synchrony, there have been conflicting results regarding this correlation. Semmler et al. (2000) found that short-term synchronization was not correlated to decreased force steadiness in older adults compared to younger adults performing low-level (≤ 10% MVC), non-fatiguing index finger abduction. Additionally, in a study of untrained, skill-trained, and strength-trained individuals, force unsteadiness and synchrony were not significantly correlated (Semmler and Nordstrom, 1998). However, Santello and Fuglevand (2004) found that motor unit models suggested a link between short-term synchronization and force unsteadiness and a similar model with synchronization best matched experimental tremor data for index finger abduction (Taylor et al., 2003).

Another way to assess motor unit synchrony is a spectral measure of the linear dependency between pairs of motor units, known as coherence. However, instead of quantifying the above-chance occurrence of near-simultaneous spikes in the time domain, coherence measures the strength and frequency of a periodic common input to a pair of motor neurons. These common inputs are thought to originate in supraspinal CNS regions or as branched common inputs in the spinal cord (Conway et al. 1995, Farmer et al. 1993, Halliday et al. 1998).

This finding suggests that using two synchronization metrics that measure two different aspects of synchronization may produce different indications of synchrony strength. In other words, although short-term synchronization and coherence both quantify motor unit synchronization, they present results in different domains (time vs. frequency) and by using different mathematical processes (cross-correlation vs. cross-spectral analyses). Also, short-term synchronization can reveal a firing time lag, whereas coherence is useful for measuring the strength and frequency of one or more common

inputs. Therefore, concurrent examination of motor unit synchrony using both techniques is essential to a comprehensive analysis.

Although there is a singular definition for coherence, there are several computational options regarding the way spike train times are processed. After the original spike train has been subdivided into segments of equal duration, individual coherence values for each segment are then averaged to find a mean coherence for the full trial duration. Larger segment size produces better frequency resolution, but also increases the variance by allowing for fewer segments. This inverse relationship between higher resolution and smaller variance forces a balance between these two factors and produces inconsistencies based on the priorities of the investigator. Increasing the trial duration improves coherence results by increasing the number of segments, but trial duration can be limited if fatigue effects are undesirable.

To improve both resolution and reduce variance, segment overlap and tapering can be applied (Bendat and Piersol, 2000). Overlapping segments, as is done for a moving average, increases the number of segments and thereby reduces the variance. Tapering the segments reduces the spectral leakage that produces false readings caused by data near the segment boundaries. A combination of both techniques has been shown to improve the accuracy for the analysis of continuous signals (Welch, 1967), but we do not know how effectively either process or the combination of these two processes will reduce spike train coherence variability and spectral leakage.

To establish levels of motor unit synchrony, the calculation of short-term synchronization is expressed as one of several indices, each of which can produce significantly different between-trial and across-subject results. There are also a number of techniques and parameter choices that can be used to compute coherence. For example, several studies have used different window tapering and sampling rates to simplify

computation and reduce signal leakage (Semmler et al., 2003; Myers et al., 2004). Preliminary studies have shown that, for the same data, these different techniques can yield markedly different results. Therefore, before we can make definitive statements about the existence of synchrony assessed in both temporal and spectral domains, we must establish a consistent, reliable technique for performing these measurements.

Experiments are conducted by different investigators for different purposes using different techniques, and because synchronization levels are not known a priori, the most effective way to examine and validate these analytical techniques is through the use of a computational model, which can produce many motor unit firing patterns with controlled features and more predictable output. A computational technique that maximizes coherence and a better understanding of how spike train properties affect this measurement will greatly improve our confidence in future motor unit synchronization study designs and their findings.

To address the suspected correlation between force steadiness and motor unit synchrony and the techniques used to assess synchrony, this study pursued the following specific aims:

1. Develop a computational model to establish the best technique for computing coherence by using simulated motor unit firing events (spike trains) with varying firing frequency, common input frequency, noise (variability), and common input strength to find the method that produces the highest significant coherence value for a pool of synchronized motor unit pairs.

   Hypothesis: Simulated spike trains with known synchronization characteristics can be analyzed using a variety of computational parameters for detection of coherence, thereby revealing an optimum technique for performing these measurements.

2. Establish that a significant correlation exists between synchronization of adductor pollicis (AdP) and first dorsal interosseous (FDI) motor units and force steadiness during a steady submaximal pinch.

   Hypothesis: A negative correlation between coherence or synchronization indices and force steadiness at the corresponding digit (AdP-thumb or FDI-index finger) will show that increased synchronization, measured in both time and frequency domains, may reduce force steadiness by degrading twitch force tetanus.

3. Validate and refine the computational model using actual motor unit data including mean firing rate, firing rate variability, and synchronization levels.

   Hypothesis: Experimental motor unit firing characteristics will allow for refinement of computational parameters such as variability (noise), mean firing rates, and synchronization levels.

Although it is unlikely that motor unit synchrony is the only factor that contributes to force steadiness, it may very well be one of the most significant. This study provided vital information that will elucidate the way in which the CNS works to minimize force unsteadiness. Understanding how motor unit synchronization is related to force steadiness will provide fundamental knowledge about the normal functioning of the human CNS and how it produces and maintains steady muscle force. It will also reveal more about how the corticospinal and other pathways responsible for motor control function to perform simple tasks. Knowing how muscles maintain their force will provide critical insight into therapeutic techniques for neuromuscular pathologies that produce abnormal levels of force tremor, such as essential tremor, Parkinson's disease and Amyotrophic Lateral Sclerosis (ALS). For instance, several studies have found significant cortical and thalamic oscillatory activity in the 3-6 Hz range related to tremor

(Volkmann et al., 1996; Vaillancourt and Newell, 2000). Knowledge of the source of this behavior could lead to better pharmacological or surgical treatments for these disorders.

TECHNIQUES

Figure 1-1 shows the anatomy and location of the first dorsal interosseous (FDI) and adductor pollicis (AdP) muscles in the hand. Although pinching involves the activation of nearly 20 different muscles, these two intrinsic muscles are two of the most active during pinch (Maier and Hepp-Raymond, 1995a). Additionally, intrinsic muscles have been shown to be more highly synchronized (Maier and Hepp-Raymond, 1995b) and are better adapted for maintaining precision forces (Milner and Dhaliwal, 2002) than the extrinsic muscles, such as the flexor digitorum profundus (FDP) or flexor pollicis longus (FPL) of the fingers and thumb, respectively. Although the intrinsic muscles are both innervated by the ulnar nerve, separate branches extend to each muscle, allowing for independent excitation, but increasing the likelihood of synchronization.

Spike Identification

Individual motor unit potentials for each electrode were identified off-line with the Spike2 waveform discrimination system which allowed for time coding of each motor unit action potential (MUAP), or "spike". For each EMG channel, one to three spikes were selected. Using a template of the each spike, the software performed the initial tracking of this motor unit throughout the experiment using a "template matching" algorithm, where a template was built from a small set of spikes belonging to the same motor unit and then matched to all spikes that appear in the EMG data. Those spikes matching the template within the bounds set by the user were classified as belonging to that spike train. After automated processing, spikes were manually scanned to ensure that spikes were not misclassified due to noise or superposition. For superpositioned spikes, the spike was classified as one of each spike, if the spikes in the superpositioned

waveform can be clearly identified. If individual spikes could not be clearly discriminated they were not included in that spike train. This manual spike screening eliminated a significant portion of the misclassified spikes coded automatically by the software.

As an example, Figure 1-2 shows the traces for four electrodes (two AdP and two FDI) from the hand of a subject performing a pinch. For one of the AdP channels, spikes from two different motor units have been identified. The superpositioned spike would be classified as belonging to each spike train for classification. Note that the three other EMG channels all have spikes that are both clearly identifiable and ambiguous in origin. Only those spikes that can be confidently attributed to a single motor unit were used for further analysis.

Once all identifiable spikes were classified, each spike was converted to an event (time) marker by recording the first crossing of a unique (to that spike) threshold and each set of event markers was saved as a separate file for that motor unit so that synchronization and coherence calculations could be performed. An example of this conversion is shown in Figure 1-3.

Short-term Synchronization Analysis

Synchronous motor unit activity was measured using cross-correlation analysis of motor unit firing times during the constant force contraction (Sears and Stagg, 1976). The cross-correlation histogram was constructed using MATLAB code that used a time-window of ±100 milliseconds and a bin width of 1.0 millisecond (Figure 1-4). The 200 millisecond span of this window ensured the inclusion of correlation of all motor units that fire at a minimum of 5 Hz, which is below the minimum firing rate of the slowest-firing human motor units (Marsden et al., 1971; Macefield et al., 1993). Using a one-

millisecond bin width provides a smooth histogram and sufficient resolution for action potentials, which are typically ~1 millisecond in duration.

Once the histogram was complete, the cumulative sum (CUSUM) of counts below or above the mean was calculated and tracked from the minimum to the maximum offset time. The CUSUM technique is used to identify peaks in the cross-correlation histogram typical of synchronized spike trains by identifying large deflections in the CUSUM plot (Ellaway, 1978; Wiegner A.W. and Wierzbicka, 1987; Nordstrom et al., 1992). Deflections were determined either visually or by tracking the variance (V of the CUSUM and defining a peak region boundary as a location where the CUSUM exceeds 3 $\sqrt{V}$ (Bremner et al., 1991a,b). Once the peak regions were established, the synchronization index can be calculated. There are a number of synchronization indices, but the one found to be least sensitive to firing rate is the common input strength (CIS) (Nordstrom et al., 1992). The CIS is the ratio of the area of the histogram peak region above the mean (A) and the trial duration in seconds (d), as shown in equation (1).

$$CIS=A/d \quad (1)$$

Therefore, CIS gives frequency of synchronous action potentials in excess of those expected by chance.

Coherence Analysis

Calculating the coherence of two stochastic point processes, such as two spike trains (denoted as x and y), involves a series of summations to find the Fourier transform of each spike train and the cross- and auto-spectra of these transforms (Rosenberg et al., 1989). To perform the summations, the spike train was subdivided into L number of equal-sized, non-overlapping segments of length T for the entire train duration (L x T). The value of T in seconds establishes the frequency resolution of the coherence plot as $1/T$. Each spike train was transformed using the equation:

$$d_x^T(f) = \int_0^T e^{-ift} dN(t) = \sum_{0<\tau_j \le T} \exp(-if\tau_j), \quad (2)$$

where x is the spike train designator, τ_j is the spike time in seconds and f is the frequency in Hz. To find the cross- and auto-spectra of these two spike trains, the function Φ_{xy} is calculated for each frequency using:

$$\Phi_{xy}(f) = \frac{1}{2\pi LT} \sum_{l=1}^{L} d_x^T(f,l)\overline{d_y^T(f,l)}, \quad (3)$$

where l represents the l^{th} epoch for which the auto- or cross-spectra is being calculated as the summation of products of the transform (d^T) and its conjugate. Equation (3) is set up to calculate the cross-spectra. To find the auto-spectra equation of the x train, each y subscript would be replaced by x and vice versa for the y train auto-spectra. Once the auto- and cross-spectra are calculated at each frequency, the spectral coherence can be calculated using:

$$|R_{xy}(f)|^2 = \frac{|\Phi_{xy}(f)|^2}{\Phi_{xx}(f)\Phi_{yy}(f)}, \quad (4)$$

where $R_{xy}(f)$ represents the coherence for spike trains x and y at frequency f.

The coherence analyses made use of MATLAB code, which utilized a 1 kHz sampling rate and non-overlapping segments of 1.024 seconds (T), allowing for a 0.96 Hz resolution as a baseline coherence measurement technique. A confidence level was established using the equation, $Z = 1-(\alpha)^{1/(L-1)}$, where α is the desired type 1 error level (Brillinger, 1978). Coherence values exceeding the 95% confidence value ($\alpha = 0.05$) were regarded as significant as outlined in the literature (Rosenberg et al., 1989).

Computational Evaluation of Cross-Correlation and Coherence Measurements

No published studies have compared the effect of parameter selection, noise, or computational techniques on short-term synchronization indices or coherence values or their variability. One study has examined the correlation of motor unit firing rate and

force (Moritz et al., 2005), but not the validity of the analysis techniques. Also, as mentioned previously, two studies that examined synchrony and its relation to steadiness also found conflicting results. Short-term synchronization was not found to be correlated (Semmler et al., 2000) to force steadiness, while motor unit coherence measurements were (Semmler et al., 2003), indicating a possible inconsistency in the correlation of short-term synchrony and coherence or an inconsistency in the way in which these measurements were calculated.

Calculation of each quantity depends on both parameter selection and computational technique. Parameter choices for short-term synchronization include histogram bin width, criteria for finding deflection points used to measure peak widths, and synchronization indices. Coherence measurement parameters include coherence frequency resolution/segment size, window overlap and tapering, and sampling rate. Other signal conditioning techniques, such as the application of overlapping and/or Hanning or other tapering windows, have been used to reduce signal leakage and variance (Myers et al., 2004, Halliday et al. 1998).

In addition to parameter selection and signal conditioning, the effects of trial duration were also not well established. There must be some threshold trial duration that produces coherence and short-term synchronization results with an acceptable level of variation. We developed a detailed analytical model to test the effects of each of these variables so that the minimum sample size, most appropriate parameters and most accurate techniques can be used in this study.

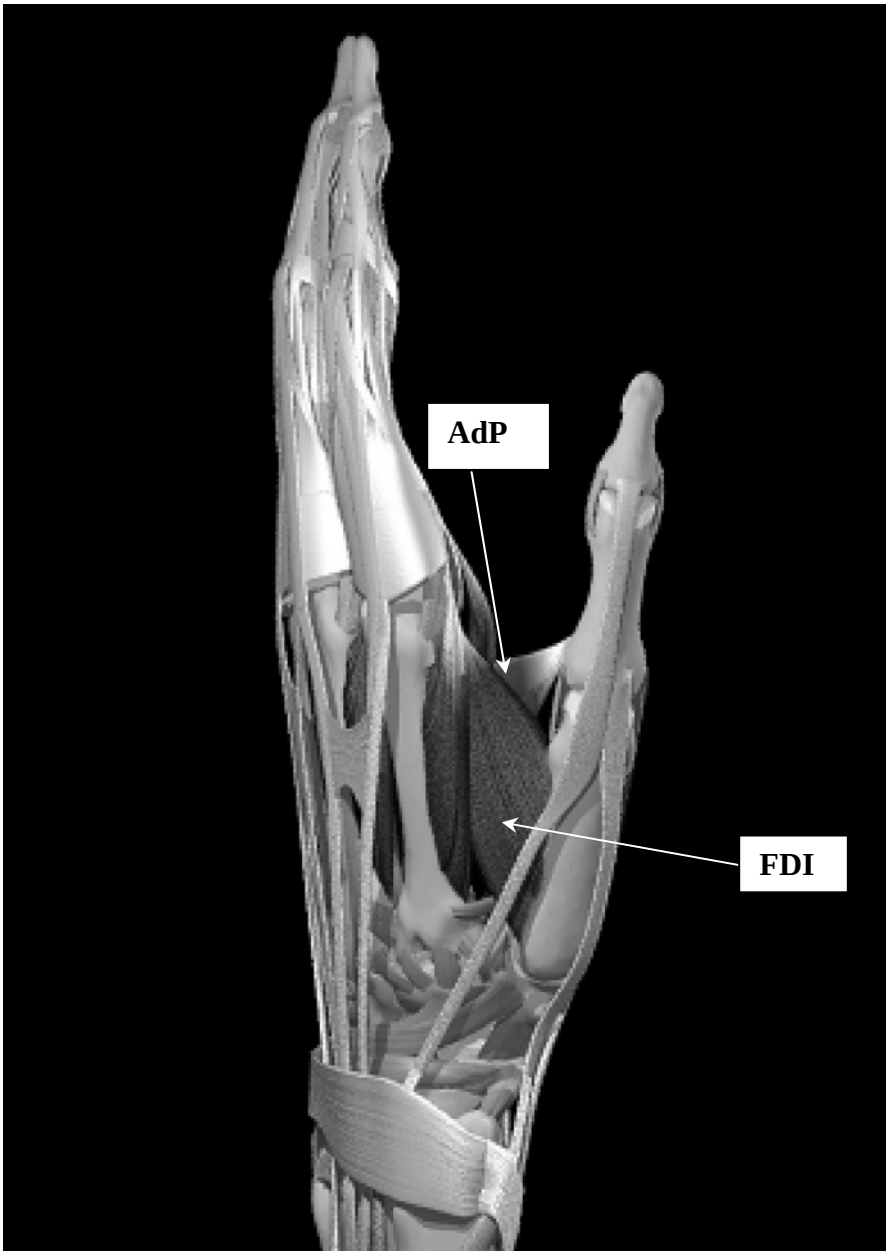

Figure 1-1. Locations of the FDI and AdP muscles in the human hand.

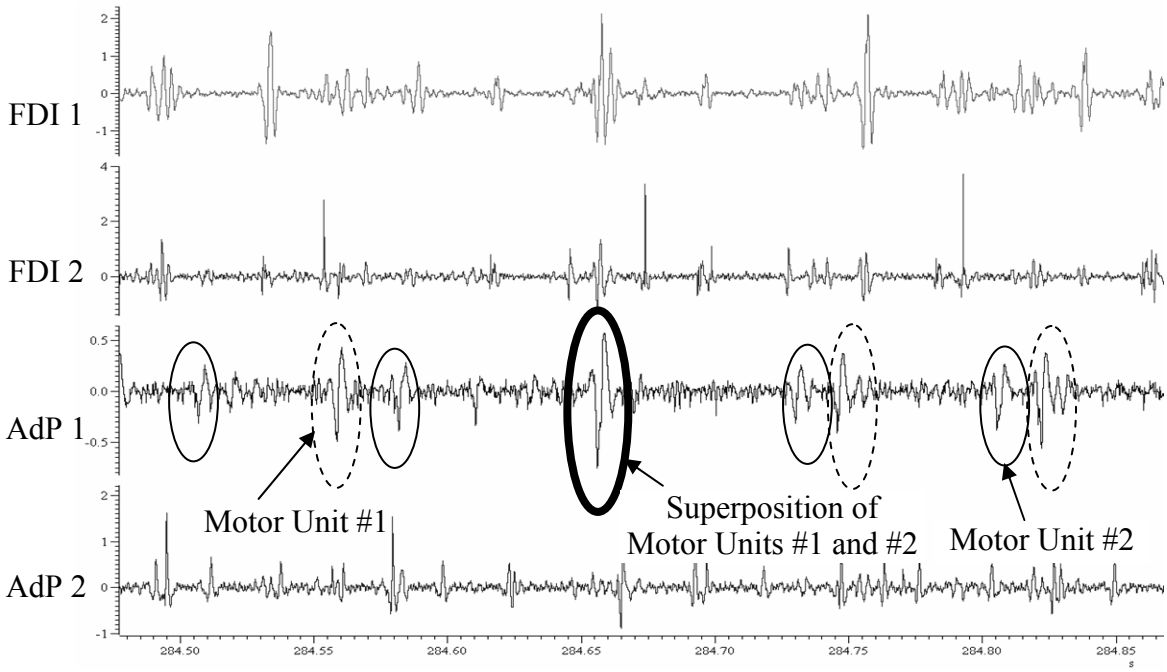

Figure 1-2. Hand muscle motor unit potentials recorded simultaneously from four locations in the AdP (two lower traces) and in the FDI (two upper traces) during a pinch. Two different motor units have been identified for the second AdP location as an example of motor unit discrimination needed for this study.

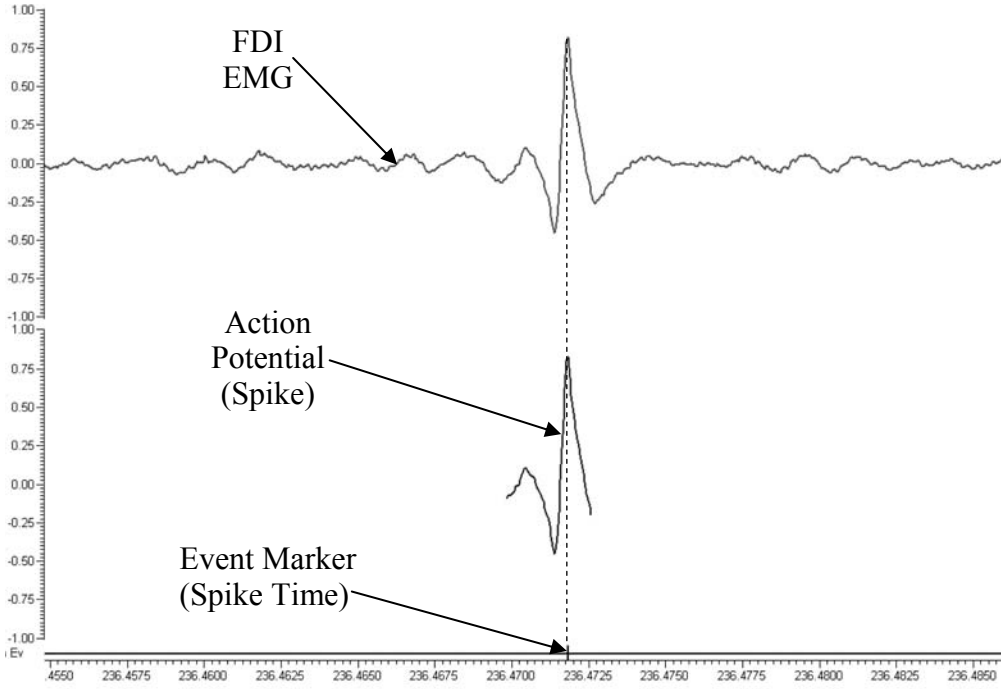

Figure 1-3. Typical spike identification process. From top to bottom, traces showing raw intramuscular AdP EMG, a spike identified from template matching, and the event marker corresponding to the spike's first maximum peak.

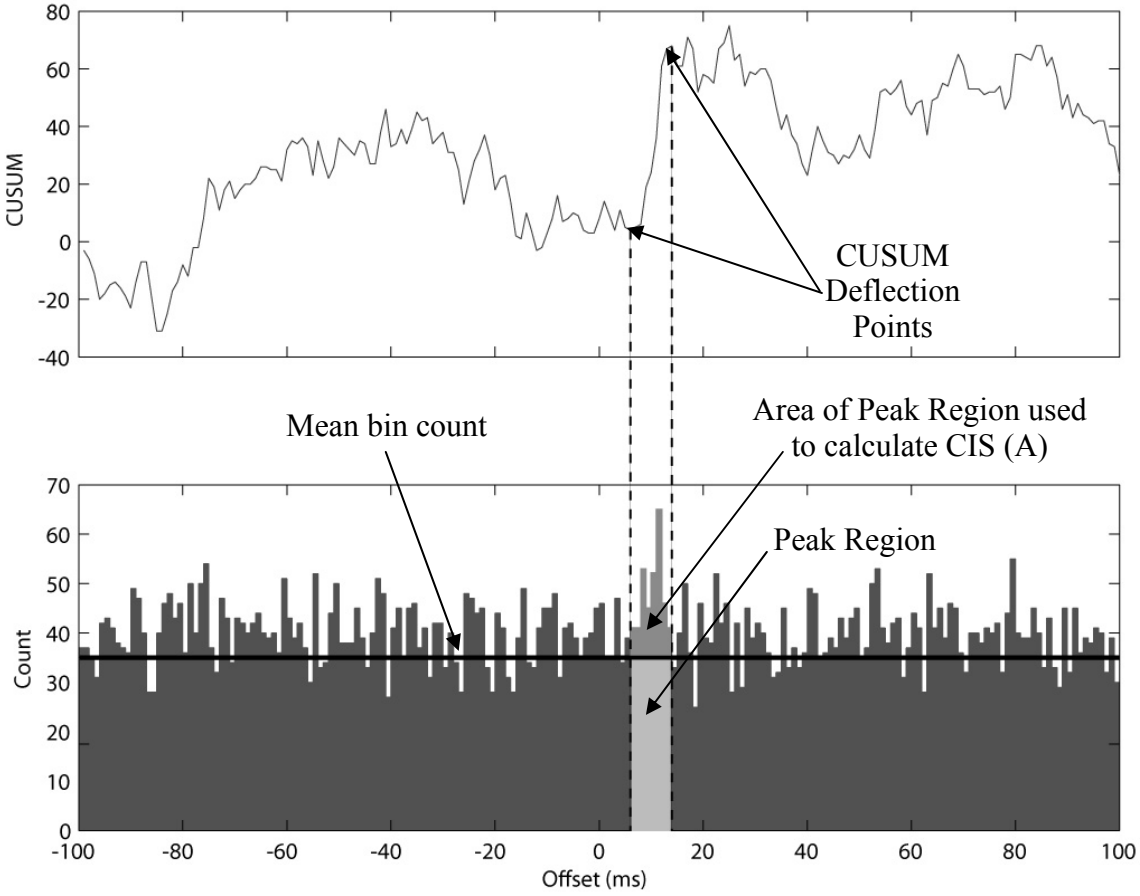

Figure 1-4. Sample cross-correlation histogram with CUSUM plot showing deflection points and definition of peak region.

Chapter 2: How computational technique and spike train properties affect coherence

ABSTRACT

Spike train coherence is an important metric used to characterize common inputs that drive motor unit synchrony. However, data segmentation, overlap, and taper can significantly affect coherence magnitude, thereby influencing the sensitivity of its detection. Also, increasing spike train variability can significantly reduce coherence for a fixed synchrony level.

To address these issues, we used a pool of simulated synchronized spike trains with various firing rates (7-19 Hz), coefficients of variation (CV) (0.05-0.50), common input frequencies (10, 20, and 30 Hz, CV: 0.05-0.50) and trial durations (30, 60, 90 and 120 sec.) and synchronization strength to explore the effects of segment length (1024 and 2048 1-ms samples), tapering (Hann, Nuttall, and rectangular), and overlap (0, 37.5, 50, 62.5, and 75%) on coherence detection. The model incorporated a leaky integrator that modeled a branched common input as a periodic pulse train acting on two independent motor neurons.

Tapered segments overlapped by at least 50% maximized coherence, regardless of taper type. Even at the highest synchronization level, coherence measurements for 30-second trials failed to reveal significant coherence for even half of the motor unit pairs, even though a common input was present for all of them, demonstrating the need for the longest practical trial duration when measuring coherence. Also, 2048-sample segments produced similar coherence values with twice the frequency resolution. Finally, for a given synchrony level, increasing variabilities of firing rate and common input from 0.15-

0.50 significantly reduced coherence detection by approximately 5% and 60%, respectively.

INTRODUCTION

Synchronized firing of motor units has been an area of increasing interest since it was first discovered. Studies have examined the relationship between motor unit synchrony and force steadiness (Semmler et al., 1995; Amjad et al., 1997; Santello and Fuglevand, 2004), task performance (Semmler et al., 1998; Maier et al., 1995a, b), and strength training (Semmler et al., 2004). Understanding these and other relationships regarding synchrony and neuromuscular performance could produce significant insights into human motor control regarding neuromuscular mechanisms, adaptation, and pathologies. However, to produce meaningful synchrony analyses, a consistent and reliable synchrony metric must be established.

In the time domain, motor unit synchrony usually refers to short-term synchronization, quantified as one of several synchronization indices based on the cross-correlation of motor unit spike trains: CIS, SI, S (Bremner et al., 1991a,b; Datta and Stephens, 1990; Ellaway and Murthy, 1985; Hamm et al., 1985, Harrison et al., 1991; Logigian et al., 1988; Nordstrom et al., 1992; Wiegner and Wierzbicka, 1987). However, the number of different indices impedes effective synchrony study comparison. The indices are also sensitive to variability (Nordstrom et al., 1992) and lack a consistent predetermined scale that indicates relative or absolute strength of synchrony. As an alternative, motor unit synchrony can be assessed by using a frequency-domain metric known as coherence.

Coherence is derived from the auto- and cross-spectral density of the two trains and provides a different perspective of the synchronization process by examining the periodic patterns in the appearance of synchronized spikes as opposed to direct

comparison of the spike times. Whereas short-term synchronization indices express the incidence of above-chance temporal synchrony, coherence reveals the strength and frequency of common inputs that drive the synchronous discharges. It is a bounded measure, ranging from 0 (incoherent) to 1 (fully coherent) and can be easily applied in across-study comparisons. Also, unlike short-term synchronization, there is no need to establish a peak region using subjective criteria. However, comparison of motor unit coherence across studies may be invalid if there are significant differences in coherence caused only by differences in the way it was calculated.

Although there is a singular definition for coherence, there are several computational options regarding the way spike train times are processed. After the original spike train has been subdivided into segments of equal duration, individual coherence values for each segment are then averaged to find a mean coherence for the full trial duration. Larger segment size produces better frequency resolution, but also increases the variance by allowing for fewer segments. This inverse relationship between higher resolution and smaller variance forces a balance between these two factors and produces inconsistencies based on the priorities of the investigator. Increasing the trial duration improves coherence results by increasing the number of segments, but trial duration can be limited if fatigue effects are undesirable.

To improve both resolution and reduce variance, segment overlap and tapering can be applied (Bendat and Piersol, 2000). Overlapping segments, as is done for a moving average, increases the number of segments and thereby reduces the variance. Tapering data near the segment boundaries reduces the spectral leakage that produces false positive readings at the wrong frequency. A combination of both techniques has been shown to improve the accuracy for the analysis of continuous signals (Welch,

1967), but we do not know how effectively either process or the combination of these two processes will reduce spike train coherence variability and spectral leakage.

With no accepted standard for data segmentation, there are notable differences in how they were applied across motor unit synchronization studies. For example, Rosenberg et al. (1989) used 1.024-second segments with no overlap or taper, Semmler et al. (2004) used 1.24-second segments with no overlap or taper, Farmer et al. (1993) used 1.024-second non-overlapped segments that were tapered with a Hann window, and Myers et al. (2004) used 2.048-second segments with 62.5% overlap and a Hann taper. Each of these studies used coherence to assess motor unit spike train synchrony, but their findings may have been partly dependent on which segment parameters were chosen.

In addition to issues related to coherence calculation, there are concerns about how coherence accuracy is affected by intrinsic motor unit properties. One prominent characteristic is synaptic noise, as indicated by firing rate variance (Nordstrom et al., 1992; Enoka et al., 1989), which may significantly reduce coherence as noise increases. This variance is likely a characteristic of the common input as well, which adds another dimension to motor unit synchrony's complexity. Because of the way coherence is calculated, coherence can be attenuated when a motor unit firing rate and common input frequency are similar, because the signal power for the individual motor unit firing rate will negate the cross-spectral power for that frequency.

To assess the effects of segment size, taper, and overlap and the impact of spike train and branched common input frequency and variability, we used different combinations of segment parameters to measure spike train coherence for motor unit pairs with various firing rates, common input frequencies, and their associated variances for various trial durations. To create a broad database, we used a computational model to produce a large pool of spike train pairs with controlled features and synchronization

levels. By comparing the coherence levels for methods that use different segmenting parameters on spike trains with various properties, we were able to find the segment parameters that maximized coherence and understand how spike train properties influenced its magnitude.

METHODS

Equipment

All computer code for spike simulation, coherence calculations, and statistical analyses were written in Matlab® version 7.1 with the Signal Processing and Statistics toolboxes. Computations were performed on a PC with a Pentium® D 3.0 GHz processor and Windows® XP OS.

Spike Train Generation

We created a pool of 108,000 spike trains with firing rates and variabilities that approximated those of physiological motor units during submaximal contractions of hand muscles. For hand muscles exerting constant, submaximal force, motor unit firing rates were found to vary from 6-23 pulses per second (pps) (Kukulka and Clanann, 1981; Fruend et al., 1975; Moritz et al., 2005). Firing rate variabilities have been measured, as coefficients of variation (CV), from as low as 0.13 (Masakado et al., 2000) up to 0.49 (Enoka et al., 1989). For the simulations, the range of firing rates was 7-19 pps and CVs varied from 0.05 to 0.50 for both the motor unit firing rate and the common input frequency (Table 2-1). The pool of firing rates was subdivided into reference and response pools, with each reference rate being paired with each response rate, for a total of 36 firing rate combinations. Firing rates of 10 and 20 pps were excluded to minimize resonance effects expected for 10 and 20 Hz common input frequencies.

To simulate the nature of motor unit firing, a “leaky integrator” model (Halliday, 1998) was used to create the spike trains. This model uses an integrate-to-threshold firing

mechanism that sums input voltages until a threshold voltage is reached. Membrane voltage *(v)* increases at each time step as a function of the current membrane voltage and the input voltage *(x)*. The voltage input for each time step *(Δt)* represents the graded potential contributed by one or more upper motor neurons and was found using equation (1), where μ is the mean voltage input at each time step.

$$x_t = \mu + \sigma * n_{rand}(t) \tag{1}$$

The input voltage variance *(σ)* is applied by adding the product of the variance and n_{rand}, which is selected from an array of normally distributed random numbers (zero mean, unity variance). Membrane voltage at each successive time step *(v_{t+1})* was then found using equation (2).

$$v_{t+1} = \frac{\tau}{\Delta t + \tau} v_t + \frac{\Delta t}{\Delta t + \tau} x_{t+1} \tag{2}$$

The time constant *(τ)* controls the rate at which the membrane voltage dissipates during each time step *(Δt)*, creating an exponential charging curve, like that of a capacitor. The first term on the right-hand side of equation (2) represents the membrane voltage *(v_t)* retained during the current time step, while the second term is the contribution from the voltage input. For this study, a τ of 0.0125 produced stable results for a time step of 0.5 ms, which provided sufficient temporal resolution for spike times that would eventually be assigned to 1 ms intervals (1 kHz sampling rate).

With known voltage inputs at all time steps established by equation (1) and the initial membrane voltage *(v_0)* assigned at a random value such that $0 \leq v_0 \leq v_{th}$, the threshold voltage (1.0), membrane voltage was found by sequentially solving for v_{t+1} at

each successive time step. Each time v_{t+1} exceeded v_{th}, a spike firing time was recorded and v_{t+1} was reset to v_{t+1} - $v_{th.}$ The process continued until t was equal to the desired trial duration *(d)*, creating a set of spike times, or spike train. We wrote a goal-seeking optimization code to find appropriate μ and σ values for the desired firing rates and coefficients of variation. Using the tolerances from Table 2-1, the optimization incrementally adjusted the values of μ and σ until the desired firing rate and CV were obtained.

To induce synchrony, we used a voltage input common to both motor units that represented the activity of a branched common input of a last-order synapse at the spinal cord level. For a pair of motor neurons, the branched common input is the combined influence of all neurons that synapse onto both motor neurons. Although synchrony is likely driven by one or more neurons that synapse onto two or more motor neurons (Sears and Stagg, 1976), we modeled the simplest case, whereby a single branched common input influences the firing of a single motor unit pair. The common input is represented as y_{t+1} in equation (1), where it is modeled as a rectangular pulse train with a given pulse width and amplitude *(A_p)*.

$$v_{t+1} = \frac{\tau}{\Delta t + \tau} v_t + \frac{\Delta t}{\Delta t + \tau}(x_{t+1} + y_{t+1}) \tag{3}$$

$$y_{t+1} = A_p k_p \tag{4}$$

If the pulse was active during the *t+1* time step, k_p = 1 and a voltage of A_p was added to the independent input *(y_{t+1} = A_p)*. Otherwise, k_p = 0 and the membrane voltage would increase as though no common input existed. If the two motor units happen to be close to threshold when the input pulse was active, the additional input caused both

membrane voltages to cross the threshold at or near the same time, producing a synchronous firing time for both motor units.

Synchrony level increased with larger pulse amplitude or width, but fixing one of these parameters simplified the model by reducing the degrees of freedom. In keeping with the original modeling work (Halliday, 1998), the pulse width was fixed at 2 ms to simplify the process and approximate the duration of an action potential. The pulses were distributed with a given frequency (10, 20, and 30 Hz) and variance (CV = 0.05 – 0.50). Once again, we used a goal-seeking algorithm that varied pulse amplitude to attain a desired level of synchrony for each motor unit pair.

Establishing an independent index of synchrony strength for a study that assesses the accuracy of another measure of synchrony presented a methodological paradox. In addition to the basic requirement for accurate representation of the synchrony strength, the measure had to be a temporal synchrony index and it had to be kept simple to allow for computational efficiency, meaning that it needed to be independent of subjective criteria such as establishing cumulative sum deflection points, which would consume significant computational time. To address these issues, we took advantage of the knowledge inherent with simulated spike trains. First, the synchrony lag time typically seen in physiological motor unit pairs was nonexistent, which places the cross-correlation peak at zero lag time. Secondly, we knew that there was a single source of synchrony, so multiple peaks would not be an issue. Finally, by controlling how synchrony was established, peak widths would only be a few milliseconds wide.

To create and computational synchronization index, we used a cross-correlogram identical to those used for experimental synchrony indices (Bremner et al., 1991a; Datta and Stephens, 1990; Ellaway and Murthy, 1985; Logigian et al., 1988; Nordstrom et al., 1992; Wiegner and Wierzbicka, 1987), with lag times from -100 ms to 100 ms and 1-ms

bins, with lag times centered at each bin (Figure 2-1). An event is counted each time a response spike from one train is within ±100 ms of a reference spike in the other train. The event count for the bin corresponding to that lag time is then incremented by one for each of those occurrences. If synchrony existed, a peak would develop at the center of the cross-correlogram, allowing for the computation of a synchrony index based on the bin population within the peak region.

Instead of expending computational resources on finding peak regions by variance methods or visually identifying peak regions for thousands of motor unit pairs using CUSUM deflections (Ellaway 1978, Wiegner A.W. and Wierzbicka 1987, Nordstrom et al. 1992), the peak region was fixed at -4.5 ms ≤ lag time ≤ +4.5 ms (the 9 central bins). The computational synchrony index *(SI_{comp})*, was then used to express synchrony as the ratio of the mean bin population within ($binpop_{pk}$) and outside ($binpop_{npk}$) the peak region, as shown in equation (5).

$$SI_{comp} = \frac{mean(binpop_{pk})}{mean(binpop_{npk})}. \quad (5)$$

An SI_{comp} = 1.0 corresponds to an unsynchronized motor unit pair while an SI_{comp} of 1.5 indicates an average peak bin population that is 150% of the average bin population outside the peak region, indicating a large degree of synchronization.

Coherence Calculation

Calculating the coherence between two stochastic point processes such as two spike trains (denoted as *x* and *y*), requires the Fourier transform of each spike train and the cross- and auto-spectra of these transforms (Rosenberg et al., 1989). To perform the transform summations, the spike train was subdivided into *L* segments of length *T* for the entire train duration *($d = L \cdot T$)*. Once the auto- and cross-spectra were calculated at each frequency, the spectral coherence was calculated using equation (6).

$$| R_{xy}(f) |^2 = \frac{| \Phi_{xy}(f) |^2}{\Phi_{xx}(f)\Phi_{yy}(f)} \quad (6)$$

$|R_{xy}(f)|^2$ represents the magnitude-squared coherence for spike trains *x* and *y* at frequency *(f)* , which is the ratio of the squared magnitude of the cross-spectral density (Φ_{xy}) and the product of the auto-spectra of each spike train *(($\Phi_{xx}(f)$ and $\Phi_{yy}(f)$)*. After digitizing each spike train at a sampling rate of 1 kHz, each sampling interval was coded. If a spike event occurred within the bounds of a 1-ms interval, the value for that interval was set to "1", otherwise, it was set to "0". Each train was then detrended to remove low-frequency responses caused by slow drifts in mean firing rates. Coherence for each pair was then found using the Matlab *mscohere* function, which uses the described technique and allows for convenient manipulation of segment size, taper, and overlap.

Random synchronization will cause coherence to be non-zero and results in some level of noise. To establish when coherence is significant, an upper confidence bound is found using an equation based on the chi-square distribution of coherence that assumes data stationarity (Brillinger, 1978). After selecting a type 1 error (α), the significance level (*Z)* is found using equation (7)

$$Z = 1 - \alpha^{\frac{1}{L-1}} \quad (7)$$

Our focus was on 1) finding the technique that maximized significant coherence detection and 2) determining the effect of motor unit spike train parameters on the incidence of this detection. The incidence rate was found by dividing the number of times the coherence rose above the significance level divided by the number of times coherence was calculated within the detection bandwidth for a group of motor unit pairs. For all techniques examined, the detection bandwidth comprises the frequency interval containing the common input frequency and the closest adjacent interval. Ideally, this coherence incidence should be 100% for all motor unit pairs in this study, which were all

partially driven by a common input. Therefore, the incidence rate indicates how reliable a metric coherence will be for a given set of motor unit and segmentation parameters.

After the coherence was computed for each motor unit pair, the coherence incidence values were calculated so that they could be compared when grouped by parameter (firing rate, variance, etc.). The volume of computations precluded the computation of multiple copies of motor unit pairs with the same fixed set of properties. Instead, each data group consisted of each motor unit firing rate combination at each common input frequency across a range of property values, as described and as shown in each figure. If a significant correlation was found between the dependent variable under study (usually coherence incidence) and either firing rate or common input frequency, then those groups were subdivided to remove that correlation and the results were presented. Unless otherwise noted, these groups comprised a set of 36 x 3 values for the 36 reference/response firing rate combinations and three common input frequencies.

Segment Taper and Overlap

We examined two tapering windows, Hann and Nuttall, along with a non-tapered (rectangular) window. The Hann window is commonly used (Bendat and Piersol, 2000) because of its balance between narrow main lobe width (for resolution) and sidelobe suppression (for reduced spectral leakage). Compared to the Hann window, the Nuttall window has significantly better sidelobe suppression, which should make it more effective at reducing spectral leakage at the expense of poorer resolution caused by its wider main lobe (Nuttall, 1981). The equations for each window are:

Hann window

$$W(k+1) = 0.5\left(1 - \cos\left(\frac{2\pi k}{nfft - 1}\right)\right) \tag{8}$$

for segment number k = 0,…, nfft-1, where nfft is the number of segment elements (T/Δt)

Nuttall window

$$W(k+1) = a_0 - a_1 \cos\left(\frac{2\pi k}{nfft-1}\right) + a_2 \cos\left(\frac{4\pi k}{nfft-1}\right) - a_3\left(\frac{6\pi k}{nfft-1}\right) \qquad (9)$$

for k = 0,…, nfft-1, where a_0 = 0.3635819, a_1 = 0.4891775, a_2 = 0.1365995, and a_3 = 0.0106411. As these two windows are applied to spike train data in each segment, the magnitude of each spike is scaled down, or tapered, as the spike is located close to the segment boundary, until spike train magnitudes at the boundaries are scaled to zero. The shapes of the rectangular, Hann, and Nuttall windows are shown in Figure 2-2.

Equation (7) is viable for non-overlapping segments, even after tapering in the time domain. However, some accommodation must be made to account for overlapped segments. This modification (Welch, 1967) is:

$$Z_{ovlp} = 1 - \alpha^{\frac{1}{wL^*-1}} \qquad (10)$$

where L^* is the number of overlapped segments, found using equation (11).

$$L^* = floor((L-1)/(1-ovlp)) + 1 \qquad (11)$$

The variable *ovlp* is the percentage of segment overlap and *w* is a weighting factor that is dependent on the amount of overlap and taper type. For tapered segments with window *W* and *nfft* segment elements, *w* is found using equation (12).

$$w = \left\{ \frac{\left[\sum_{k=0}^{nfft-1} W(k) * W(k + (1 - ovlp) * nfft) \right]}{\left[\sum_{k=0}^{nfft-1} W^2(k) \right]} \right\}^2 \quad (12)$$

For this study, *nfft* was set at 1024 and 2048, which produced frequency resolutions of 0.98 and 0.49 Hz, respectively, when using a 1 kHz sampling rate. The comparison of coherence detection for these two segment lengths allowed us to examine the effect of temporal versus frequency resolution for different trial lengths and computational parameters.

Although tapering can improve accuracy and reduce spectral leakage, it can also eliminate synchronized spikes near segment boundaries and increase variability by reducing signal continuity. However, both of these issues can be ameliorated by overlapping tapered segments. For this study, we examined segment overlap of 0, 37.5, 50, 62.5, and 75%. A summary of all coherence segmentation parameters is shown in Table 2-2.

Statistics

Coherence is a bounded quantity ([0,1]) that follows a chi-squared distribution (Bendat and Piersol, 2000). Therefore, nonparametric tests were used to compare means between two or more groups. The coherence is expressed in terms of the incidence rate at which coherence exceeds the significance level at the common input frequency and is referred to as the incidence of coherence detection, which is the percentage of cases which show significant coherence within the detection bandwidth. Every simulated pair was synchronized to some degree, so the incidence of detection would ideally be 100%. How far this value falls below 100% indicates the reliability of coherence measurements for the presented segmentation and motor unit parameters.

For comparison of significant coherence incidence between two groups, a Wilcoxon rank-sum test was used to identify significant differences. In the case of comparisons involving more than two groups, Friedman's ANOVA based on ranks was used, along with a Tukey-Kramer post-hoc test to determine which group interactions were significant. Differences were deemed significant only if tests produced a p-value that fell below the type 1 error level (α) of 0.05. Unless otherwise stated, errors and error bars are equivalent to the 95% confidence interval (CI).

RESULTS

To provide an equitable comparison of data segmentation parameters, we fixed the sampling rate at 1 kHz and the frequency resolution at 0.97 Hz (1.024-second segment length) and varied only segment taper (rectangular or Hann) and overlap (0 or 50%). The application of tapered or overlapped segments provided gains in coherence incidence that were found to be significant in the Friedman test, but failed rank-sum significance tests (Figure 2-3). The combination of 50% overlap and a Hann taper yielded highly significant increases in coherence incidence ($p<0.001$). The difference in mean coherence incidence between this technique and the baseline technique increased from 5.9% for 30-second trials ($p=0.0009$) to 9.3% for a trial lengths of 90 and 120 seconds ($p=0.0003$ and $p=0.0004$, respectively). Although the combination of Hann taper and 50% segment overlap produced consistently significant advantages over the three other combinations, we also explored the possibility that other taper/overlap combinations might yield even higher coherence incidence.

To address this issue, we compared coherence incidence for a markedly different taper window (Nuttall) and overlap amounts (0, 37.5, 62.5, and 75%). For overlap amounts of 50% or less, coherence incidence for the Hann taper were higher than for the Nuttall taper, but these differences were not significant (Figure 2-4). The increase in

coherence incidence was negligible for overlap amounts of 62.5 and 75% (Hann: 1.1%, Nuttall: 0.9%) and neither was significant. For the Hann window, the coherence incidence grew by 2.3% when overlap was increased from 50% to 75%, but this improvement was also not significant. However, this same increase in overlap produced a significant improvement of 6.2% for the Nuttall taper ($p=0.018$). Of the combinations that produced coherence incidence values not significantly different from the highest rate, the Hann taper/50% overlap combination produced the highest coherence incidence with the least overlap. Therefore, we continued to use it for the remainder of the analyses.

A comparison of coherence detection when using segment lengths of 1024- and 2048-sample segments showed that the mean coherence incidence values were slightly, but consistently, lower for the 2048-sample segments for all trial durations (Figure 2-5). However, none of these differences were significant. To take advantage of the improved frequency resolution, we used the 2048-sample segment for the remaining comparisons.

Having established the segment parameters that produced the highest coherence incidence values, we next explored the interactions between motor unit firing rate and common input frequency to ensure that they did not skew coherence detection in a way that produced misleading trends. In spite of this precaution, there was still a noticeable interaction between these two properties (Figure 2-6). Each successively longer trial produced significantly higher coherence incidence values for all three input frequencies, with only one exception (10 Hz, 120-s trial). More importantly, the coherence incidence for all trial durations was significantly lower for common input frequencies of 10 Hz than that of the 30 Hz case ($p=0.0007$ for 120-second trial). There were also significant differences between the coherence incidence values for the 20 and 30 Hz cases for the 90- and 120-second trial ($p=0.0428$ and $p=0.0328$, respectively).

Unlike the relationship between motor unit firing rate and common input frequency, the correlation between coherence incidence and both trial length and synchrony level were predictable and proportional (Figure 2-7). These trends were confirmed with a few exceptions. Low synchrony (SI_{comp} = 1.05) detection failed to change noticeably for trial durations of 60, 90, and 120 seconds, which is why values for that synchrony level were not included in any of this study's previous comparisons. Even for synchrony levels as high as that corresponding to SI_{comp}=1.2, 120-second trials failed to yield average coherence detection above 50%, making a false negative detection at and below this synchrony level highly likely. In general, the 30-second trials were too short to detect synchrony, failing to rise above 50% even for the highest synchrony level studied. The correlation between synchrony level and coherence incidence was nearly linear for all trial durations (R^2=0.975 for 120-s trials), but this correlation became stronger as trial duration increased, as indicated by steeper regression slopes.

Coherence detection for pairs with increasing motor unit firing rate variabilities (CV_{fr}) were adversely affected by this variance (Figure 2-8), especially when the CV_{fr} increased from 0.05 to 0.15. However, once CV_{fr} increased beyond this level, the correlation diminished. More significantly, the effect of variance of the common input frequency (CV_{com}) was far more pronounced in the range of 0.15 to 0.35, where a CV_{com} in excess of 0.25 causes coherence incidence values to drop below 50%, even for 120-second trials. This correlation also diminished as CV_{com} increased beyond 0.4, but detection incidence was below 30% at that point for all trial lengths.

Increasing common input and firing rate variance reduces incidence regardless of synchronization strength (Figure 2-9). When both variances are 0.05, the incidence quickly rises above 85% as soon as synchronization strength rises above noise level (SI_{comp}=1.05) and is near or equal to 100% for SI_{comp} values of 1.2 or higher. The

detection of coherence rapidly degrades with an increase in variance as seen in Figure 2-7. Doubling the detection bandwidth from 2 to 4 bins (0.98 to 1.96 Hz) improves incidence somewhat. However, incidence is still less than 50% for a CV of 0.35. The possibility that coherence is significant outside of the 4-bin detection band is dispelled by the low incidence for this region, which is only slightly higher than that expected for a 5% significance level (Figure 2-10). For physiological CV values (0.15-0.35), these incidence values are all between 5 and 6%.

DISCUSSION

The trends and relationships of the coherence calculation parameters and motor unit properties tested in this study have yielded some important conclusions: (1) calculating coherence using data segments tapered by a Hann window and overlapped by 50% maximizes coherence detection (2) 2048-sample segment lengths produce twice the frequency resolution of 1024-sample segments, while producing coherence incidence values that are not significantly different, (3) experimental protocols for motor unit synchrony studies should be as long as practical and no shorter than 30 seconds, (4) coherence detection for motor unit pairs with at least one firing rate near or below 10 pps may be lower than those for other pairs with the same amount of synchrony but higher firing rates, (5) the increase in firing rate variances over the range seen in physiological experiments does not significantly reduce coherence incidence, however, increases in common input variance across this same range produces a pronounced reduction in coherence incidence.

The impetus behind this study was to determine if spike train coherence was affected by data segmentation, synchronization level, trial duration, and spike train parameters. Motor unit coherence studies might be altered by differences in data segmentation parameters. To explore this possibility, we reviewed the methods used for

previous motor unit coherence studies (Table 2-3). Of the 32 studies reviewed, 19 used no segment taper or overlap, 4 used only a taper, and 3 used a taper and overlap. None of the studies used overlapped segments exclusively and 6 studies did not identify any coherence calculation parameters. The broad range of sampling rates, segment sizes, tapering windows, and segment overlap demonstrates the need to assess how these choices affect coherence detection. Several findings in this study show that these choices will have significant impact on study results, which could mean the difference between a positive and negative finding of coherence. This effect may be particularly important for experiments with short trial durations or small subject pools, which are common in this field of study.

Subdividing spike train data into segments allows for computation of a mean coherence for the entire spike train (Welch, 1967). Note that in equation (7), in addition to reducing variance, a larger number of segments, L, reduces the significance level. Ideally, trials should be as long as practical to maximize the number of segments without inducing fatigue effects, unless those are desired. In addition to overlapping segments, they can also be tapered to reduce the spectral leakage caused by non-periodicities inherent with data segmentation. Spectral leakage is detrimental to coherence studies in that it can result in displacement of signal power to adjacent frequencies, causing the coherence to be more broadly distributed in a way that may result in failed detection or detection at the wrong frequency. Using one of a number of windows, data near the center of each segment is essentially unchanged, while data near the segment bounds is attenuated.

For the comparison of the four taper/overlap combinations, we found that the combination of segment taper and overlap produced significantly higher coherence incidence values as compared to the other three taper/overlap combinations. Most likely,

the reduced leakage through tapering is countered by the attenuation of data that represents synchronized motor unit spikes. Similarly, overlapping may reduce the variance, but creates more leakage by introducing the additional discontinuities created by a larger number of segments. The drawbacks of each technique appear to be reduced by using them together. Overlapping tapered segments helps prevent portions of data from being marginalized by tapering and also removes the effect of discontinuities at the segment bounds caused by the larger number of segment boundaries generated by overlapping. The Hann window produced coherence incidence values that were consistently higher than those for the Nuttall window, but the differences were not significant, which indicates that window choice is not critical, considering these windows are near opposite ends of the spectrum in window design. Also, increasing the overlap beyond 50% did not produce higher coherence incidence values for either window type, which shows that there is no need to use a segment overlap of more than 50%.

Regardless of segment overlap and taper, longer trials increased coherence detection. Low synchrony (SI_{comp} = 1.05) produced coherence incidence values that were essentially insensitive to trial duration. Most likely, the synchrony is so small that the SI_{comp} index fails to consistently detect synchrony due to the variability of the index and the error level of 5%, which makes random and stimulated synchrony indistinguishable. Even for motor unit pairs with double that synchrony (SI_{comp} = 1.10), the coherence incidence is still below 20% for 120-second trials, indicating that coherence studies will most likely fail to detect this level of synchrony. The synchrony level had to exceed an SI_{comp} of 1.2 in order to get coherence incidence above 50% for a 120-second trial, which indicates that, regardless of how coherence is calculated, it may be less sensitive than cross-correlation techniques for detecting synchrony and may be unreliable in detecting lower synchrony levels. In general, increasing a trial duration by 30 seconds always

produced significantly higher coherence incidence values, but because those rates never exceeded 50% for the highest synchrony level, motor unit synchrony studies should be designed to record continuous spike trains that are as long as practical. If longer trials are not possible, an experiment incorporating the use of aggregate results, such as pooled coherence (Amjad et al., 1997), should be considered.

Another spike train property that affects coherence detection is the common input frequency. The lower coherence incidence for motor unit pairs synchronized at a 10 Hz frequency is most likely caused by the predominance of simulated motor units with firing rates at or near 10 pps. This effect may be worthy of further study for motor units that commonly fire at a rate of <10 pps at low forces (Moritz et al., 2005; Nordstrom et al., 1992; Enoka et al., 1989; Kukulkan and Clanaan, 1981; Fruend et al., 1975). This feature is important for understanding trends seen in physiological synchronization studies because lower coherence incidence rates may be driven, at least in part, by the close proximity of the motor unit firing rate(s) to the common input frequency(ies). Delineating the difference between interference from the common input frequency and the lack of a common input would be difficult, but one option would be to examine the coherence of multiple pairs from the same subject and muscle. If a correlation existed between the lack of coherence for motor unit pairs that had at least one motor unit firing at a rate near the peak coherence frequency for other pairs from the same location, it might be possible to attribute low coherence incidence to interference between the firing rate and common input frequency. This effect is also important to consider for studies that attempt to compare coherences at frequencies that are near or below 10 Hz.

Common input frequency and the motor unit firing rates have some variability, which greatly reduced coherence incidence as variances increased. For the firing rate variability, this effect was minimal for variances seen in physiological studies, which

generally vary from 0.15 to 0.50. However, the effect of common input frequency variability is larger than that of the motor unit firing rate, particularly for values higher than 0.15. The combined effect of these variances on coherence incidence with regard to synchronization strength (Figures 2-8 and 2-9) show that coherence measurements are extremely effective for motor units and common inputs with small variances, with incidences near or at 100% even for low synchronization levels. Unfortunately, this effectiveness rapidly diminishes with increasing variances to the point that incidence at the highest synchronization level is still below 50% for a CV of 0.35, which is still well within the physiological realm of synaptic noise. Assuming that the variabilities for the common input are equivalent to those for the firing rate, this property may create problems for studies that include highly variable common inputs, which cannot be measured directly, or for long-term studies, where the firing rate variance has increased as time progressed (Nordstrom et al., 1992; Enoka et al., 1989). The effect of this spike train parameter will be difficult to isolate, however, we may be able to reduce our uncertainty by dividing long trials into shorter epochs and tracking mean coherence detection and its variability in both magnitude and frequency for the entire trial, which is essentially an extension of the data segmentation techniques examined here.

In addition to revealing the effect of data segmentation and motor unit properties on coherence measurements, this study also exposed some potential weaknesses of the coherence metric itself. Results of this pool of simulated motor unit pairs produced many cases for which temporal synchronization was clearly evident but coherence calculations failed to detect a common input more than half the time. And, if the common input was particularly noisy, there was a pronounced likelihood that highly synchronized motor unit pairs would be classified as non-synchronous if only coherence was measured. These discoveries serve to emphasize the need to use the most reliable coherence calculations,

complement them with temporal synchrony measurements, and fully understand the characteristics of the motor units under study. These findings should be carefully considered when planning and analyzing future motor unit synchronization studies so that we can produce reliable results and enable fair study comparisons that are critical to the advancement of this area of neurophysiology.

Table 2-1. Summary of motor unit firing properties and synchrony parameters used for simulated spike trains

Parameter	**Range**	**Increment**	**Tolerance**
Firing Rate (pps)	Reference: 7, 11, 12, 15, 16, 19 Response: 8, 9, 13, 14, 17, 18	1.0	0.05
Firing Rate Variance (CV)	0.05 – 0.50	0.05	0.005
Common Input Frequency (Hz)	10 – 30	10	-
Cmn. Input Freq. Variance (CV)	0.05 – 0.50	0.05	0.005
Trial Length (seconds)	30 – 120	30	-
Synchrony (SI_{comp})	1.00 – 1.50	0.05	0.01

Table 2-2. Data segmentation parameters for comparison of coherence calculation techniques

Parameter	**Value/Type**
Segment Size (samples)	1024, 2048
Frequency Resolution (Hz)	0.98, 0.49
Detection Bandwidth (Hz)	1.96, 0.98
Taper	None (rect.), Hann, Nuttall
Overlap	0, 37.5, 50, 62.5, 75%

Table 2-3. Coherence parameters for previous motor unit synchrony studies

Segmentation	# of Studies	Samp. Rate (Hz)	Seg. Size (samples)	Freq. Res. (Hz)	Taper	Overlap
No Overlap	9	200	256	0.78	-	-
No Taper	5	1000	1024	0.97	-	-
	2	500	various	various	-	-
	1	200	1024	0.195	-	-
	1	300	512	0.59	-	-
	1	400	512	0.78	-	-
Taper w/o	1	500	4000	0.125	Hann	-
Overlap	1	500	various	various	Triangular	-
	1	1000	1024	0.97	Hann	-
	1	2000	4096	0.49	Hann	-
Taper w/	1	1000	2048	0.49	Hann	62.5%
Overlap	1	1000	not spec.	not spec.	not spec.	not spec.
	1	not spec.	not spec.	not spec.	not spec.	not spec.
Not Specified	6	-	-	-	-	-

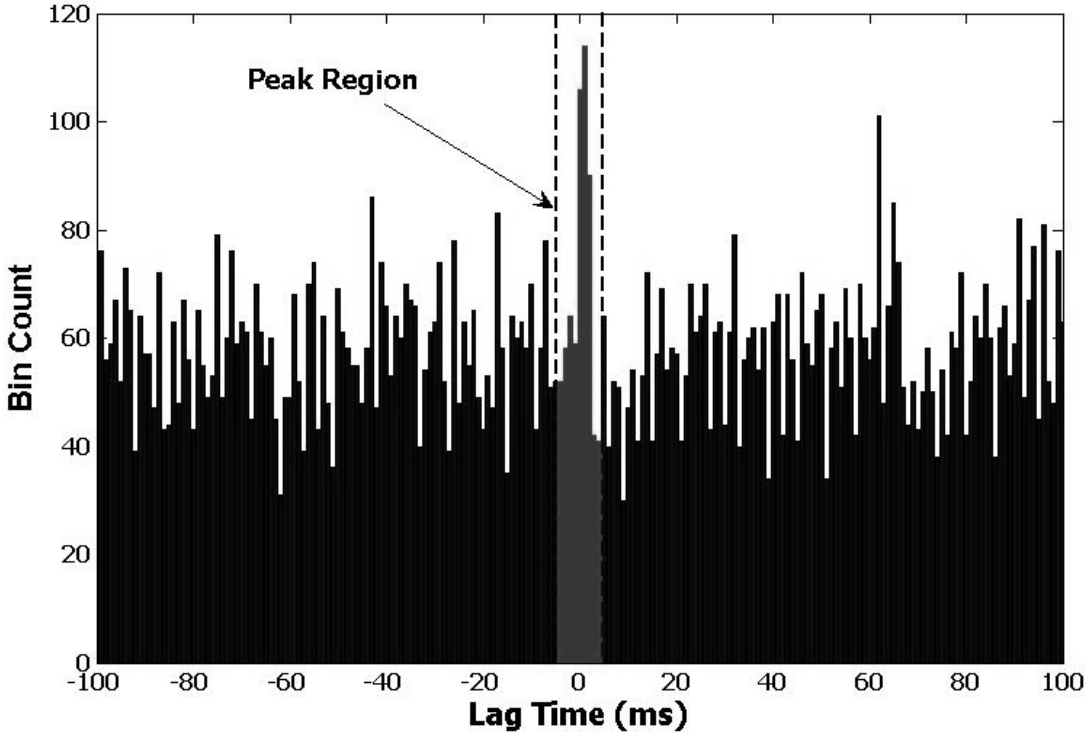

Figure 2-1. Typical cross-correlogram used for computation of the synchronization index, SI_{comp}. This particular result was for a motor unit pair from a 120-second trial with an SI_{comp} of 1.20.

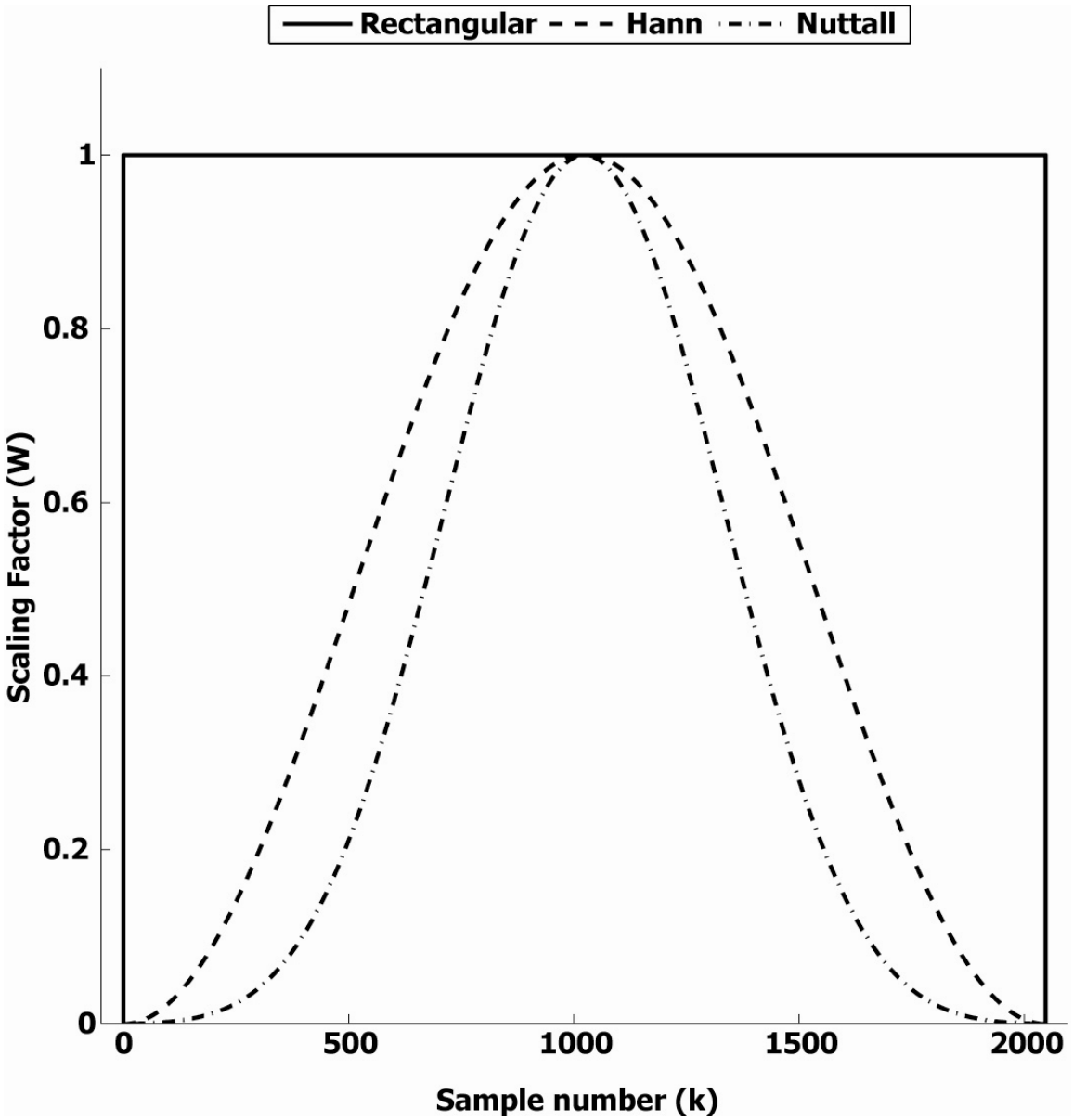

Figure 2-2. Representative curves for each of the taper windows used in this study. While the rectangular data passes all data for processing, the Hann and Nuttall windows attenuate data located near the segment bounds while passing most of the data at the segment's center.

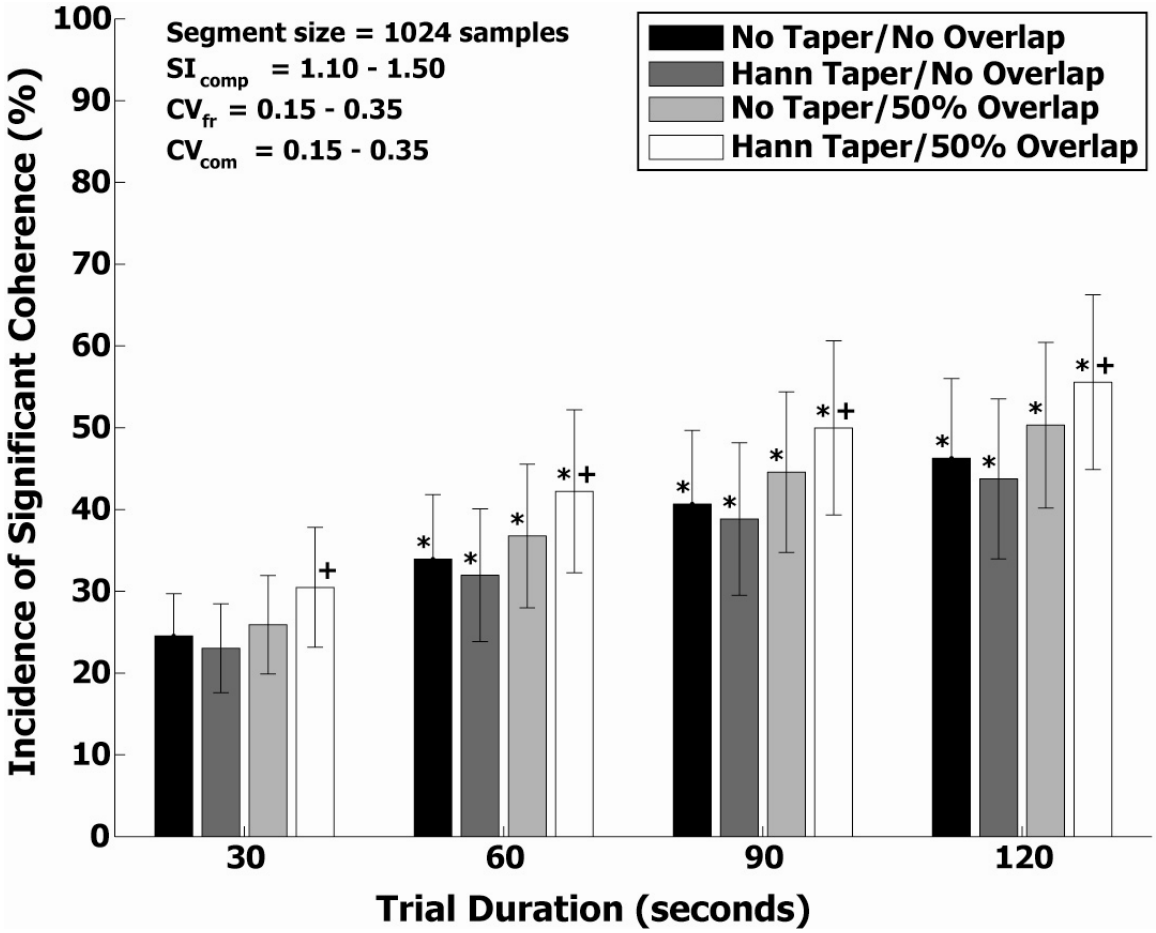

Figure 2-3. Coherence incidence for calculation methods using the four segment taper and overlap combinations for the same pool of simulated spike train pairs. Using a combination of segment taper and overlap produces significantly higher coherence incidence than the baseline method (no taper/no overlap). An asterisk (*) indicates a significant difference between coherence incidence at that trial duration and the next shorter duration, whereas a plus (+) indicates a significant difference between that method and the no taper/no overlap method at that trial duration.

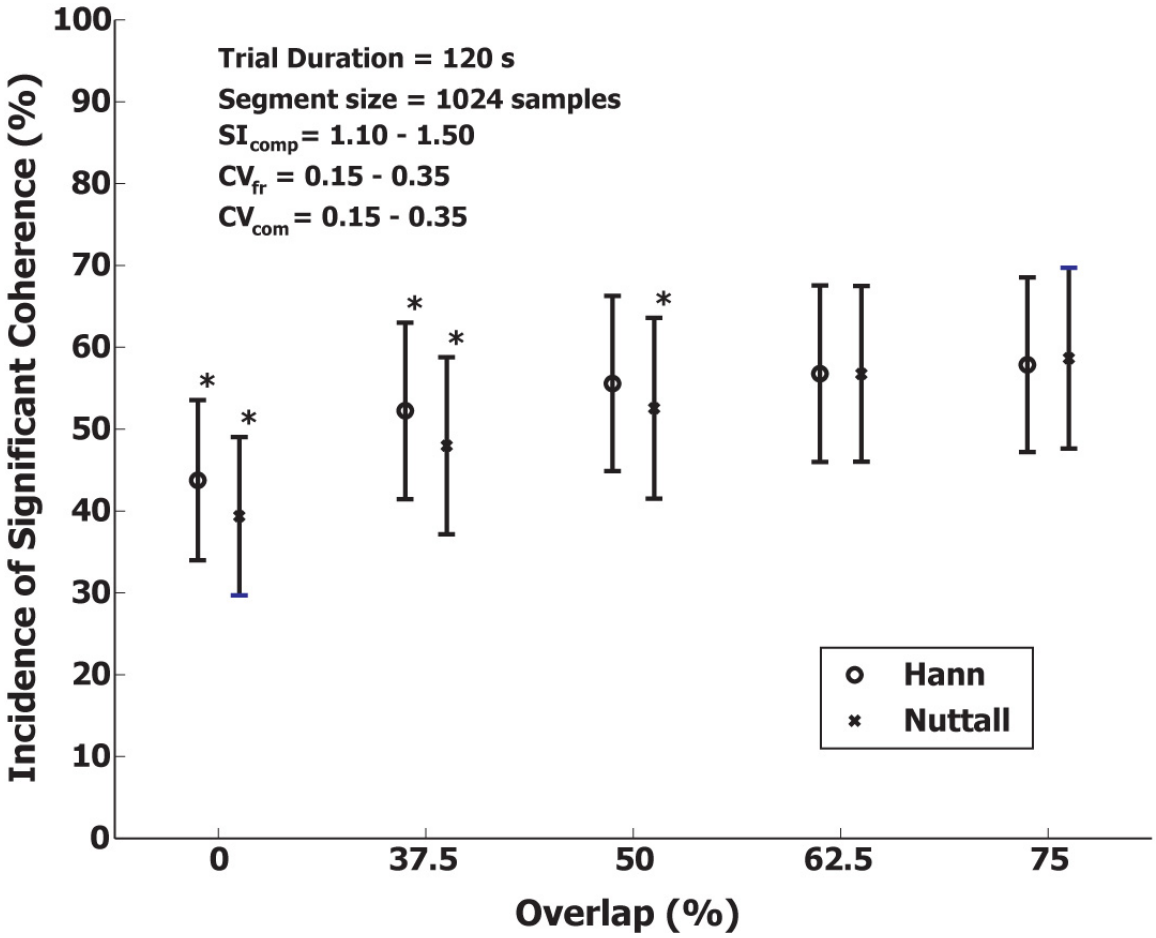

Figure 2-4. Coherence incidence for Hann and Nuttall windows at different segment overlap. As compared to the Hann window, the Nuttall window yielded slightly lower mean coherence incidence for overlaps of 50% or less, but this difference was never significant. An asterisk (*) denotes a significant difference between the mean coherence incidence for that overlap and 75%, for the given window type.

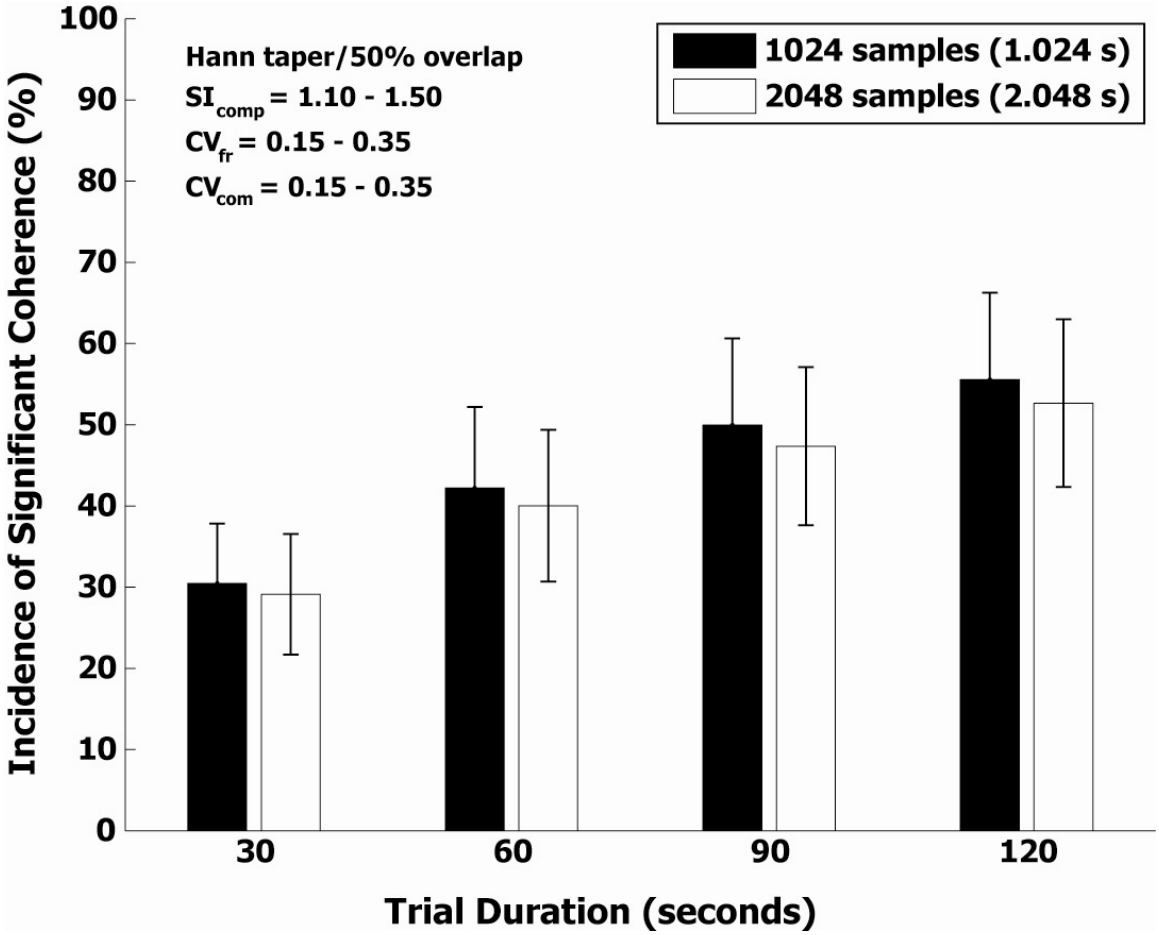

Figure 2-5. Comparison of coherence incidence for segments with 1024 and 2048 samples. Doubling the segment length produced small reductions in mean coherence incidence that were not significant for any trial duration. This finding allows for the use of longer segments without concern for reducing detection incidence rates.

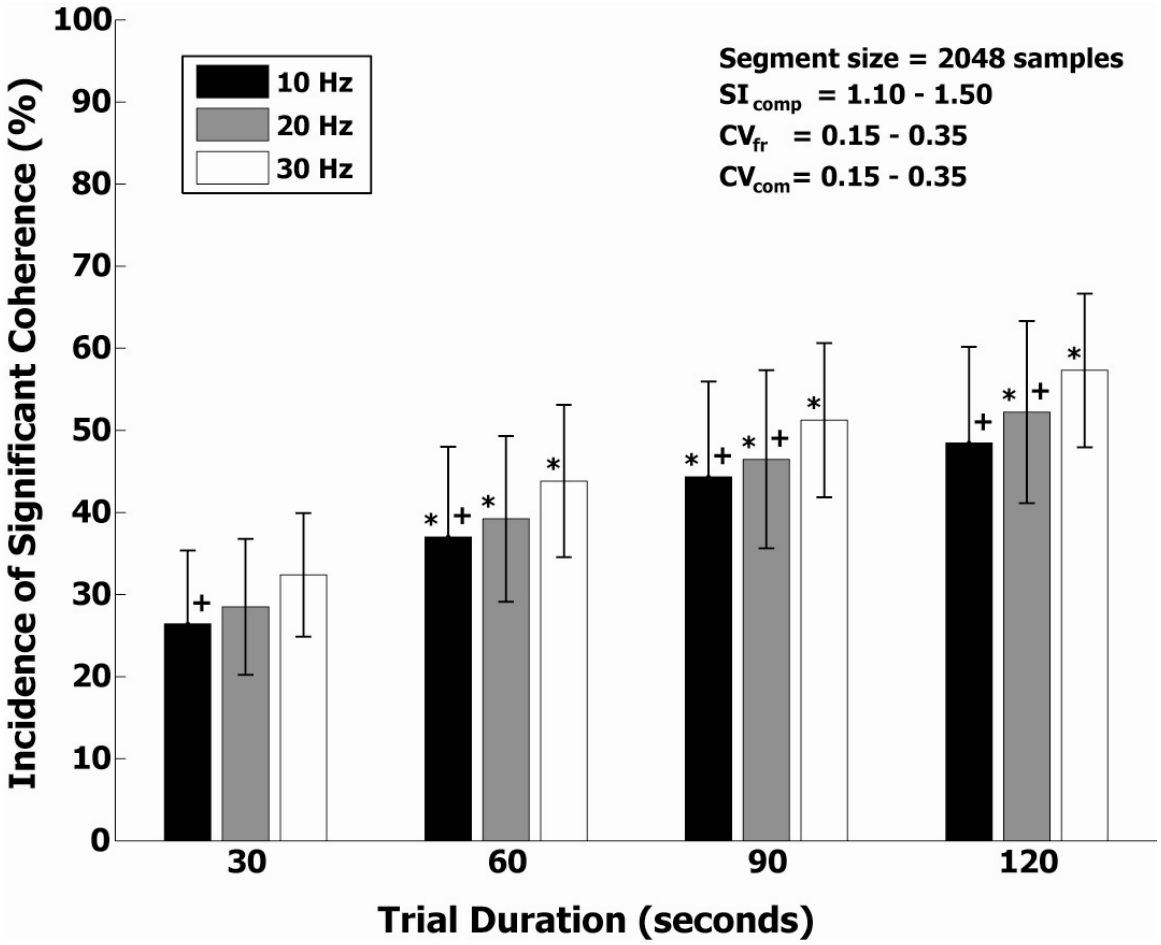

Figure 2-6. Comparison of coherence detection for different common input frequencies. When coherence incidence values are categorized by common input frequency, they were significantly lower when the common input frequency is 10 or 20 Hz, as compared to those for 30 Hz, as indicated by the plus (+) sign. As in previous figures, an asterisk (*) indicates a significant difference between coherence incidence values at that trial duration and the next shorter duration, for a given common input frequency.

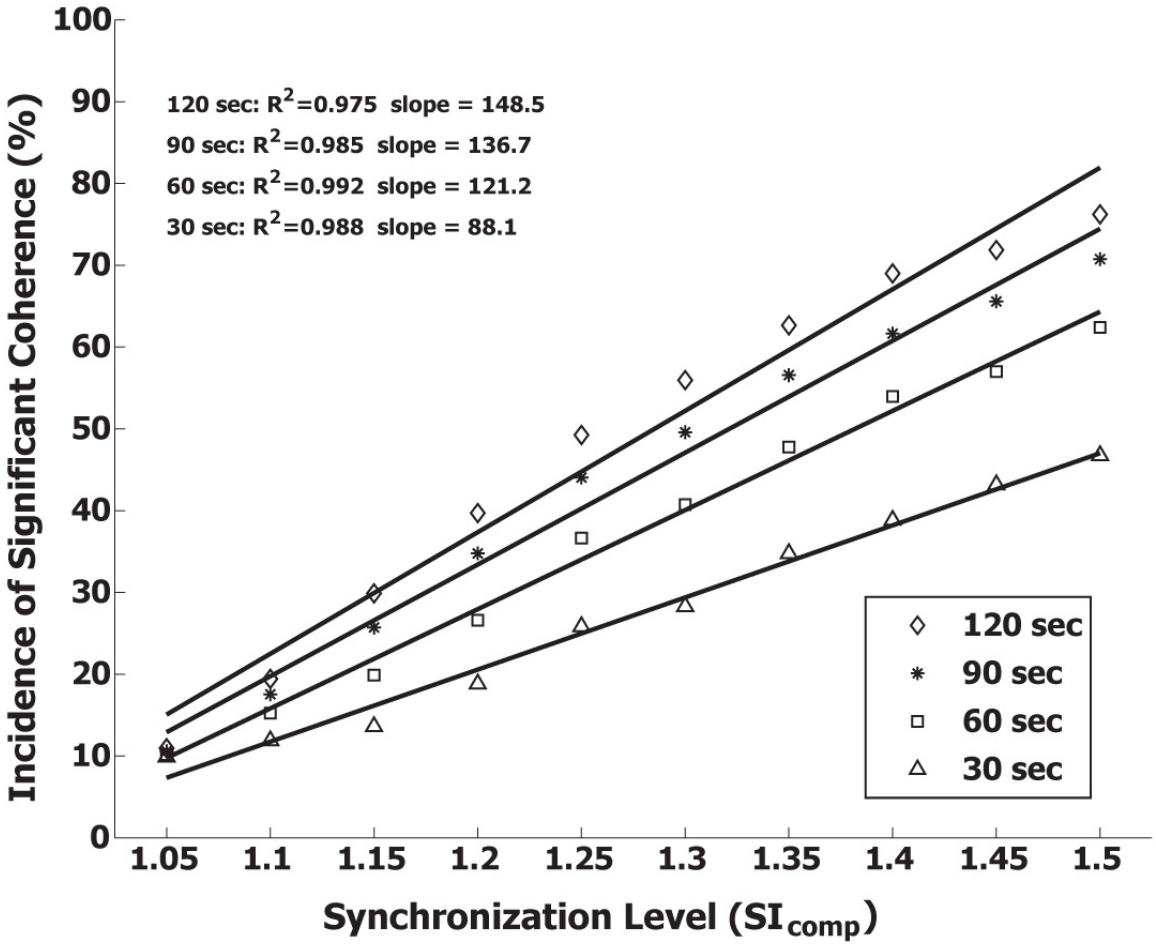

Figure 2-7. Linear regression of coherence incidence versus synchronization level (SI_{comp}). Coherence incidence is strongly correlated to the synchronization level of the simulated motor unit pair, as indicated by SI_{comp}. Higher regression slopes indicate this correlation strengthens as trial duration increases.

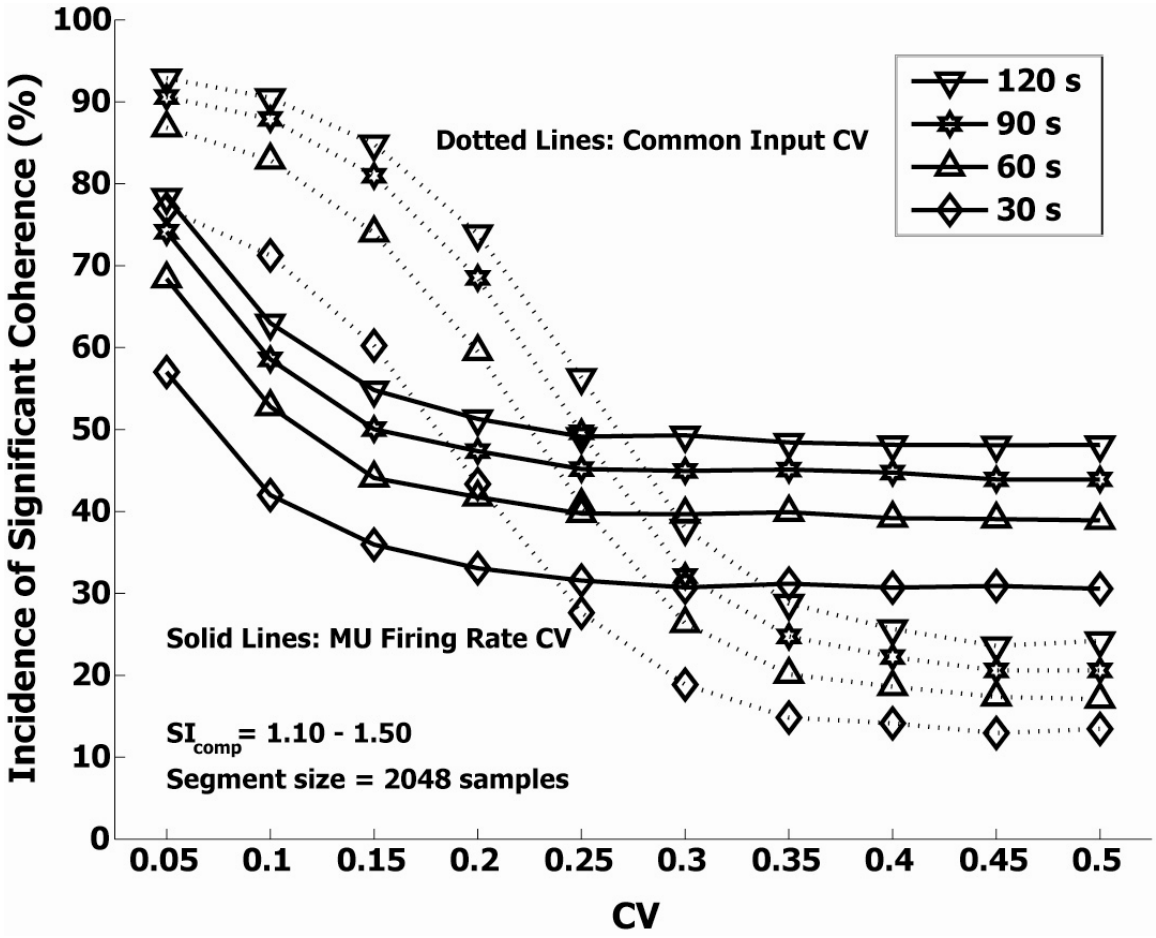

Figure 2-8. Variabilities of the firing rate (CV_{fr}) and common input frequency (CV_{com}) adversely affect coherence incidence as they increase. For the variabilities commonly seen in motor unit studies (CV=0.15-0.50), this effect is far more pronounced for the common input variability (dotted lines) than the firing rate variability (solid line).

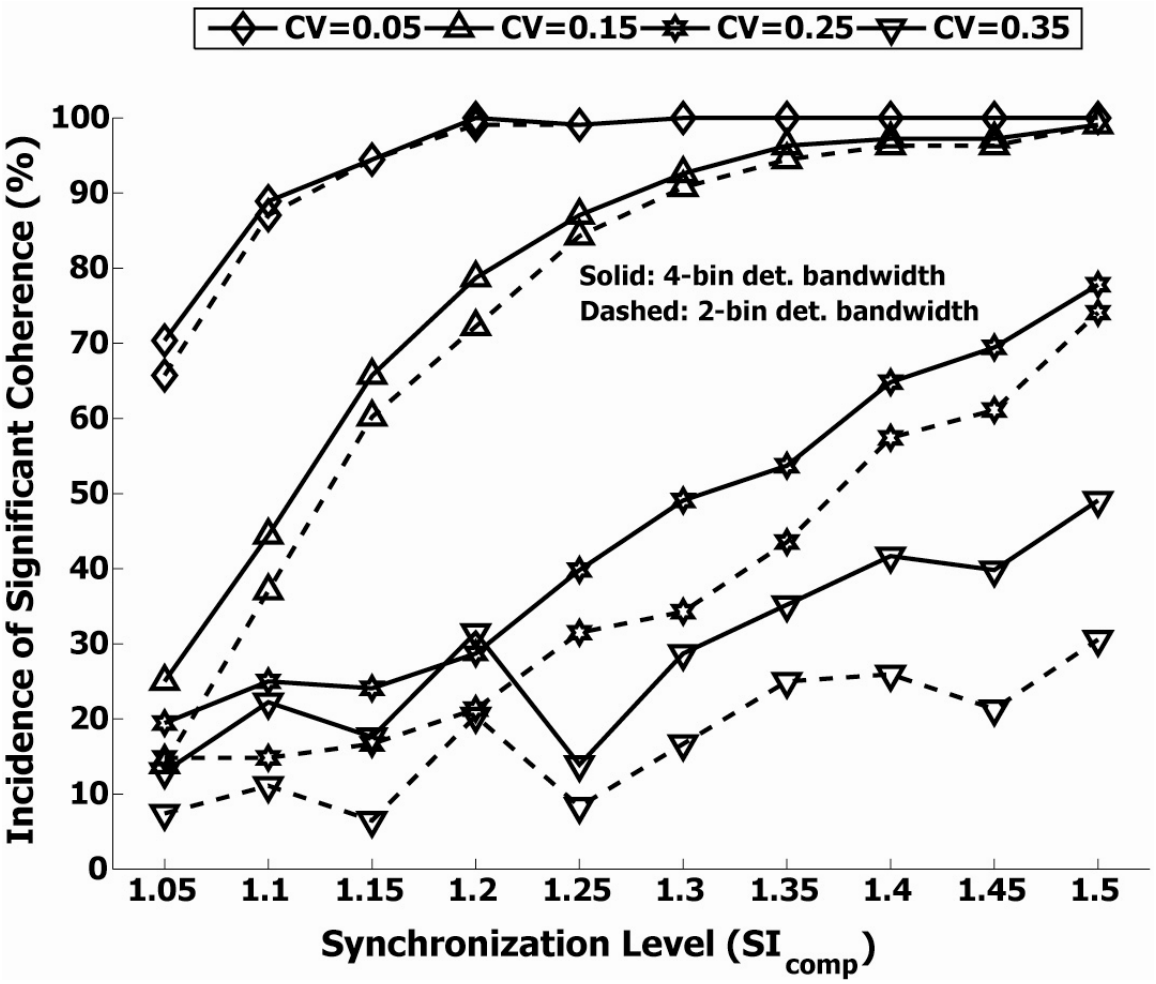

Figure 2-9. Average coherence incidence for detection bandwidths of 2 bins (dashed) and 4 bins (solid) wide. The difference in incidence rates increase with CV, but incidence rates are still below 50% when CV=0.35. Note that coherence incidence exceeds 85% when variance is low.

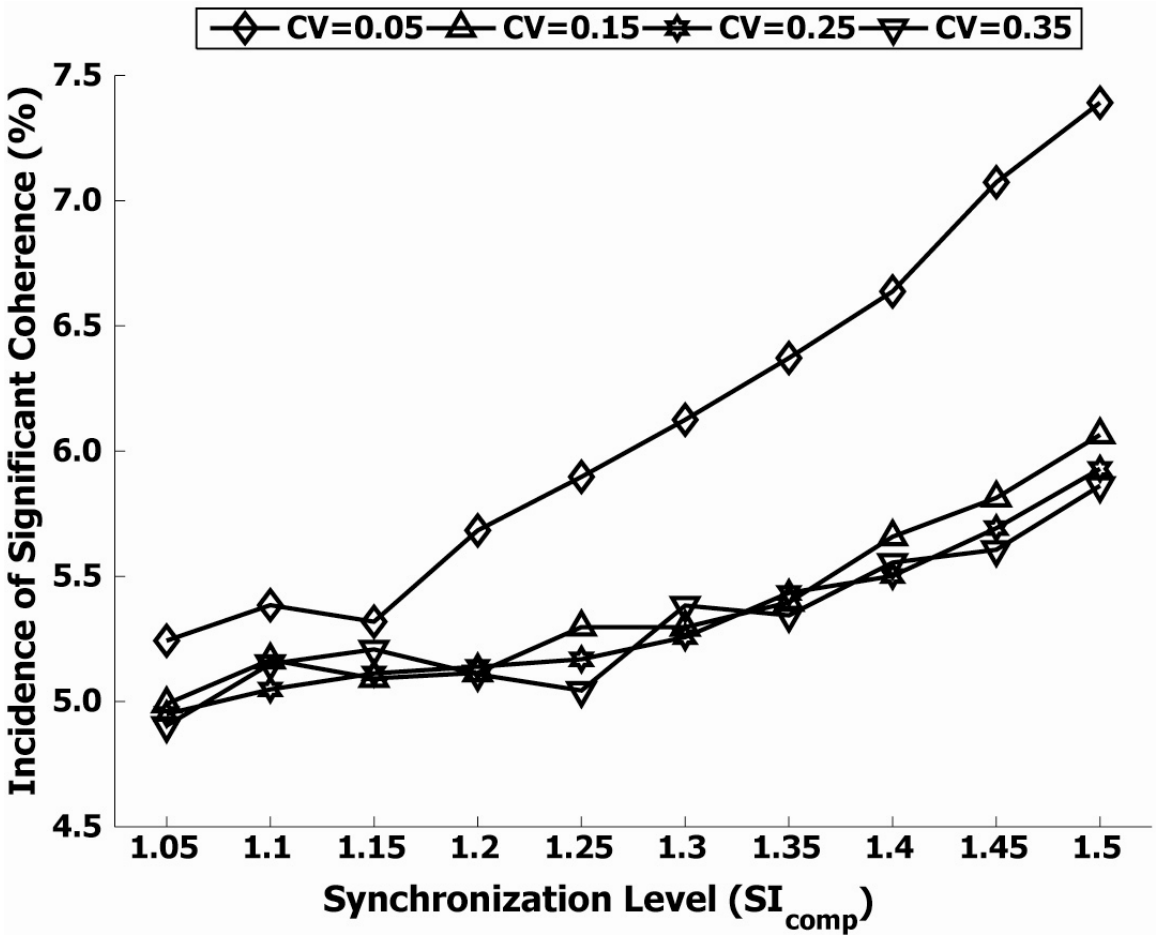

Figure 2-10. Coherence incidence for significant coherence detected outside of the 4-bin (1.96 Hz) detection bandwidth. For physiologically representative CV values (0.15-0.35), the 5% significance level is well-matched by the noise level, however, there is a slight underprediction of the significance level as synchronization increases. Incidence is higher for a CV of 0.05, indicating that false positive detections outside the detection bandwidth will be more common.

Chapter 3: Motor unit synchrony is not correlated to submaximal pinch force steadiness in younger adults

ABSTRACT

Non-pathological force steadiness has been shown to decrease as force falls below about 10% of maximum. One possible mechanism that could reduce force steadiness is a corresponding increase in motor unit synchronization, which could reduce force tetanus by aligning motor unit twitch forces. To establish whether this correlation existed, we recorded the intramuscular EMG from the first dorsal interosseous (FDI) and adductor pollicis (AdP) muscles and individual digit force variation during a two-minute isometric pinch at four submaximal forces: 2, 4, 8, and 12% of maximum pinching force (MPF) for each digit. MPF varied from 39.2 to 112.3 N (70.2±19.0 N) for the thumb and from 35.7 to 103.1 N (62.2±17.2 N) for the finger. For the AdP, 119 motor unit pairs were recorded, with motor unit discharge rates from 11.6 (±2.04) pulses per second (pps) at 2% MPF to 14.9 (±3.68) pps at 12% MPF, with a good linear fit (R^2=0.95). The FDI motor units comprising the 133 pairs for that muscle had firing rates increased at a similar rate, with a rate of 11.3 (±2.33) to 14.6 (±3.58) pps over the same force range.

There was a strong correlation between digit force and force CV for the thumb (R^2_{th}=0.91, p=0.044) and the index finger (R^2_{fg}=0.94, p=0.032). For the thumb force, CV decreased from 0.0778 (±0.0098) 2% MPF to 0.0365 (±0.009) at 12% MPF. Index finger force CVs were nearly identical, with a CV of 0.0789 (± 0.0151) 2% MPF to 0.0362 (± 0.0108) at 12% MPF. Pooled coherence for all 549 motor unit pairs (grouped by force) revealed a dominant peak for the 2-10 Hz for all forces and a much smaller peak for the 16-34 Hz band for the 4, 8, and 12% MPF forces. For frequency bands below 10 Hz, the 2%, 4%, and 8% MPF coherences were significantly lower than those for 12% (p<0.001).

There was a weak correlation of the thumb force to coherence for within-AdP pairs (R^2=0.32, p<0.001) and CIS (R^2=0.26, p<0.001), but no significant correlations for coherence or any of the short-term synchronization indices (CIS, SI, S, E, k'-1) were found for the index finger force. These findings do not support motor unit synchronization as a strong driver of force unsteadiness for isometric tasks at these forces.

INTRODUCTION

Muscle force steadiness is critical to precision task performance and depends on twitch force properties (Allum et al., 1978), number of active motor units (Hamilton et al., 2004), recruitment order consistency (Jones et al., 2002), rate-coding (Dietz et al., 1974), and doublet discharges (Laidlaw et al., 2000). One example of non-pathological force steadiness is its degradation with decreasing force once force falls below about 10% of maximum (Galganski et al., 1993; Keen et al., 1994; Laidlaw et al., 2000; Semmler et al., 2000). Focus has also been placed on the correlation between force steadiness and motor unit synchronization, more specifically known as short-term synchronization, is defined as the higher than chance tendency for motor units to fire within a few (0-5) milliseconds of each other and is believed to be driven by either branched common inputs at the spinal cord level (Sears and Stagg, 1976; Kirkwood and Sears, 1978) or oscillatory input to upper motor neurons at the cortical or subcortical level (Farmer et al., 1993; Baker et al., 2001). The near-simultaneous firing of motor units within and across muscles, has been extensively investigated as a possible source of force unsteadiness during non-fatiguing voluntary contractions (Allum et al., 1978; Christakos et al., 2006; Semmler and Nordstrom, 1998; Semmler et al., 2000; Tracy et al., 2005) and in simulated muscle models (Yao et al., 2000; Jones et al., 2002; Taylor et al., 2003; Enoka et al.,

2003; Hamilton et al., 2004; Santello and Fuglevand, 2004; Moritz et al., 2005). However, these studies have produced conflicting results.

For instance, Santello and Fuglevand (2004) found that motor unit models supported a link between short-term synchronization and force unsteadiness and other studies have also found that motor unit synchrony was correlated to force variability (Yao et al.; 2000, Taylor et al., 2003; Enoka et al., 2003; Moritz et al., 2005). Semmler et al. (2000) found that short-term synchronization was weakly correlated to decreased force steadiness in younger adults performing low-level (≤ 10% MVC), non-fatiguing index finger abduction, but the force and motor unit data were collected during separate sessions and motor unit activity was recorded at a single force level that did not necessarily match any of those used for measuring force steadiness (2.5, 5, 7.5, and 10% of maximum). In another study, the force steadiness across groups of untrained, skill-trained, and strength trained young adults was not correlated to synchronization strength (Semmler and Nordstrom, 1998).

In addition to mixed results, there are several other characteristics of these studies that made a complete assessment and comparison difficult or impossible. None of these studies addressed motor unit coherence, which reveals frequency and strength of the common inputs that can drive synchronization. Most of the studies used a single short-term synchronization index in preference to four others. They are all single-digit experiments that did not allow for the study of across-muscle synchronization during a coordinated task; an area of interest for which there is little information. Also, for those studies that examined multi-digit tasks, one examined motor unit synchrony, but only during brief exertions (Huesler et al., 2000), which precluded useful coherence measurements. Another examined only the FDI for short (8-second) durations (Kilner et

al., 2002), which precludes across-muscle synchrony measurements or coherence calculations, which require a much longer trial duration to reduce coherence variance.

To address all of these issues, we chose an isometric precision grip task that was performed at four different force levels to examine force effects across the range for which the largest changes in steadiness have been recorded. We measured synchronization in both time and frequency domains and examined multiple temporal synchronization indices to ensure that none of them produced preferential correlations. The pinch task involved simultaneous thumb adduction and index finger abduction so that across-muscle synchrony and possible differences in motor unit activity could be investigated. By monitoring muscle activity in the first dorsal interosseous (FDI) and adductor pollicis (AdP), we hoped to maximize the likelihood for synchronization, because intrinsic hand muscles have been shown to be more highly synchronized for within- and across-muscle pairs and the FDI-AdP demonstrated a consistent synergy for a precision grip (Maier and Hepp-Raymond, 1995a). Intrinsic muscles may also be better adapted for maintaining precision forces (Milner and Dhaliwal, 2002).

We tested the hypothesis that, during submaximal pinching, both short-term synchronization and coherence of the motor unit pairs would increase with force unsteadiness as isometric force level was reduced. Additionally, we investigated relationships between force steadiness and motor unit firing rate and firing rate variability to determine if either of these motor unit properties was associated with force steadiness during an isometric precision grip at multiple forces.

MATERIALS AND METHODS

Participants

Nine right-handed people (five male) between the ages of 20 and 45 (28.2 ± 9.5) years participated in this study. They were free of neuromuscular disorder and did not

have a prior history of extensive hand-use/training. Each participant was fully informed of the experimental procedures during an orientation session before signing a consent form. All experimental procedures were approved by the Institutional Review Board and were performed at the Neuromuscular Physiology Laboratory at The University of Texas at Austin. Each person participated in two experimental sessions separated by approximately four weeks.

Experimental Set Up and Design

Participants were seated with their left forearm, wrist, and hand stabilized in a splint to prevent postural changes during the experiment. The hand was secured in the supinated (palm-down) position and the thumb and index finger were placed against opposite sides of a cantilevered force transducer that measures independent force from each digit (Figure 3-1). An additional restraint immobilized the 3rd, 4th, and 5th digits to prevent supplemental force generation from interfering with pinch forces.

To standardize the applied forces across subjects, forces were expressed as a percentage of maximal pinching force (MPF). To measure the MPF, the left hand was positioned so that the proximal joint of each digit was in full contact with the edge of each arm of the force transducer. To prevent involvement of supplementary muscles, the subject was instructed to pinch by bringing the index finger and thumb together while relaxing the arm and shoulder and to apply the force through the proximal joints of each digit. A pinch that comprised a combination of thumb adduction and index finger abduction was chosen so that the two tasks most commonly performed as part of hand motor unit synchronization studies. The combination of an uncommon task performed by the non-dominant hand was also most likely to produce the highest level of motor unit synchronization (Semmler and Nordstrom, 1998). The subject was then asked to pinch maximally for three seconds three times in succession with five-second rest intervals.

When the maximal forces showed consistency (± 5%) for three consecutive pinches, the average of the two highest forces was established as the MPF for each digit.

Following MPF measurements, the subject was given time to become familiar with the apparatus and protocol by practicing ramp-hold-ramp (±0.67% MPF/sec ramp speed) contractions at 2, 4, 8, and 12% MPF for 60-second periods with progressively longer rest periods at higher forces (15, 15, 30, and 60 seconds, respectively) to prevent fatigue. These particular force levels were selected to track low-force steadiness while preventing the recruitment of too many motor units, which would impair accurate spike discrimination. The practice protocol consisted of a series of two pinches at each force in increasing succession. A monitor was positioned in front of the participant to enable manipulation of their thumb and finger forces to track a target force cursor that moved from the lower left corner of the monitor to a position above and to the right of its origin. The actual force cursor moved horizontally with thumb force and vertically with finger force. As the maximum force increased, the final position of the target cursor would move higher and further to the right, so that scale was maintained. For the ramp-hold-ramp series, the target cursor would move from the origin to the final position at the stated rate, hold for 60 seconds, and then return to the origin at the same rate. During a subject's first session, this protocol was repeated once to ensure familiarity with the set-up, but was performed only once when the subject returned for the second session.

After the practice protocol was completed, the dorsal surface of the hand was cleaned and abraded before inserting two monopolar needle electrodes (25 mm long, 0.010" dia., FHC) into the AdP and two electrodes into the FDI. A surface electrode was placed at the ulnar styloid process of the wrist to be used as a ground and another surface electrode was placed over the proximal FDI tendon as a reference. Another monitor, not

visible to the subject, was used by the experimenter to monitor motor unit recording quality and force.

Before starting pinch trials at each force level, the subject performed brief pinches at the target force as EMG signals from each electrode were monitored. If motor units were not clearly distinguishable, the corresponding electrode was carefully repositioned until at least one clearly defined motor unit action potential was consistently visible when the target force was maintained. This process continued until clearly defined motor units could be seen on at least three channels. If the experimenter could not see consistent motor unit spikes during a trial, the experiment was stopped and the electrodes were repositioned again.

Subjects increased each digit force as practiced. The only difference was that the hold period was two minutes and the rest periods were longer. At least two trials were performed at each force level with rest periods of 30, 30, 60 and 90 seconds for the 2, 4, 8, and 12% MPF levels, respectively. To ensure that steadiness and force order of progression were not correlated, five subjects performed the trials in reverse order (12%→8%→4%→2%). The experiment concluded once acceptable data had been collected for at least two trials (ramp up-hold-ramp down) at each force level.

Data Collection and Analysis

A PC (Pentium IV with Windows XP OS) with dual monitors was used to provide real-time displays of target and actual forces and EMG recordings for each electrode. All data was analyzed offline using Spike2 for Windows (version 5) software package (CED). The signals from the force transducers were amplified at a gain of 500 and digitized at a sampling rate of 1000 Hz (Micro 1401 Mk II ADC, Cambridge Electronic Design (CED)). Force recordings were only analyzed during the steady-state portion of each trial. A mean and standard deviation for each force recording was computed and

used to check for outliers caused by momentary fluctuations. All force values lying outside the 99% bounds (± 2.58 SD) were deleted and the mean and SD were recalculated. This process continued until all force values fell within the 99% probability bounds. Force PSD calculations were performed after linear detrending so that spectral power would be correlated only to force variance.

Intramuscular EMG recordings were digitized at a rate of 25 kHz and high-pass filtered at 13 Hz (Micro 1401 Mk II ADC, CED). Each EMG recording was examined for spurious noise by performing a PSD on the signal and low-pass filtering below the frequency of the lowest noise source, without removing signal content. After removing high-frequency noise, the signal was then linearly detrended to remove signal drift.

All computer code for spike simulation, coherence calculations, and statistical analyses were written in Matlab® version 7.1 with the Signal Processing and Statistics toolboxes. Computations were performed on a PC with a Pentium® D 3.0 GHz processor and Windows® XP OS.

Spike Identification

Individual motor unit potentials for each electrode were identified off-line with waveform discrimination system which allowed for time coding of each motor unit action potential, or "spike". The software performed the initial tracking of this motor unit using a "template matching" algorithm, where a template was built from a small group of spikes belonging to the same motor unit and then matched to all spikes in the EMG data. After automated processing, spikes were manually scanned to ensure that spikes were not misclassified due to noise or superposition. For superpositioned spikes, the spikes were classified as a spike in each train, if the spikes in the superpositioned waveform could be clearly identified. Otherwise, those spikes were not included in the analysis. Once all identifiable spikes were classified, each spike was converted into an event (time) marker

by recording the increasing threshold crossing time of the first voltage deflection. This process converted each action potential train into a set of event times needed for the computation of motor unit synchrony in time and frequency domains. Before calculating coherence or short-synchronization indices, data segments that did not contain data for both trains were removed to prevent attenuation of these measurements that would be caused by intermittent spike train data.

Short-term Synchronization

Synchronous motor unit activity across the AdP and FDI was measured using cross-correlation analysis of motor unit firing times during the constant force contraction (Sears and Stagg, 1976). The cross-correlation histogram was constructed with a time-window of ±100 milliseconds from the reference spike event time and a bin size of 1.0 millisecond. The 200-millisecond span of this window ensured the correlation of all motor units that fire at a minimum of 5 Hz, which is below the minimum firing rate of the slowest-firing human motor units (Marsden et al., 1971; Macefield et al., 1993). Using a one-millisecond bin width provides a smooth histogram and sufficient resolution for action potentials, which can typically be discriminated well within this time span.

To establish a peak region for those motor unit pairs exhibiting synchrony, the cumulative sum (CUSUM) of counts below or above the mean was calculated and tracked (Ellaway 1978, Wiegner A.W. and Wierzbicka 1987, Nordstrom et al. 1992). Deflection points were determined by tracking the variance (V) of the CUSUM and defining a deflection point as a location where the CUSUM exceeds $3\sqrt{V}$ (Bremner et al., 1991) and verified visually. Figure 3-2 shows a typical cross-correlogram and CUSUM plot used to find the peak region for a motor unit pair.

An event is counted each time a response spike from one train is within ±100 ms of a reference spike in the other train. The mean bin count is found by dividing the bin

populations outside the peak region by the number of non-peak bins. Within the peak region, two quantities are important to the calculation of synchronization indices. Extra events are equal to the area within the peak region above the mean bin count, while expected events are found as the peak region area below the mean. Once the peak region was established, extra, expected and total event counts could be used to calculate the synchronization indices. Computation of synchronization indices is simple and there is no consensus on the best index, so we computed all of the following indices:

$$\text{CIS} = \text{extra events/trial duration} \quad (1)$$

$$\text{SI} = \text{extra events/total events} \quad (2)$$

$$\text{S} = \text{extra events/total no. of spikes} \quad (3)$$

$$\text{k'-1} = (\text{extra events/expected events}) - 1 \quad (4)$$

$$\text{E} = \text{extra events/no. of reference spikes} \quad (5)$$

All of these indices are dependent on the number of extra events and will therefore be correlated to some degree. However, the index E will be more dependent on the reference train firing rate, as the indices S and SI will be dependent upon the combined firing rate of both trains. The index k' will be the most dependent on accurate selection of the peak region, because only counts in that time span are used to calculate it. The CIS index does not rely upon spike counts or event counts outside the peak region and was the only index found to be insensitive to motor unit firing rates (Nordstrom et al., 1992). However, a more recent study (Halliday et al., 2006) found that all of these indices were equivalent except for a scale factor and offset. Still, we included all five indices to ensure that our results were not skewed by preferential selection of one index over the others.

Coherence Analysis

Calculating the coherence of two stochastic point processes, such as two spike trains (denoted as spike trains x and y), involves a series of summations to find the Fourier transform of each set of event times and the cross-power spectral density (CPSD - Φ_{xy}) and auto-power spectral densities (APSD - Φ_{xx}, Φ_{yy}) of these transforms (Rosenberg et al., 1989), as shown in equation (6),

$$| R_{xy}(f) |^2 = \frac{| \Phi_{xy}(f) |^2}{\Phi_{xx}(f)\Phi_{yy}(f)} \tag{6}$$

where $|R_{xy}(f)|^2$ represents the coherence for spike trains x and y at frequency f and the cross- and auto-spectra of these two spike trains are represented by the functions $\Phi_{xy}(f)$, $\Phi_{xx}(f)$, $\Phi_{yy}(f)$.

Before processing, event times for each spike train were sampled at 1 kHz (1-ms bins). Each sampling bin was set to "1" if it bounded a spike event time or "0" if not and the converted event record was detrended to remove signal drift. Coherence for each motor unit pair was found using the MATLAB function mscohere with a segment size of 2.048 seconds (2048 samples), a 50% segment overlap and a Hann taper, to reduce variance and prevent spectral leakage as discussed in Chapter 2.

The coherence confidence level was established using equation (7),

$$Z_{ovlp} = 1 - \alpha^{\frac{1}{wL^*-1}} \tag{7}$$

where L* is the number of overlapped segments, found using equation (8),

$$L^* = floor((L-1)/(1-ovlp)) + 1 \tag{8}$$

where L was the maximum possible number of non-overlapped segments of length T into which the spike train could be subdivided. α was the desired type 1 error level (Brillinger, 1978). For this study, coherence values exceeding the 95% confidence value ($\alpha = 0.05$) were regarded as significant.

The variable *ovlp* is the percentage of segment overlap and w is a weighting factor that is dependent on the amount of overlap and taper type. For tapered segments with window W and nfft segment elements, w is found using equation (9).

$$w = \left\{ \frac{\left[\sum_{k=0}^{nfft-1} W(k) * W(k + (1 - ovlp) * nfft) \right]}{\left[\sum_{k=0}^{nfft-1} W^2(k) \right]} \right\}^2 \tag{9}$$

For a Hann taper, the window equation is:

$$W(k+1) = 0.5\left(1 - \cos\left(\frac{2\pi k}{nfft - 1}\right)\right) \tag{10}$$

for k = 0,…, nfft-1, where nfft is the number of segment elements ($T/\Delta\tau$). For this study, nfft was 2048.

Coherence was quantified in three ways. Coherence incidence describes the number of cases for which coherence exceeded the significance level at a given frequency and is used to express coherence for a group of motor unit pairs. The coherence index is used to describe the percentage of frequency bins between 5 and 50 Hz for which the coherence exceeded the significance level and was used to describe the overall strength of coherence for a single motor unit pair.

The third quantification of coherence was the technique of pooled coherence (Amjad et al., 1997), a comparison of coherence for pools of motor unit pairs at each force level. This technique allows for the aggregate computation of coherence that have

been normalized according to trial duration. Coherence measurements for different trial lengths with identical segment sizes as were recorded in this experiment had different segment numbers (L) that resulted in different had different significance levels (equation 7). To find this quantity for a set of motor unit pairs, the cross-power spectral density (CPSD), auto-power spectral densities, and number of segments are calculated independently and then summed before the coherence relation is applied, as shown in equation (11),

$$Pooled \ |R_{xy}(f)|^2 = \frac{|\sum_{i=1}^{k} \Phi_{xy_i}(f) * L_i|^2}{\left(\sum_{i=1}^{k} \Phi_{xx\,i}(f) * L_i\right)\left(\sum_{i=1}^{k} \Phi_{yy_i}(f) * L_i\right)} \quad (11)$$

where k is the total number of motor unit pairs and L_i is the number of segments for *i*th pair. The significance level (7) is modified to:

$$Z_{pool} = 1 - \alpha^{\frac{1}{w\sum L_i * -1}} \quad (12)$$

for each *i*th motor unit pair. For our study, the CPSD and APSDs were found using the same segment length, overlap, and taper used to find the independent coherence for each motor unit pair.

Statistical Analysis

The means and distributions of groups were compared using a one-way ANOVA using force level as the independent variable and Tukey-Kramer corrections for multiple comparisons. Linear regressions were used to examine trends for force variability and coherence versus force level and to find correlations between coherence and synchrony indices. Coherence follows a chi-square distribution (Bendat and Piersol, 2000), so non-parametric Kruskal-Wallis tests with Tukey-Kramer corrections were used in place of the one-way ANOVA when coherence values were directly compared. Stated errors are the

standard deviation (SD), whereas those shown in figures are the 95% confidence intervals. All findings were considered significant if the p-value fell below a value of 0.05.

RESULTS

MPF forces varied from 39.2 to 112 N (70.2±19.0 N) for the thumb and 35.7 to 103 N (62.2±17.2 N) for the finger. These forces translated to torques of 3.38-9.69 N-m and 3.08-8.90 N-m for the thumb and finger, respectively. The number and distribution of motor unit pairs are shown in Table 3-1.

Motor Unit Properties

Mean motor unit firing rates systematically increased with force level for motor units of both muscles (Figure 3-3, top). For the AdP, motor units discharged from 11.6 (±2.04) pulses per second (pps) at 2% MPF to 14.9 (±3.68) pps at 12% MPF, with a good linear fit (R^2=0.922, p=0.040). FDI firing rates increased at a similar rate, with a rate of 11.3 (±2.33) to 14.6 (±3.58) pps over the same force range (R^2=0.972, p=0.014). The mean coefficient of variation (CV) of the motor unit firing rate also increased with force for both muscles, but neither of these regressions was statistically significant (Figure 3-3, bottom).

Force Steadiness and Spectral Power

We also examined the correlation between digit force level and force steadiness (Figure 3-4). There was a strong correlation for the thumb (R^2_{th}=0.91, p=0.044) and the index finger R^2_{fg}=0.94, p=0.032) and close tracking between force CV for each digit. For the thumb force, CV dropped from 0.0778 (±0.0098) to 0.0365 (±0.009) as force level increased from 2% to 12% MPF. This same change in force resulted in an index finger force CV change from 0.0789 (±0.0151) to 0.0362 (±0.0108). The CV decrease was largest from 2% to 4% MPF, with smaller decreases for each successive force increase.

Also shown in Figure 3-4 are the subgroups according to the order in which the force levels were applied. Regardless of whether force increased or decreased with each trial, the overall trends of decreasing force steadiness with force and closely matched finger and thumb force steadiness were consistent with that seen for the group correlation.

Force spectral power shows that power at all force levels was concentrated in the 0-2 Hz bandwidth, with no indication of tremor peaks at higher frequencies (Figure 3-5). Power increased with force, indicating that the force deviations also increased with force. Spectral power for the 12% MPF level was only found to be significantly higher than that for 2 and 4% MPF in the 0-0.5 Hz band ($p<0.001$).

Motor Unit Synchrony

Overall coherence indices were computed for all motor unit pairs and then separated by pairs within the FDI, within the AdP, and paired across the two muscles (Figure 3-6). As force level decreased, the correlation between coherence for within-FDI pairs and force level was the only one that was significant ($R^2=0.09$, $p=0.001$). To find the coherence for all motor unit pairs at each force level, we found the pooled coherence for each group. There was a dominant peak for the 2-10 Hz for all forces and a much smaller peak for the 16-34 Hz band for the 4, 8, and 12% MPF forces. When examining trends on a spectral basis for the entire frequency range (Figure 3-7), pooled coherence was not significantly different for any two force levels ($p=0.160$). However, for frequency bands below 10 Hz, the 2%, 4%, and 8% MPF coherences were significantly lower than that for 12% ($p<0.001$). Note that as frequency increased beyond 40 Hz, all coherence incidence rates approached the 5% significance level, indicating that significant coherence values found at these frequencies were only due to chance.

Correlations between the force CVs for each digit and both coherence and short-term synchrony indices are shown in Figure 3-8. The upper plot shows a very weak

correlation for the thumb force CV and coherence for within-AdP pairs (R^2=0.32, p<0.001) and CIS (R^2=0.26, p<0.001), but no significant correlations for coherence or the CIS index were found for the index finger force. To ensure that our findings were not based on choice of synchrony index, we checked the correlation between coherence and five other synchrony indices (Figure 3-9). Correlations between each synchronization index and coherence were similar to or less than that for the CIS index (R^2=0.57), with the S and E indices (R^2=0.57) showing nearly identical agreement. The SI index correlation was slightly weaker (R^2=0.42), while the k'-1 correlation was very small (R^2=0.05). All correlations had p-values of less than 0.001.

DISCUSSION

The primary purpose of this study was to establish whether a correlation between motor unit synchrony and force steadiness existed across multiple force levels during an isometric pinching task. Motor unit synchronization was expected to increase with the increase in force unsteadiness as force was reduced from 12% to 2% MPF. However, both short-term synchronization indices and coherence measurements failed to reveal any correlation between these two properties.

The trends seen in Figure 3-6 show that overall coherence was not significantly correlated to force level, nor were there consistent trends for any of the four groups. This figure shows that the lower values of coherence were predominantly due to the across-muscle coherence, whereas the higher values of coherence were from within-muscle pairs. Other studies have shown that across muscle synchronization is generally lower for across-muscle pairs (Maier and Hepp-Raymond, 1995a; Santello and Fuglevand, 2004), but we expected this difference might be smaller or undetectable for a task involving the coordinated effort of two digits and considering the close agreement between thumb and index finger force steadiness.

The correlation between force steadiness and force level was consistent with those seen in previous studies (Taylor et al., 2003; Enoka et al., 2003; Hamilton et al., 2004; Moritz et al., 2005; Tracy et al., 2005), which was important for establishing that a progressive change in force steadiness was consistently present for each experiment. The consistency of this correlation for the increasing force and decreasing force progression indicates that there was no advantage gained by performing the low force task from practice at higher levels, nor was there a disadvantage produced by fatigue from performing the earlier trials. Establishing the positive correlation between force level and force steadiness was critical to this study, enabling assessment of correlation between synchrony and steadiness across different force levels.

Coherence for motor unit pairs within each muscle was not correlated to the corresponding digit's force steadiness and there was only a weak correlation between short-term synchronization (CIS) of FDI pairs and index finger force steadiness (Figure 3-8). This finding conflicts with those of recent simulation studies (Yao et al., 2000; Jones et al., 2002; Taylor et al., 2003; Enoka et al., 2003; Hamilton et al., 2004; Santello and Fuglevand, 2004; Moritz et al., 2005; Lowery and Erim, 2005), but are similar to those for other physiological experiments (Logigian et al., 1988; Semmler and Nordstrom, 1998; Semmler et al., 2000). With the exception of one study, the simulations used a post-generation alignment of spikes referenced to a single train to produce short-term synchronization, which is not representative of a physiological process. However, a study that incorporated a common input to drive synchronization (Lowery and Erim, 2005) also found that force unsteadiness, measured as force CV, was correlated to synchronization level. However, this effect was only present for common input frequencies below 10 Hz and highest at 2 Hz. For cortical activity, this spectral region is not associated with typical beta-band (13-30 Hz) oscillations, but it is associated with

what is typically referred to as “common drive”, which slowly changes motor unit firing rates at a 1-2 Hz rate. Therefore, synchronization driven by a common input may increase low-frequency force fluctuations, but not the higher frequency adjustments normally associated with force unsteadiness.

The concentration of spectral power in the 0-2 Hz band has been seen for isometric forces in several similar single-digit studies (Vaillancourt et al., 2002; Taylor et al., 2003). The increase in spectral power with increasing force level indicates that the fluctuations were larger at higher forces, which is consistent with earlier studies (Sutton and Sykes, 1967; Cresswell and Loscher, 2000). However, the increase in fluctuation size (standard deviation) does not keep pace with the increase in isometric force, resulting in a decreasing force CV, as recently reported (Vaillancourt et al., 2002; Hamilton et al., 2004; Sosnoff and Newell, 2006; Spirduso et al., 2005). The isolation of force spectral power in a bandwidth for which motor control EEG activity is not seen indicated that force variability and synchronization were not related.

We also examined pooled coherence for all motor unit pairs at each force level (Figure 3-7). This plot showed two dominant bands of motor unit coherence similar to those established previously at 1-12 Hz and 16-32 Hz (Halliday et al., 1999). Although there were no significant differences between pooled coherence for each force, the coherence was approximately 2-3 times greater for the 12% MPF force than that for the other three forces in the 2-10 Hz band, which indicates that coherence may be a way to produce higher forces beyond a certain threshold. This spectral region is normally not of primary interest, however, because the cortical activity is usually most prominent in the 10-35 Hz region. However, if a correlation to force variability were to exist, it would most likely be in the same spectral bandwidth as the force spectral power, which was 0-2 Hz.

Mean motor unit firing rate increased with higher isometric forces as expected. However, we did not see a decrease in firing rate CV as reported in previous studies (Semmler and Nordstrom, 1998; Enoka et al., 2003). The increase in firing rates was important for establishing that the motor units being recorded were responsible for the increased force and not just maintaining postural stability. However, the discrepancy in firing rate variability is an important finding because the increase of firing rate variability has been postulated as a source of force unsteadiness (Taylor et al., 2003; Enoka et al., 2003; Hamilton et al., 2004; Moritz et al., 2005; Tracy et al., 2005). In particular, the study by Moritz et al. (2005) was built upon earlier modeling related to the Enoka et al. (2003) and Taylor et al. (2003) studies and found significant positive correlations between firing rate variability and force unsteadiness. Conversely, there is also experimental evidence that firing rate variability and force steadiness are not correlated, as seen in young versus older adults (Semmler et al., 2000), which agrees with our findings.

Other findings support a difference in findings based on how the protocols were administered. For instance, unrestrained force application normally produces a large mechanical tremor component that can obscure neurogenic activity in spectral measurements, making comparisons between restrained and unrestrained force protocols difficult. Taylor et al. (2003) found that synchrony increased force fluctuations, but only for anisometric forces. Kilner et al. (2002) experimented with how synchrony changed with compliance of the resistive device used as a force transducer and discovered that synchrony increased as the compliance, or flexibility, increased. There have also been several investigators who found significant correlations between tremor and synchrony when the digit is unconstrained (Halliday et al., 1999, Kakuda et al., 1999). This second

study also found that coherence was non-existent for isometric forces, but the duration was only 5 seconds, which is typically too short for finding significant coherence.

Force steadiness and motor unit firing rate or its variability do not appear to drive force unsteadiness. Similarly, the connection between force steadiness and synchrony is nonexistent for the FDI as it controls the index finger during isometric contractions and was only weakly correlated for the AdP and thumb force. Across-muscle synchrony also had no effect on force steadiness, in spite of the coordinated nature of the performed task. The absence of correlations may be due to the restrained nature of isometric force generation as opposed to unrestrained tasks that allow for oscillatory movement seen in normal physiological tremor, where this correlation is typically found. However, the weak correlation between force steadiness and AdP synchrony in both the time and frequency domain, which indicates a different physiological mechanism for force production between the AdP and FDI muscles. This difference could be due to muscle motor unit number, size, or difference in primary function of pressing versus grasping. Most importantly, motor unit synchrony does not appear to be a possible driver of force steadiness for steady, isometric, multidigit tasks across multiple force levels, regardless of the metric used to quantify motor unit synchronization.

Table 3-1. Summary of recorded motor unit pairs by muscle and force

	2% MPF	4% MPF	8% MPF	12% MPF	**Total**
AdP	11	53	27	28	**119**
FDI	29	49	28	27	**133**
Across	53	112	72	60	**297**
Total	**93**	**214**	**127**	**115**	**549**

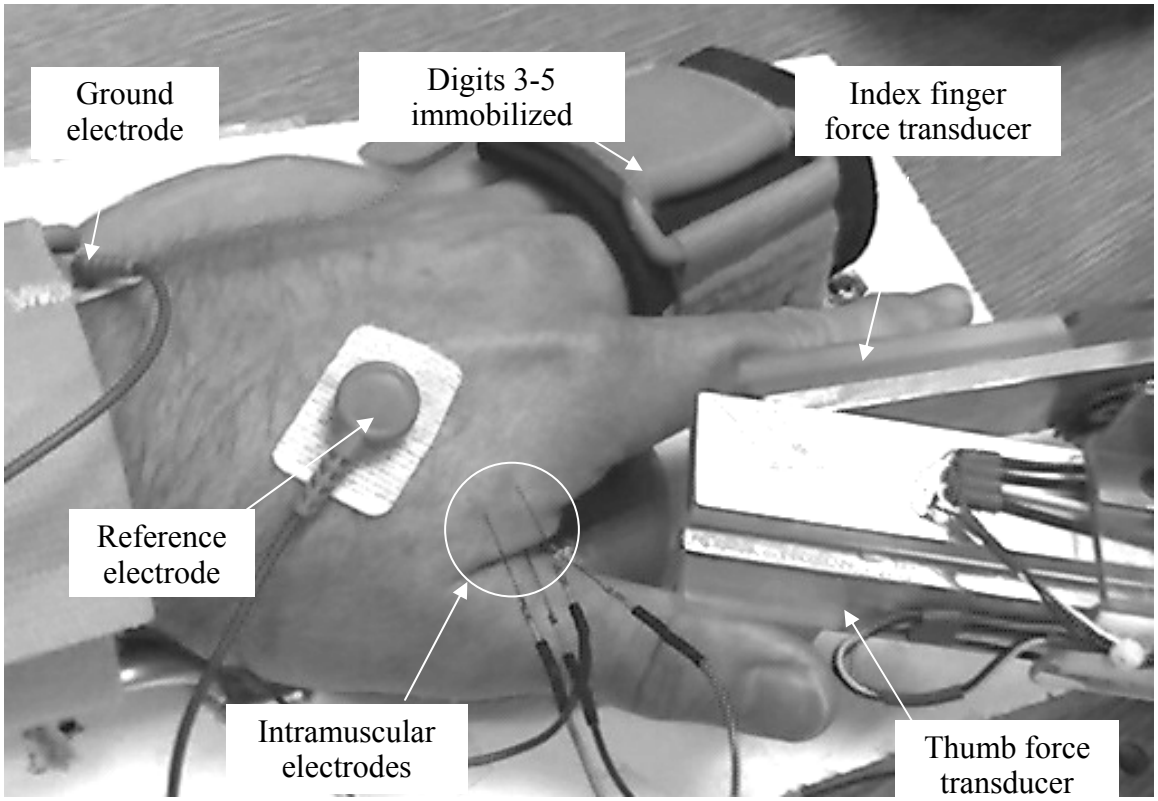

Figure 3-1. Photo of experimental set-up showing restrained left hand and electrode placement while index finger and thumb were placed against force transducers.

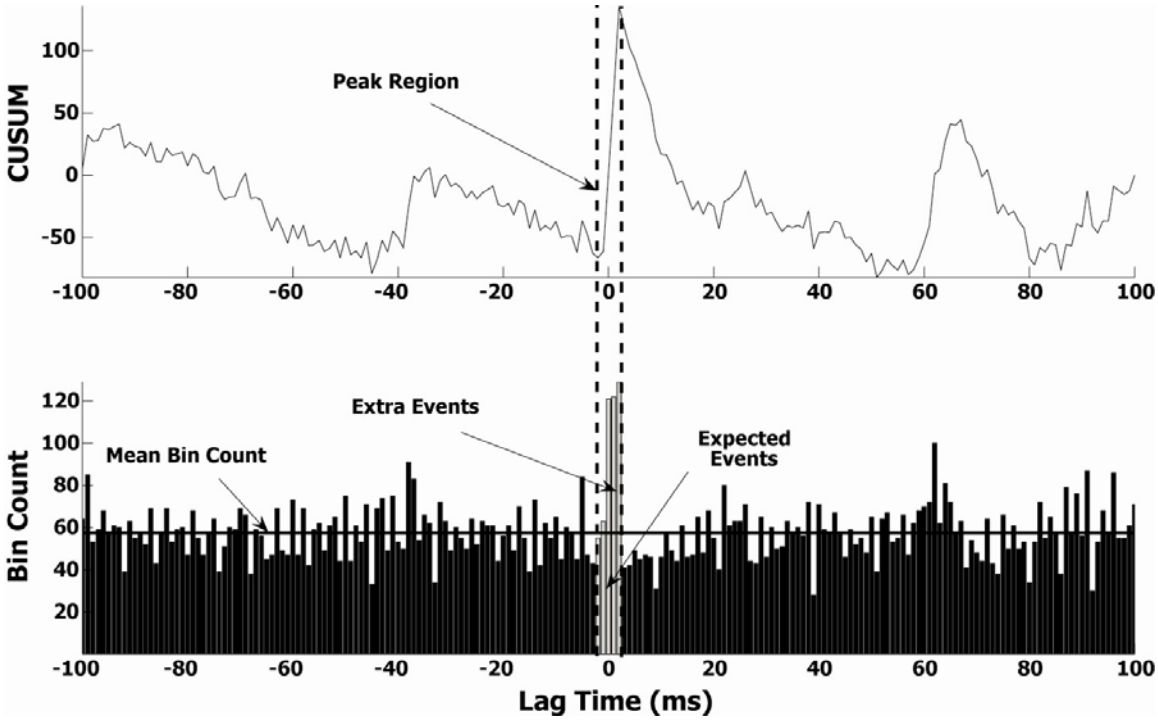

Figure 3-2. Sample cross-correlation histogram with CUSUM plot showing deflection points and definition of peak region, extra events, and expected events.

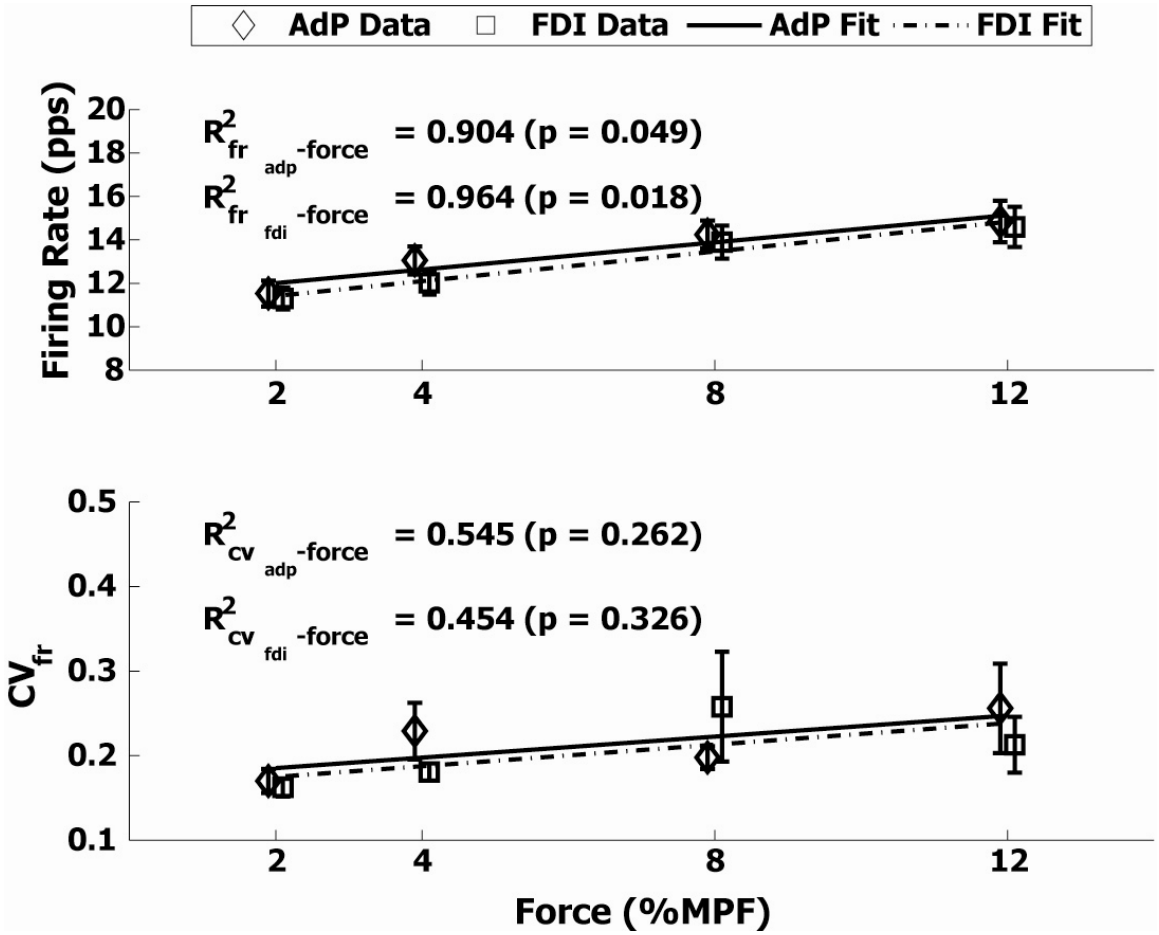

Figure 3-3. Correlation of mean motor unit firing rates (upper) and firing rate CVs (lower) with force level. Linear regression confirms that both firing rate and firing rate CV increase as force increases.

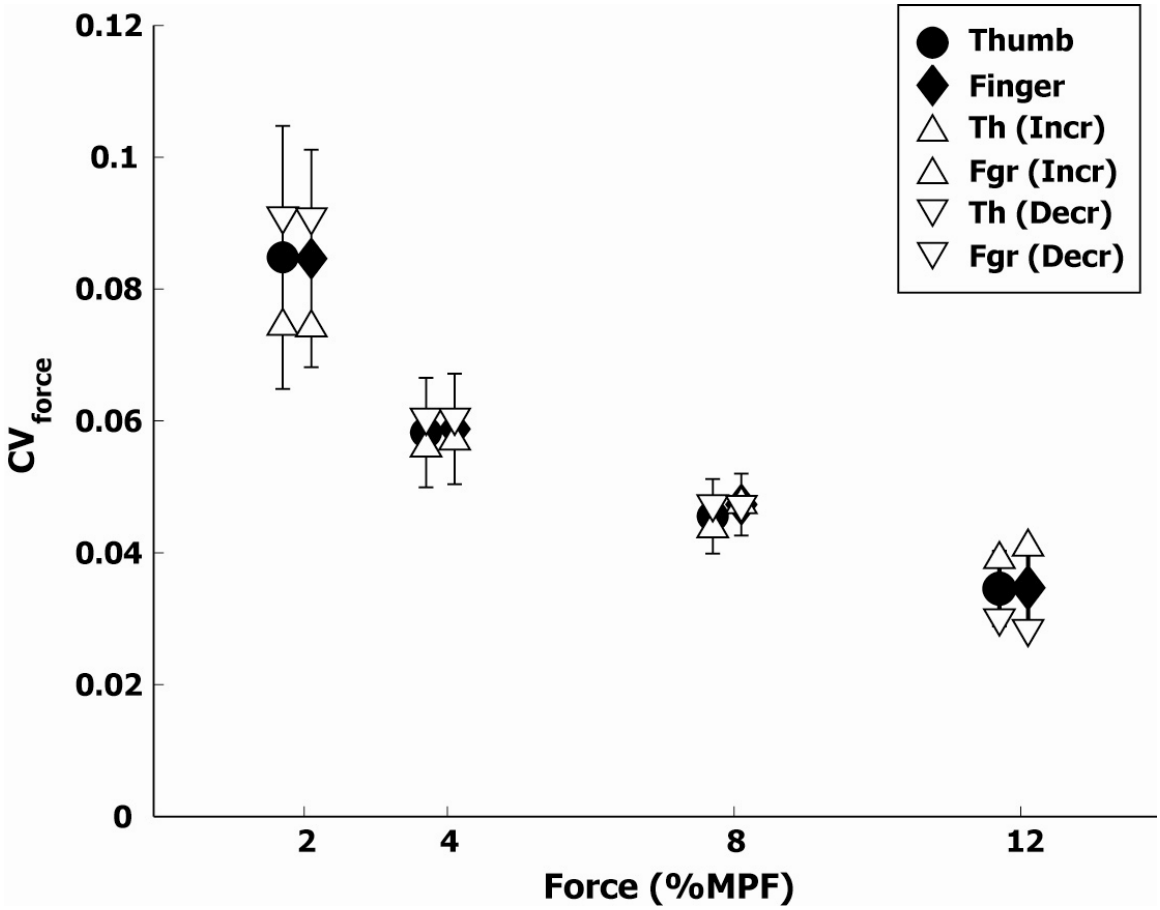

Figure 3-4. Force steadiness decreases with force for both the thumb and index finger. Also shown are digit force CV values for the subjects subgroup that applied progressively increasing or decreasing force during the experiment.

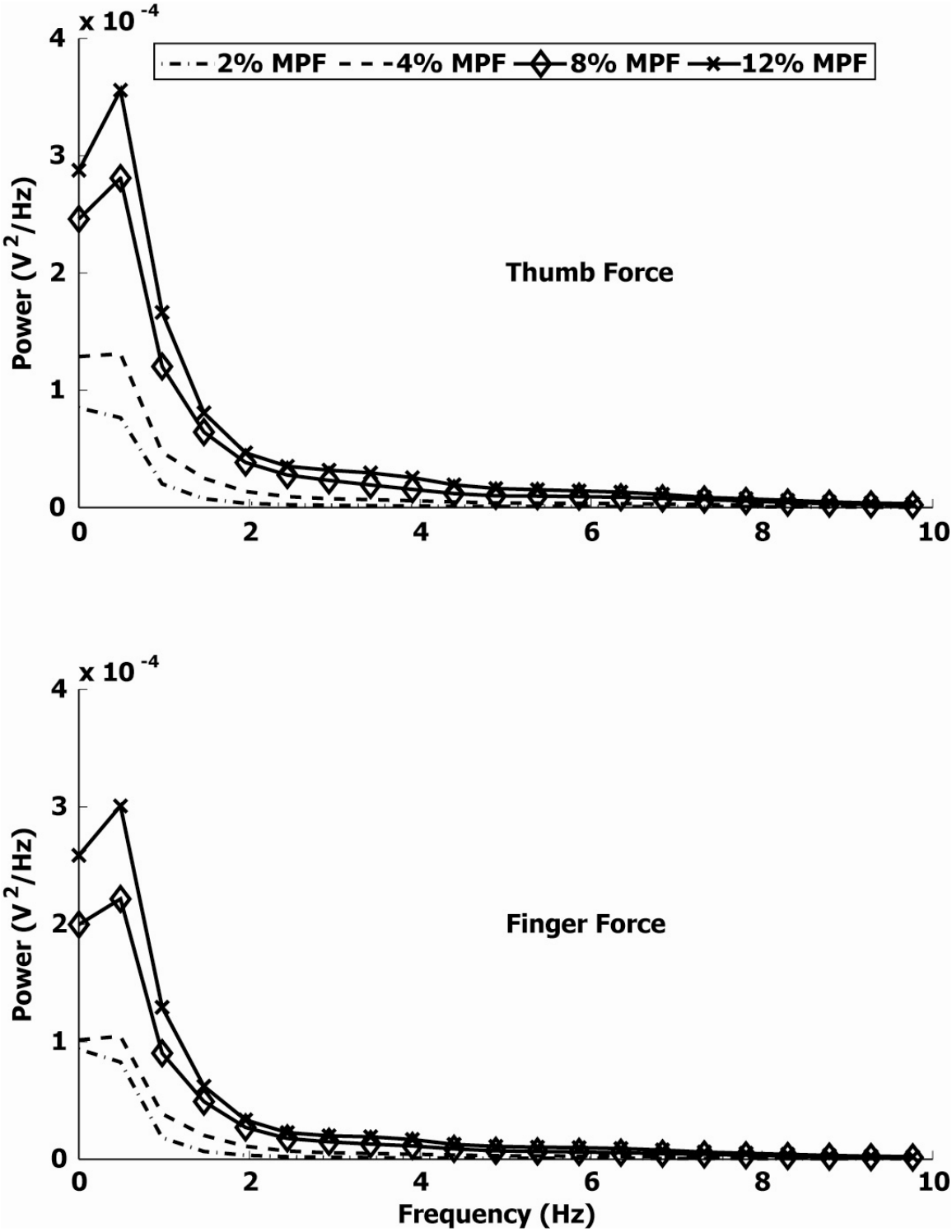

Figure 3-5. Detrended PSD plots for the thumb and index finger forces. No measurable force power was found above 10 Hz for either digit.

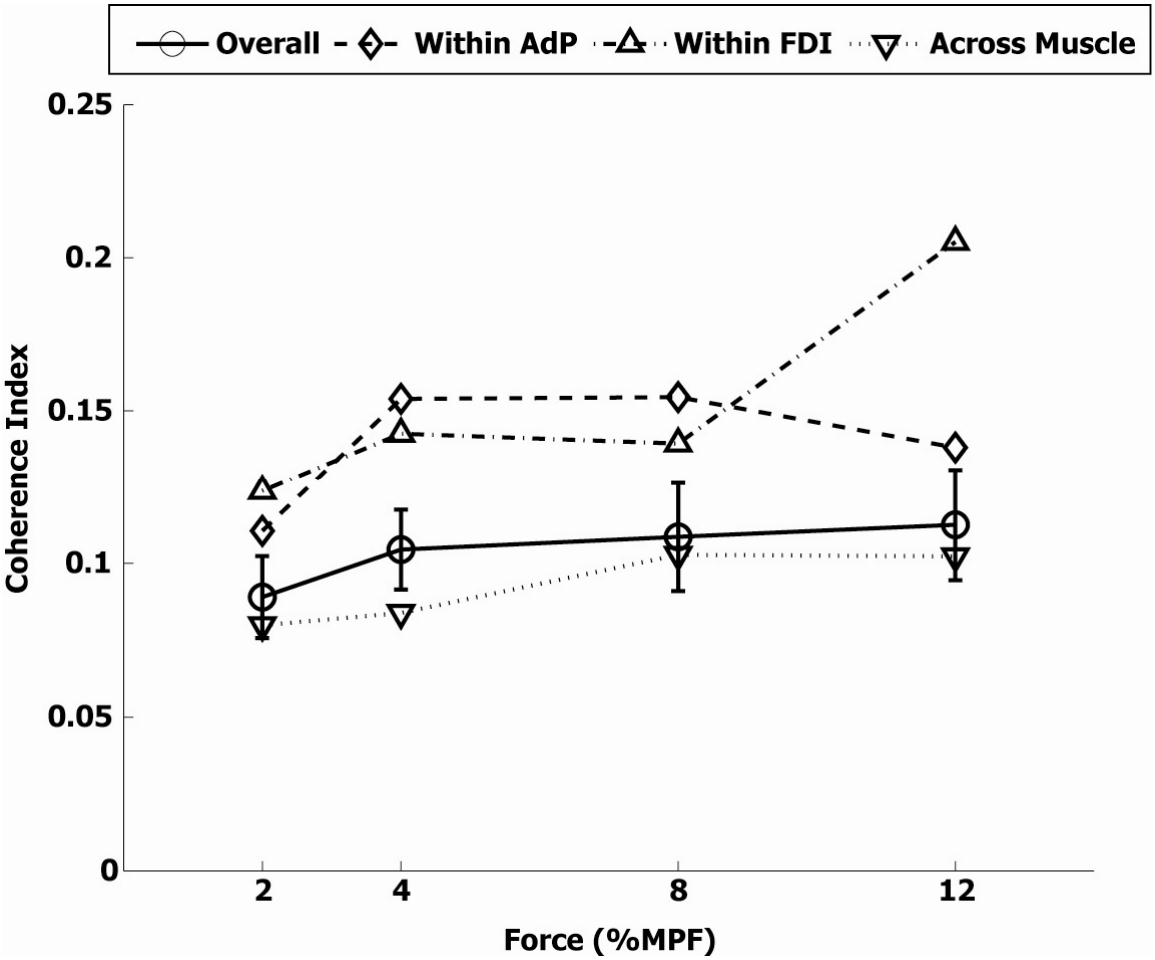

Figure 3-6. Mean coherence at each force level for all motor unit pairs with 95% CI. Also shown are mean coherences for pairs grouped by type (AdP, FDI, and across-muscle). The only significant regression was for within-FDI pairs (R^2 = 0.093, $p<0.001$).

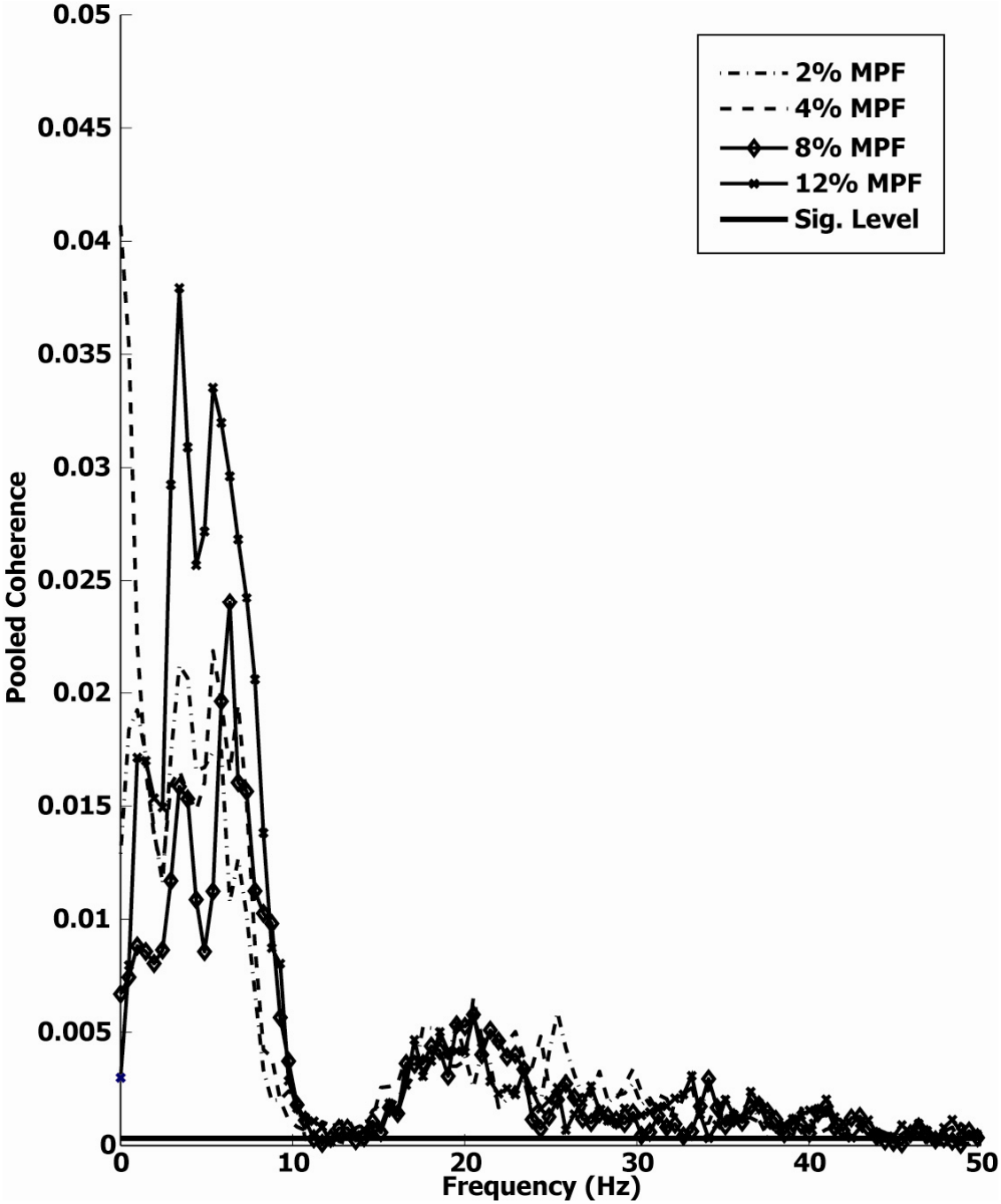

Figure 3-7. Pooled coherence for all trials at each force level. Coherence for different force levels shows little difference except in the 2-10 Hz bandwidth. For 12% MPF, coherence was significantly higher than that for 2, 4 and 8% MPF ($p<0.001$).

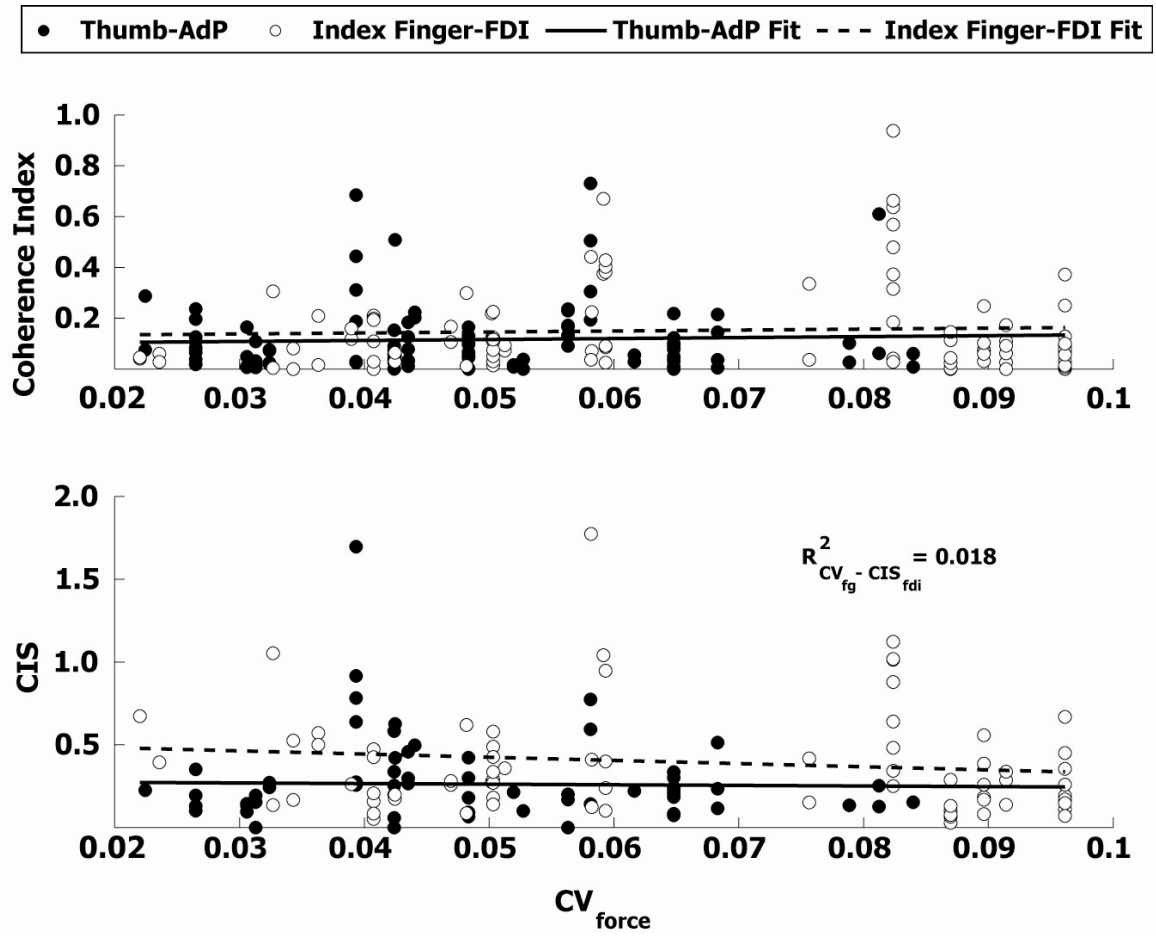

Figure 3-8. CIS and coherence indices plotted against force CV. AdP values are paired with thumb force CV and FDI indices are paired with index finger CVs. Regression for FDI pair CIS values were correlated to finger force CV ($p<0.001$). However, neither index for AdP pairs was significantly correlated to thumb force.

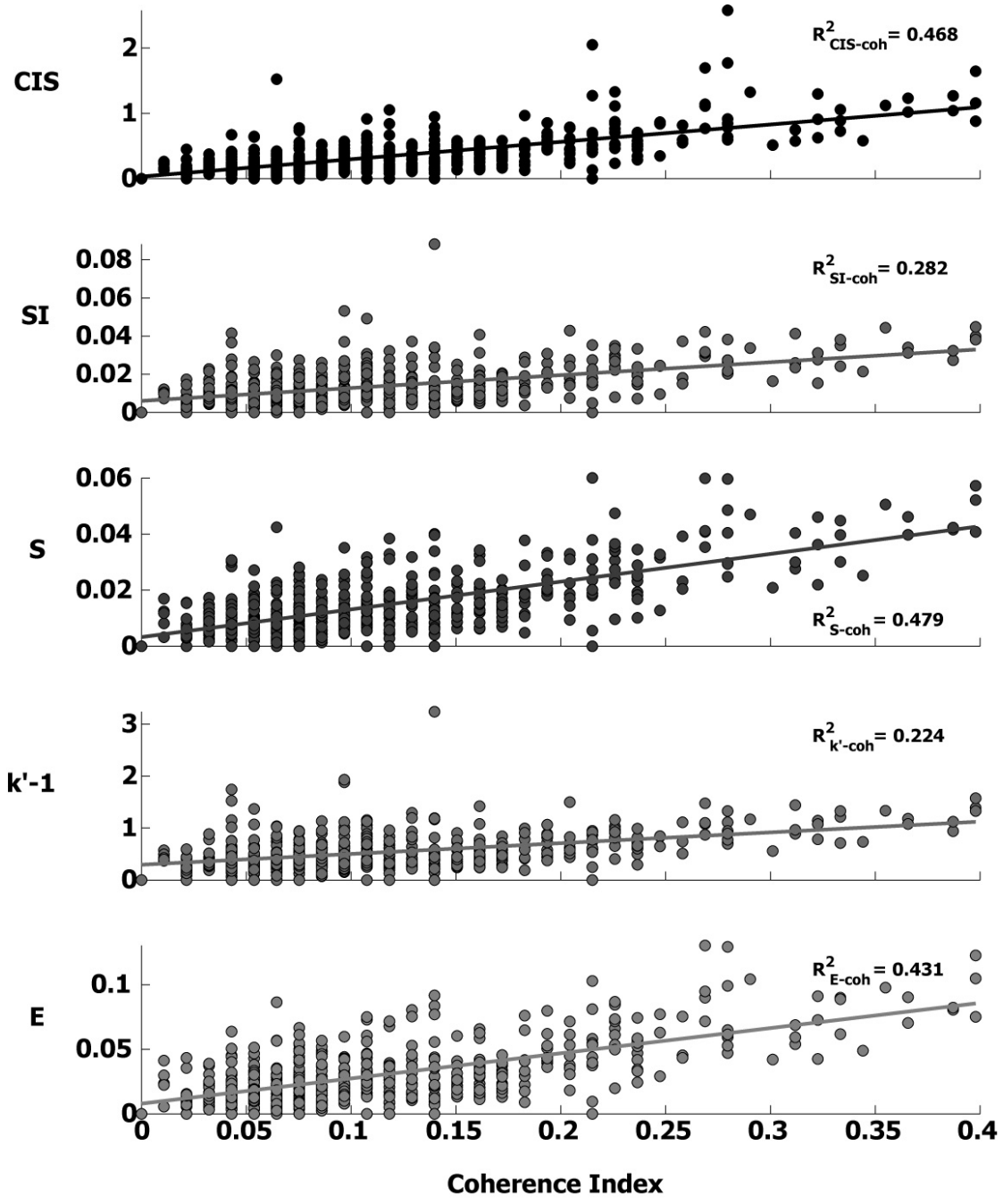

Figure 3-9. Correlation of coherence versus synchronization indices. Five different short-term synchrony indices were correlated to coherence indices for each pair. Indices CIS, S, and E were the most strongly correlated, but all correlations were significant ($p<0.001$).

Chapter 4: How spike train nonstationarity affects coherence detection

ABSTRACT

Motor unit spike trains can exhibit a high degree of variability in mean firing rate and its variance as time progresses, producing signal nonstationarity. Coherence and other power spectral measurements typically assume that data stationarity; therefore, the existence of nonstationarity could cause erroneous coherence measurements, which would lead to inaccurate analyses.

To determine if the effect of firing rate nonstationarity is significant, we produced a set of simulated spike train pairs that had firing rates and variances in the same range as those for physiological motor units active during a submaximal isometric pinching task. We also incorporated a nonstationarity factor that caused firing rates to vary up to the highest amount seen for the physiological motor units. Bootstrap approximations of the significance level were within 3% of the theoretical values and were invariant across all levels of synchrony and stationarity.

Three different stationarity indices based on firing rate and its standard deviation were used to quantify stationarity and were correlated to each other by a minimum r of 0.747. Linear regressions that used each of these indices as independent variables showed no significant correlation between the level of nonstationarity and the peak coherence value (max $R^2 = 0.082$) nor was there a systematic increase in correlation with increasing nonstationarity. Therefore, we have demonstrated that coherence measurements of spike train data with characteristics similar to those of the simulated trains will be robust in the presence of nonstationarities related to mean firing rate and its variance.

INTRODUCTION

Synchronized firing of motor units can be assessed in the frequency domain by measuring the coherence of two spike trains, which can reveal inputs common to both motor units. This information can then be used to assess the frequency, magnitude, and potential sources of a common input. However, there are some limitations to the effectiveness of coherence measurements. Spike train variability and, more significantly, common input variability can reduce coherence detection by over 50% as variances increase over a range of physiologically typical values. Variances in firing rate create irregular firing patterns that broadens the dispersion of signal power, making the detection of common inputs more difficult. Similarly, another limiter which must be considered when assessing spike train coherence is the assumption of signal stationarity, which expresses the signal stability throughout the data record.

Strictly speaking, a signal is stationary if all of its statistical properties are constant for the entire data record. More precisely, a random signal is said to be stationary if its probability distributions are invariant with time. A broader classification, commonly referred to as "weak stationarity", can be applied if the signal's mean, variance, and autocorrelation are stable over time. For most purposes, this less restrictive form of stationarity is sufficient to justify the use of common power spectral computations, such as coherence (Bendat and Piersol, 2000). Unfortunately, even an assumption of weak stationarity does not hold for most biosignals.

Although the effect of spike train nonstationarity on coherence has not been investigated, there have been a number of studies that have examined the presence, detection, and effects of nonstationary data on other types of signal analysis. Mananas et al. (2001) found EMG and vibromyography (VMG) recordings from respiratory muscles were nonstationary, but also found traditional power spectral measurements to be

effective in diagnosing respiratory diseases. In a study of optokinetic nystagmus, Shelhamer (1997) found significant changes in the correlation parameter used to track eye movement. The nonstationarity in heart rate recordings has also been evaluated as a potential indicator for cardiac anomalies (Srinivas and Yeragani, 2003). The effect of nonstationarity on power spectral measurements was analyzed by comparing results for stationarity segments of heart rate recordings to those for the entire recording (Weber et al., 1992). Significant differences in power were found for the two data sets, but the record length for the stationary segments were as short as 10% of the full record length, introducing inconsistencies driven by the higher variabilities and significance levels of the shorter records. These studies showed that biosignal nonstationarity is prevalent and that there is well-founded concern about its effect on spectral power measurements. The recordings they examined are similar to spike trains in that they are physiological patterns that can be represented by a point process with mean rates and variances that drift with time, which improves the likelihood that these findings apply to spike train data as well.

Like cardiac and respiratory data, signal nonstationarity is a prominent characteristic that could affect the study of motor unit activity and synchronization. For example, during maximal contractions, motor unit firing rates drop rapidly after the first few seconds (Marsden et al., 1983) and firing variability has been shown to vary during fatiguing contractions (Enoka et al., 1989; Jensen et al., 2000; Johnson et al., 2004). Also, many studies have demonstrated the rate-coding property of motor units since it was first discovered (Adrian and Bronk, 1929), where firing rates increase with force before reaching a plateau at full tetanus. Even in our study of submaximal isometric force production in Chapter 3, we showed that mean firing rates decreased 5-25% for a 2-minute trial, even though experimental conditions were static. Therefore, spike train stationarity is usually not a valid assumption. De Luca et al. (1979) stated that

nonstationarity of motor unit spike trains could result in an indication of nonexistent interdependence of interspike intervals (ISIs) that would create inaccurate assessment of train autocorrelations. Finally, Englehart and Parker (1994) extensively evaluated motor neuron firing statistics as they related to nonstationarity, but did not examine their effects on spectral analyses. However, the issue more critical to this study is whether or not the nonstationarity of spike train firing rates can affect spectral measurements such as coherence.

Our goal was to determine if spike train firing rate nonstationarity had a negative impact on coherence measurements for motor unit spike trains. We addressed this concern by producing a pool of simulated spike trains with nonstationarity that varied from nearly nonexistent to that severe enough to result in average drop of 25% in mean firing rate. By creating simulated spike trains that had firing rates and variabilities with stationarity levels that were similar to those of physiological units, the need to collect large amounts of motor unit data was eliminated. If coherence of this pool of spike train pairs was affected by increasing nonstationarity, we intended to establish a threshold level of stationarity that would still allow for reliable coherence measurements.

MATERIALS AND METHODS

Experimental Set Up

Nine people (five male) between the ages of 18 and 45 participated in this study. All participants were free of neuromuscular disorder and did not have a prior history of extensive hand-use/training. They were fully informed of the experimental procedures during an orientation session prior to the experiment and before signing a consent form. All experimental procedures were performed at the Neuromuscular Physiology Laboratory and were approved by the Institutional Review Board at The University of Texas at Austin.

The details of the experimental set-up were addressed in Chapter 3, but are summarized here. Participants were seated with their left forearm, wrist, and hand stabilized in a splint to prevent postural changes during the experiment. The hand was secured in the supinated (palm-down) position and the thumb and index finger were placed against opposite sides of a cantilevered force transducer that measured independent force from each digit. An additional restraint immobilized the 3rd through 5th digits to prevent ancillary hand movement. To keep the applied forces scaled among subjects, we used forces expressed as a percentage of maximal pinching force (MPF). To measure the MPF, subjects pinched maximally for three seconds three times in succession with five-second rest intervals. When the maximal forces showed consistency (± 5%) for three consecutive pinches, the average of the two highest forces for each digit was established as the MPF for that digit.

Following MPF measurements, each subject was given time to become familiar with the set-up by practicing ramp-hold-ramp (±0.67% MPF/sec ramp speed) contractions at 2, 4, 8, and 12% MPF for 60-second periods with progressively longer rest periods (15, 15, 30, and 60 seconds, respectively) at higher forces to prevent fatigue. The practice protocol consisted of a series of two pinches at each force in increasing succession. After practicing, the dorsal surface of the hand was cleaned before inserting two monopolar needle electrodes (25 mm long, 0.010” dia., FHC) into the AdP and two electrodes into the FDI. A surface ground electrode was placed at abraded regions over the ulnar styloid process of the wrist and a reference was placed at the proximal FDI tendon. Another monitor, not visible to the subject, was used by the experimenter to assess EMG and force recordings.

To begin the experiment, subjects increased each digit force as practiced. The only task difference was the 2-minute hold period with proportionally longer rest periods.

At least two ramps were performed at each force level with rest periods of 30, 30, 60 and 90 seconds for the 2, 4, 8, and 12% MPF levels, respectively. The experiment was concluded once acceptable data had been collected for at least two trials (trial: ramp up-hold-ramp down) at each force level.

Data Collection and Analysis

A PC (Pentium IV with Windows XP OS) with dual monitors was used to provide real-time displays of target and actual forces and EMG recordings for each electrode. All EMG records were analyzed offline using Spike2 for Windows (version 5) software package (CED). The signals from the force transducers were amplified at a gain of 500 and digitized at a sampling rate of 1000 Hz (Micro 1401 Mk II ADC, Cambridge Electronic Design (CED)). Intramuscular EMG recordings were digitized at a rate of 25 kHz and high-pass filtered at 13 Hz (Micro 1401 Mk II ADC, CED). Each EMG recording was examined for spurious noise by examining the PSD of the signal and low-pass filtering below the frequency of the lowest noise source, without removing signal content. After removing high-frequency noise, the signal was then linearly detrended to remove signal drift.

All computer code for spike simulation, coherence calculations, and statistical analyses were written in Matlab® version 7.1 with the Signal Processing and Statistics toolboxes. Computations were performed on a PC with a Pentium® D 3.0 GHz processor and Windows® XP OS.

Spike Identification

Individual motor unit potentials for each electrode were identified off-line with waveform discrimination system. The software performed the initial tracking of this motor unit using a "template matching" algorithm, where a template was built from a small group of spikes belonging to the same motor unit and then matched to all spikes in

the EMG data. After automated processing, spikes were manually scanned to ensure that spikes were not misclassified due to noise or superposition. For superpositioned spikes, the spikes were classified as a spike in each train, if the spikes in the superpositioned waveform could be clearly identified. Otherwise, those spikes were not included in the analysis. Once all identifiable spikes were classified, each spike was converted into an event (time) marker by recording the increasing threshold crossing time of the first voltage deflection. This process converted each action potential train into a set of event times needed for the coherence computation.

Spike Train Generation

Simulated spike trains were produced using the same model used in Chapter 2, with the additional feature of variable firing rates and coefficients of variation (CV) that covered the range of variabilities seen in experimental results of Chapter 3. Spike train length was set to 120 seconds, to match the duration of the physiological spike trains. To simplify this study, we also fixed several of the spike train parameters. The common input frequency used to synchronize the spikes was held at 30 Hz with a CV of 0.20. Also, the number of reference and response firing rates were cut in half and their CVs were limited to the range of 0.15 to 0.35. All spike train parameters are summarized in Table 4-1.

Spike trains were generated as membrane voltage repeatedly crossed a threshold value when independent and common voltage inputs were added at each time step. For non-synchronized motor units, membrane voltage (v) increased at each time step as a function of the current membrane voltage and the independent input voltage (x). The voltage input for each time step (Δt) represented the graded potential produced by a branched upper motor neuron and was found using equation (1), where μ is the mean voltage input at each time step.

$$x_t = \mu + \sigma * n_{rand}(t) \quad (1)$$

The input voltage variance (σ) was applied by adding the product of the overall variance and n_{rand}, which is a vector of normally distributed random numbers (zero mean, unity variance).

With known voltage inputs at all time steps established and the initial membrane voltage ($v_0 = v_{t=0}$) assigned at a random value such that $0 \leq v_0 \leq v_{th}$, the threshold voltage (v_{th} = 1.0), membrane voltage was found by sequentially solving for v_{t+1} at each successive time step using equation (3).

$$v_{t+1} = \frac{\tau}{\Delta t + \tau} v_t + \frac{\Delta t}{\Delta t + \tau} x_{t+1} \quad (3)$$

The time constant *(τ)* controls the rate at which the membrane voltage dissipates during each time step *(Δt)*, creating an exponential charging curve, like that of a capacitor. The first term on the right-hand side of equation (2) represents the membrane voltage *(v_t)* retained during the current time step, while the second term is the contribution from the voltage input. For this study, a τ of 0.0125 produced stable results for a time step of 0.5 ms, which provided sufficient temporal resolution for spike times that would eventually be assigned to 1 ms intervals (1 kHz sampling rate).

With known voltage inputs at all time steps established by equation (1) and the initial membrane voltage *(v_0)* assigned at a random value such that $0 \leq v_0 \leq v_{th}$, the threshold voltage (1.0), membrane voltage was found by sequentially solving for v_{t+1} at each successive time step. Each time v_{t+1} exceeded v_{th}, a spike firing time was recorded and v_{t+1} was reset to $v_{t+1} - v_{th}$. The process continued until *t* was equal to the desired trial

duration *(d)*, creating a set of spike times, or spike train. We wrote a goal-seeking optimization code to find appropriate μ and σ values for the desired firing rates and coefficients of variation. Using the tolerances from Table 2-1, the optimization incrementally adjusted the values of μ and σ until the desired firing rate and CV were obtained.

To induce synchrony, we used a voltage input common to both motor units that represented the activity of a branched common input of a last-order synapse at the spinal cord level. The common input is represented as y_{t+1} in equation (1), where it is modeled as a periodic rectangular pulse train with a given pulse width and amplitude (A_p).

$$v_{t+1} = \frac{\tau}{\Delta t + \tau} v_t + \frac{\Delta t}{\Delta t + \tau}(x_{t+1} + y_{t+1}) \tag{3}$$

$$y_{t+1} = A_p k_p \tag{4}$$

If the pulse was active during the $t+1$ time step, $k_p = 1$ and a voltage of A_p was added to the independent input $(y_{t+1} = A_p)$. If the two motor units happen to be close to threshold when the input pulse was active, the additional input caused both membrane voltages to cross the threshold at or near the same time, producing a synchronous firing time for both motor units. Otherwise, $k_p = 0$ and the membrane voltage of each motor unit would increase as though no common input existed.

Synchrony level increased with larger pulse amplitude or width, but fixing one of these parameters simplified the model by reducing the degrees of freedom. In keeping with the original modeling work (Halliday, 1998), the pulse width was fixed at 2 ms to simplify the process and approximate the duration of an action potential. Once again, we used a goal-seeking algorithm that varied pulse amplitude to attain a desired level of

synchrony for each motor unit pair. Synchrony was quantified using the same index used in Chapter 2, SI_{comp}.

Our intent was to create spike train pairs with a fixed synchrony level and a broad range of nonstationarity, so we fixed only the synchrony level and allowed the mean firing rates and nonstationarity levels to vary. Still, mean firing rates were always well within 1 pps of the desired rate. We did not try to induce increased variability because the decrease in firing rate was accompanied by an increase in variability.

To induce nonstationarity in each spike strain, we applied a nonstationarity factor, F_{ns}, to the desired mean motor unit firing rate (fr_{targ}) using equations 2a and 2b to obtain the firing rate at the beginning (fr_{targ1}) and end (fr_{targ2}) of each simulated trial.

$$fr_{targ1} = fr_{targ}\left(1 + \frac{F_{ns}}{2}\right) \tag{2a}$$

$$fr_{targ2} = fr_{targ}\left(1 - \frac{F_{ns}}{2}\right) \tag{2b}$$

The relationship between μ, σ, and firing rate is exponential and varies with firing rate, so the change in firing rates was not easily predictable, so the factor was set to increasingly higher levels until mean firing rate change for that value (F_{ns}=0.5) resulted in a approximate firing rate decrease of 25%, which was the largest mean firing rate change seen in the motor units recorded for the study in Chapter 3. The range for F_{ns} was then subdivided into equal increments of 0.1 so that mean nonstationarity would vary from 0% (F_{ns} =0.0) to 25% (F_{ns}=0.5).

Once the starting and ending firing rates were calculated, a lookup table was used to find the corresponding μ and σ values for these rates and intermediate values of μ and

σ were found for every 0.025 pps increment. The trial duration of 120 seconds was divided into subsegments equal to the number of firing rate increments (plus one) and for each subsegment, a spike train was created. These subsegment spike trains were then concatenated to create a full spike train with variable firing rate. This process created spike trains with smoothly varying firing rates without using unique μ and σ values for each spike, which would have created instability and unnecessary computational effort in producing thousands of unique μ and σ values. Additionally, the inherent variability in the spike train would have made the effect of such efforts undetectable.

Stationarity Indices

Stationarity was quantified using three indices: StIn (Srivinas and Yeragani, 2002), StatAv (Pincus et al., 1993), and Δfr, which is simply the change in firing rate. StIn is a measure of how much the mean firing rate varies and is found by calculating the standard deviation of the ratios of mean firing rates of spike train subsegments and the overall mean firing rate (equation 4). Change in variance is tracked by StatAv, which is the mean of all subsegment ISI standard deviations divided by the overall standard deviation (equation 5). For stationary data, StIn would be 0 and StatAv would be 1. As stationarity increased, these two indices would be negatively correlated. For consistency, the subsegments for these calculations were always 2 seconds long and overlapped by 1 second (119 subsegments), to parallel the way in which coherence was calculated. The Δfr index was simply the difference between starting and ending firing rates divided by the starting firing rate. Each train's starting and ending firing rates were found for the first and last 50 spikes of the train, respectively.

$$StIn = std\left(\frac{mnfr_{sub}(1:n_{sub})}{mnfr_{train}}\right) \tag{4}$$

$$StatAv = mean\left(\frac{sd_{sub}(1 : n_{sub})}{sd_{train}} \right) \quad (5)$$

$$\Delta fr = \left(fr_{start} - fr_{stop} \right) / \ fr_{start} \quad (6)$$

Coherence Analysis

The details of coherence calculations were also described in Chapter 2. Based on the outcome of that study, 2048-element segments (1 kHz sampling rate) were overlapped by 50% and tapered using a Hann window to reduce spectral leakage and variance of the coherence estimate. Coherence calculations were performed on detrended spike trains using the mscohere function of Matlab with the appropriate variables for segment length, overlap, and taper. We also calculated coherence with no overlap or taper for a comparison of how these differences in data segmentation affected sensitivity to non-stationary data.

Stationarity could affect coherence measurements in two ways: altered coherence values or altered significance levels. The significance level typically used for coherence measurements is founded on the assumptions of a chi-squared distribution and stationary data. For coherence found with no taper or overlap, the significance level (Z) is found using equation (7).

$$Z = 1 - \alpha^{\frac{1}{L-1}} \quad (7)$$

L is the maximum number of non-overlapped segments of length T that can be created from the spike train of duration d. Theoretical coherence significance (Welch, 1967) is found using equation 8:

$$Z_{ovlp} = 1 - \alpha^{\frac{1}{wL^*-1}} \tag{8}$$

where L* is the number of overlapped segments, found using equation 9.

$$L^* = floor((L-1)/(1-ovlp)) + 1 \tag{9}$$

The variable ovlp is the percentage of segment overlap and w is a weighting factor that is dependent on the amount of overlap and taper type. For tapered segments with window W and nfft segment elements, w is found using equation (10).

$$w = \left\{ \frac{\left[\sum_{k=0}^{nfft-1} W(k) * W(k + (1-ovlp) * nfft) \right]}{\left[\sum_{k=0}^{nfft-1} W^2(k) \right]} \right\}^2 \tag{10}$$

for a Hann window,

$$W(k+1) = 0.5\left(1 - \cos\left(\frac{2\pi k}{nfft - 1}\right)\right) \tag{11}$$

for segment element k = 0,…, nfft-1, where nfft is the number of segment elements (T/Δt).

To ensure that changes in significant coherence were not the result of inaccurate significance levels, an alternative bootstrap sampling technique was used to produce a significance level that could be used to validate the theoretical level. For each spike train, each of the L non-overlapped segments was assigned a number based on order and then a new spike train was assembled by concatenating these segments as a bootstrap sampling picked the segment number randomly with replacement. This process was repeated 100 times for each train and the coherence was calculated for each repetition. The

significance level was then established as the value that exceeded 95% of the coherence values, allowing for a 5% error, to match the type 1 error (α) of the theoretical level.

Statistics

Multiple linear regressions were used to examine trends for coherence (dependent variable) versus the synchrony index values for each spike train (independent variables). Stated errors are the standard deviation (SD), whereas those shown in figures are the 95% confidence intervals. All findings were considered significant if the p-value fell below a value of 0.05 and all coherence significance levels were also established at the 5% type 1 error level.

RESULTS

Mean firing rates and firing rate CVs were found for multiple motor units during isometric force production at multiple levels (Chapter 3). Values were normalized to emphasize the amount each parameter decreased as time progressed (Figure 4-1). Firing rates slowly decreased with time at each force level, but the firing rate change increased as force increased, where mean firing rate dropped an average of 25% at the 12% MPF level. Trends for the change in firing rate CV were similar; with the largest decrease of ~30% occurring at the 12% MPF level, but the decrease with time was more erratic than those for the firing rate.

Stationarity

The nonstationarity factor was set to progressively higher values up to a maximum value of 0.5, which produced a mean firing rate drop of at least 25% at all synchronization levels. When firing rates are plotted versus trial time, the trends are similar to those seen for motor units from our earlier experiments (Figure 4-2). For the maximum nonstationarity factor of 0.5, the mean firing rate change from the beginning to

end of a trial was -22.8±13.1%, which encompassed the largest firing rate changes seen experimentally.

As the nonstationarity factor increased, the drop in firing rate and CV over the course of the 2-minute trial duration increased, demonstrating the effectiveness of the technique used to impose nonstationarity. For the nonstationarity factor of 0.5, the firing rate decreased an average of 26.1% and the mean firing rate CV dropped by 27.0%, which are values similar to the maximum changes seen in physiological motor units when isometric force was at 12% MPF.

To ensure that each stationarity index quantified nonstationarity consistently, we examined the correlation of each index to the other two. Table 4-2 shows the correlations of each index to the other two. All of the indices were strongly correlated with all p-values <0.001. The correlation for StIn to the other indices was negative as it increased with reduced stationarity, whereas the other two indices decreased as stationarity weakened. All three indices were strongly correlated to the nonstationarity factor, but the Δfr index had the strongest correlation (Figure 4-3).

Coherence Significance Levels

For the coherence calculated without overlap or taper, the theoretical significance level was 0.0512. The corresponding bootstrap value was 0.0520 (±7.31 E-6) across all stationarity and synchrony levels. The theoretical significance level for the tapered and overlapped coherence was 0.0271, which was also closely approximated by the bootstrap level of 0.0278 (±8.99 E-6) for all levels of synchrony and stationarity. Because the bootstrap and theoretical levels matched well (< 2.6%) and the bootstrap levels remained relatively unchanged as nonstationarity was increased, we used the theoretical significance levels for the comparisons that follow.

Coherence and Stationarity Correlations

After subtracting the significance level for all coherence values, multiple linear regressions between the peak coherence found near 30 Hz (common input frequency) and each of the stationarity indices for both spike trains showed that there was little contribution to the coherence variance produced by the change in stationarity (Table 4-3). For the StatAv index, only one R^2 value was significant at a moderate synchrony level and only for coherence calculated using segment overlap and taper. Most of the R^2 values for the Δfr and StIn regressions were significant; however, none of the R^2 values exceeded 0.10 for any level of synchronization, for any of the indices, or for either of the coherence calculation methods.

To avoid the use of 3-D plots, the peak coherence for each coherence calculation technique and select synchronization levels were plotted against average of the Δfr values for each spike train of each pair (Figure 4-4). These scatter plots show no visible trend of coherence increase or decrease as the nonstationarity of the spike trains increases. Regressions of coherence for physiological motor unit pairs was also not significantly correlated to any stationarity index and had no visible trend when plotted against the mean Δfr (Figure 4-5).

DISCUSSION

This study demonstrates that coherence measurements are consistent across a wide range of nonstationarity for simulated spike train pairs with synchronization, firing rates, and variabilities that are representative of those for real motor units, regardless of the technique used for calculating coherence or the level of synchronization. It also showed that peak coherence was not correlated to stationarity for physiological motor unit pairs. This finding is important for establishing the reliability of coherence measurements for a variety of experiments that record motor unit activity for a broad

range of forces and for different types of tasks. Had this investigation exposed a sensitivity of coherence to nonstationarity, previous experiments that assessed synchronization using coherence would need re-evaluation after measuring the level of nonstationarity and adjusting for its effects on coherence.

The method of measuring stationarity by tracking the mean square value (variance plus square of mean) was established by Bendat and Piersol (2000), and has been shown to be effective in identifying nonstationarity in studies of EMG and vibromyography (Mananas et al., 2001), cardiovascular activity (Pinna et al., 1996), and intracranial pressure (Aboy et al., 2005). More complex tests, such as the autoregressive techniques used by Pinna et al (1996) and Weber et al. (1992) have produced results that are only marginally better. Also, in the case of the Pinna study, comparisons of stationary and nonstationary data involved records of unequal length (up to a factor of 9x), that produce different variances, which in turn produce varying confidence intervals critical to this type of analysis. Thonet et al. (1997) also used a time-varying autoregression procedure to quantify nonstationarity in both physiological and simulated heart rate signals, but did not demonstrate that this method was superior to the much simpler method presented here.

The three indices used to measure spike train stationarity were closely correlated, indicating that none of them would likely be superior in quantifying stationarity. However, the Δfr index was the most sensitive and was the easiest to interpret in a physical sense. The other two indices, StIn, and StatAv, provided the ability to discern whether a coherence change was correlated more strongly to firing rate instability or to firing rate variability. However, the close correlation of these indices and the similarity in the trends for changes in firing rate and its variability probably would have precluded making this distinction, had a significant effect been present.

Bootstrap calculations of the 5% coherence noise level produced a significance level that closely matched the theoretical values for coherence calculation technique and were essentially invariant across all stationarity and synchrony levels. The insensitivity of the significance level to stationarity was a critical finding, because it supported the use of the theoretical significance levels in all previous studies that measured spike train coherence. This finding may also have provided a quick test for acceptable nonstationarity. Should the bootstrap significance level be affected by nonstationarity levels that exceed those studied here, then there would be reason to suspect the reliability of coherence measurements for those spike train pairs.

Similar to the significance levels, peak coherence was insensitive to increased nonstationarity, regardless of which index was used to measure nonstationarity. Multiple regressions produced R^2 values for all synchrony levels that were all less than 0.10 and, for the StatAv index, mostly insignificant. Because the other two indices were based on mean firing frequency and stationarity was driven by changing the firing rate decrease, it was understandable that these indices would be more correlated to coherence. However, the correlations were still very weak. Srinivas and Yerigani (2003) found that the StIn was correlated to the mean signal level and corrected for the mean. Unfortunately, they did not specify how that correction was accomplished. Still, there was no systematic increase of R^2 with increasing stationarity, so there was no reason to believe that the threshold level of stationarity existed for this type of experiment.

Data records that are much shorter or that exhibit greater fluctuations may require analysis by nonlinear methods investigated for analysis of other types of nonstationary signals. Several attempts to find better methods for analyzing nonstationary data have produced mixed results. White et al. (1990) created a time-frequency coherence method to study signals with finite energy components, but found the results to be similar to those

found for Fourier-based coherence. They used time–frequency and time-scale methods to identify transient phenomena in neonatal cardiorespiratory records found that wavelet transform and several time-frequency methods were more effective than short-term Fourier transforms in providing enough time and frequency resolution to identify events in short data records (<30 seconds). Additionally, chaotic analysis (Salisbury and Sun, 2004) of EKG data and EEG/MEG wavelet transform analysis (Makinen et al., 2005) have also been effective in revealing oscillatory activity in transient data not detectable using linear power spectral techniques. But, for most motor unit studies, the traditional FFT-based spectral analysis methods should be equally effective.

When the technique of modified periodograms was first introduced by Welch (1967), one of its purposes was to reduce the effect of nonstationarity on Fourier transforms of continuous signals. By dividing the signal into a series of small segments, finding transforms for each of those subsegments, and averaging the results, the stationarity assumption was closely approximated for the span of each subsegment (local stationarity) and thereby reduced variance of the transform. Because coherence is based on the transform of each spike train and their cross-correlation, this principle holds for that measurement as well. What this study shows is that even though a spike train is a point process, as opposed to a continuous signal, the stabilizing effect of this technique allows for reliable coherence measurements for a broad range of nonstationarity.

This investigation also demonstrated is that the negative correlation between common input variance and coherence incidence (detection rate) was not related to decreased stationarity, but to the ability of coherence to effectively detect a common input for signals as variabilities increase. On a broader scale, experiments that examine coherence of motor unit spike trains produced during steady, submaximal isometric forces will not be affected by the inherent nonstationarity of the spike train data.

Table 4-1. Summary of motor unit firing properties and synchrony parameters used to create simulated spike trains.

Parameter	**Range**	**Increment**	**Tolerance**
Firing Rate (pps)	Reference: 11, 15, 19 Response: 9, 14, 18	1.0	0.05
Firing Rate Variance (CV)	0.15 – 0.35	0.05	0.005
Common Input Frequency (Hz)	30	-	-
Cmn. Input Freq. Variance (CV)	0.20	-	0.005
Trial Length (seconds)	120	120	-
Nonstationarity factor	0.0-0.5	0.1	-
Synchrony (SI_{comp})	1.05 – 1.50	0.05	0.01

Table 4-2. Correlations of stationarity indices across all synchronization levels

	StatAv	**StIn**	**Δfr**
StatAv	-	-0.762	0.747
StIn	-0.762	-	-0.862
Δfr	0.747	-0.862	-

Table 4-3. R^2 values for linear regression fits of peak coherence at 30 Hz to stationarity indices for coherence. Coherence computations with and without segment taper and overlap are shown. Significant values are denoted by an asterisk (*).

	No Taper/Overlap			**Hann Taper/50% Overlap**		
SI_{comp}	**$R^2_{coh\text{-}\Delta fr}$**	**$R^2_{coh\text{-}StIn}$**	**$R^2_{coh\text{-}StatAv}$**	**$R^2_{coh\text{-}\Delta fr}$**	**$R^2_{coh\text{-}StIn}$**	**$R^2_{coh\text{-}StatAv}$**
1.05	0.003	0.010	0.008	0.001	0.000	0.001
1.10	0.005	0.006	0.008	0.006	0.001	0.018
1.15	0.014	0.026*	0.007	0.038*	0.027*	0.010
1.20	0.026*	0.008	0.011	0.049*	0.034*	0.018
1.25	0.035*	0.022*	0.007	0.082*	0.045*	0.023
1.30	0.026*	0.041*	0.017	0.082*	0.081*	0.035*
1.35	0.017	0.013	0.005	0.053*	0.027*	0.012
1.40	0.049*	0.013	0.014	0.065*	0.019	0.011
1.45	0.053*	0.028*	0.010	0.064*	0.041*	0.010
1.50	0.044*	0.029*	0.007	0.061*	0.052*	0.017

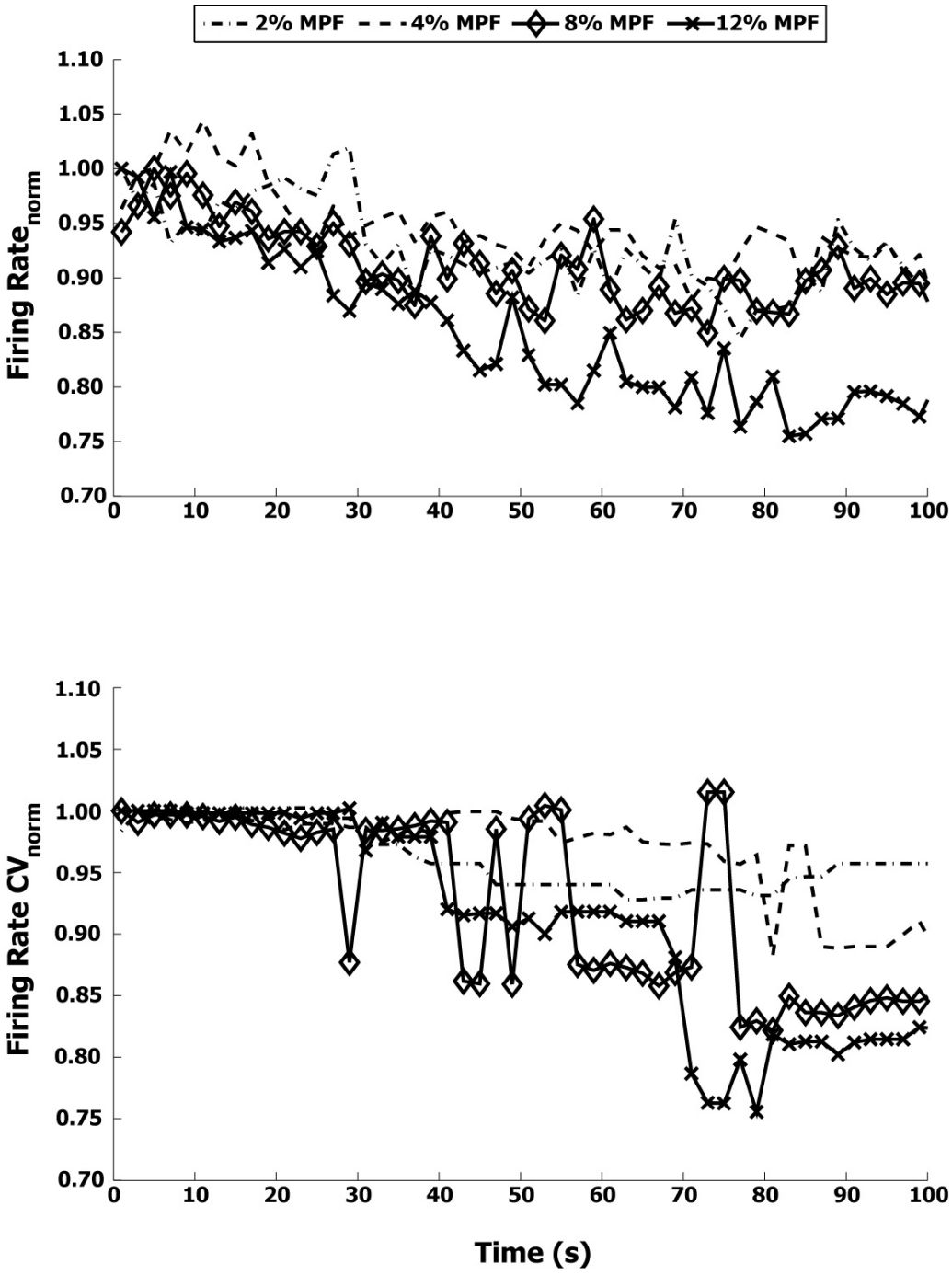

Figure 4-1. Normalized firing rate and firing rate CVs for physiological motor units from the AdP and FDI muscles during a 2-minute isometric pinch. Motor units are grouped according to force and exhibit larger decreases as force increases and time progresses.

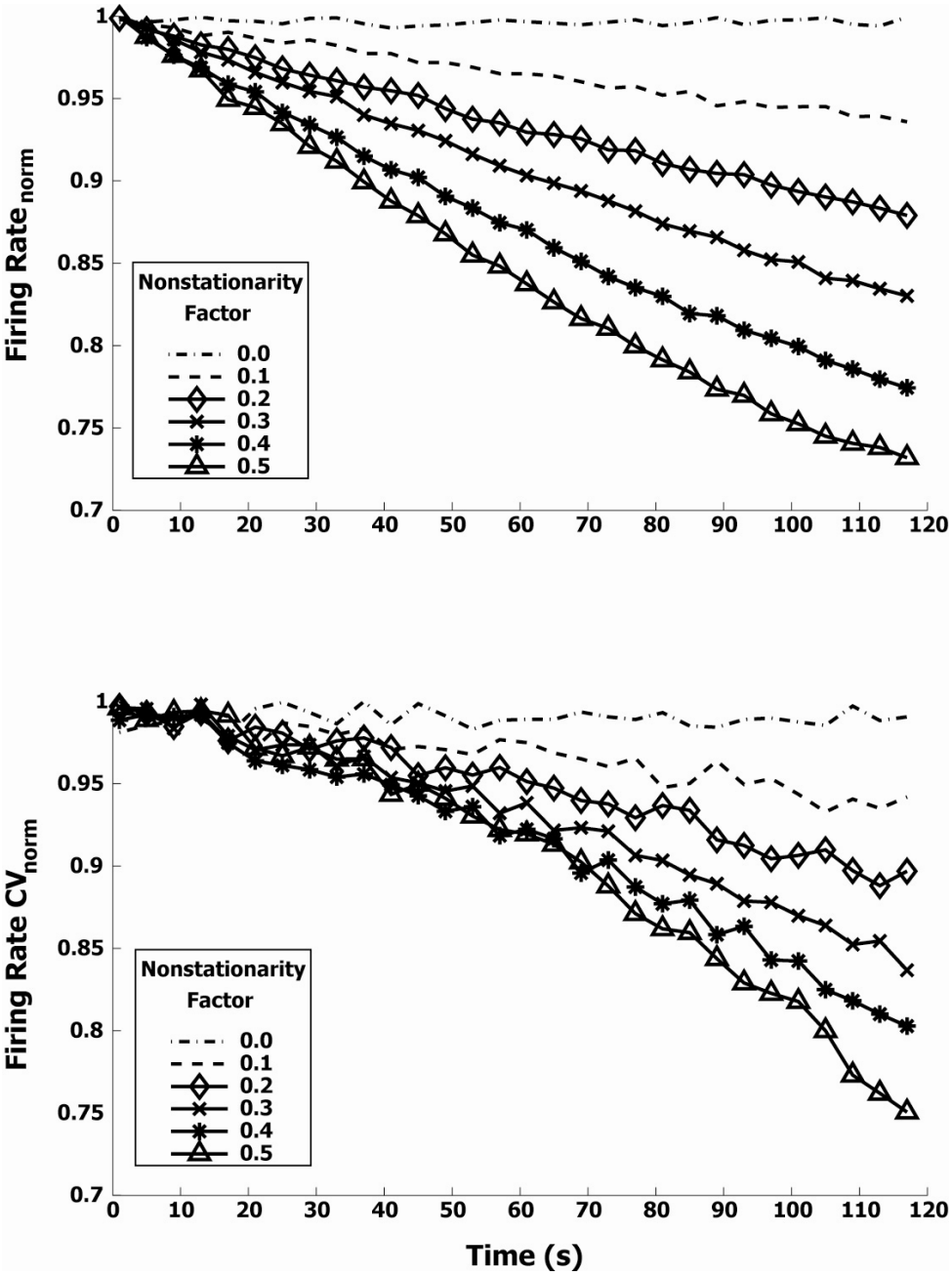

Figure 4-2. Mean normalized simulated motor unit firing rates and firing rate CVs as trial duration progresses. As nonstationarity factor increases, signal stationarity is reduced. At highest nonstationarity factor, reductions in firing rate and its CV approximate the maxima for physiological motor units (Figure 4-1).

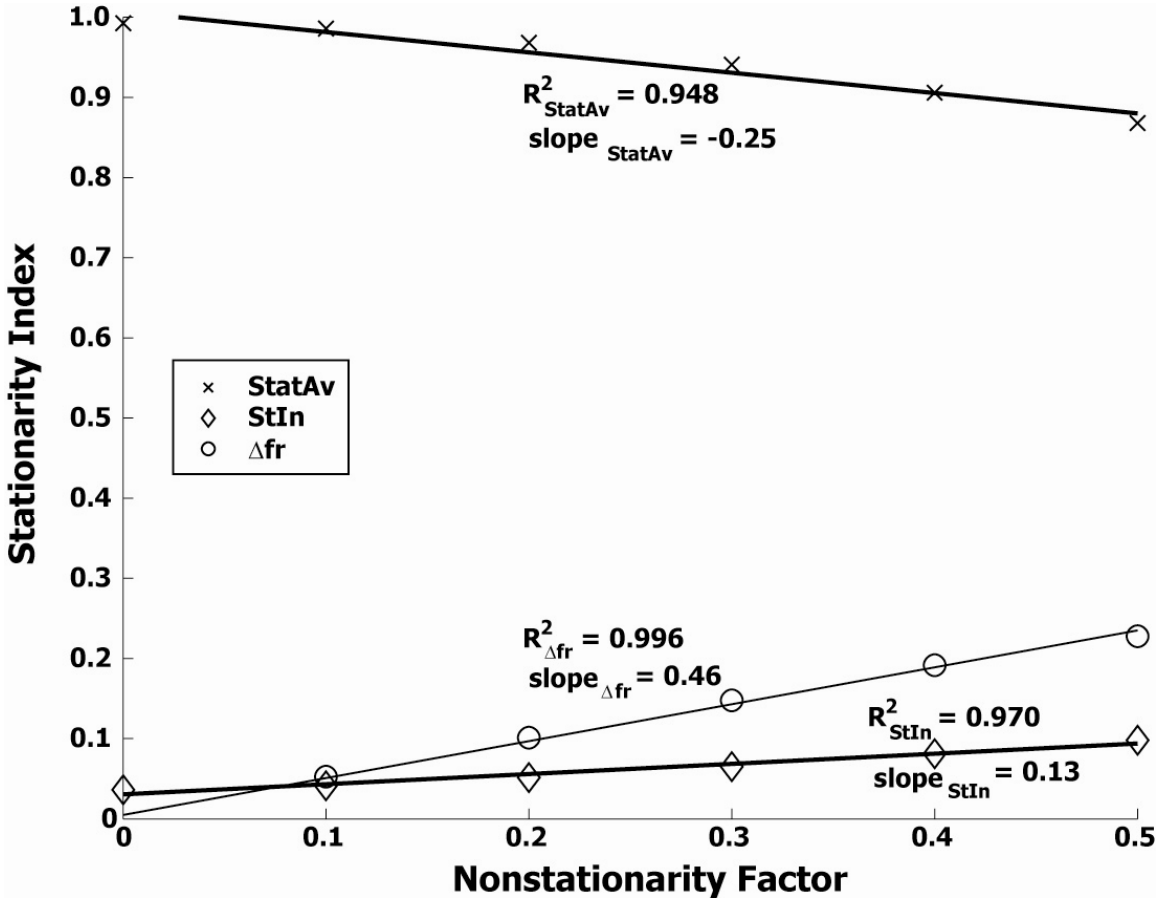

Figure 4-3. Comparison of stationarity indices as nonstationarity factor is increased. Correlation was very strong for all three indices, but largest for the Δfr index. All R^2 values have a p-value of < 0.001.

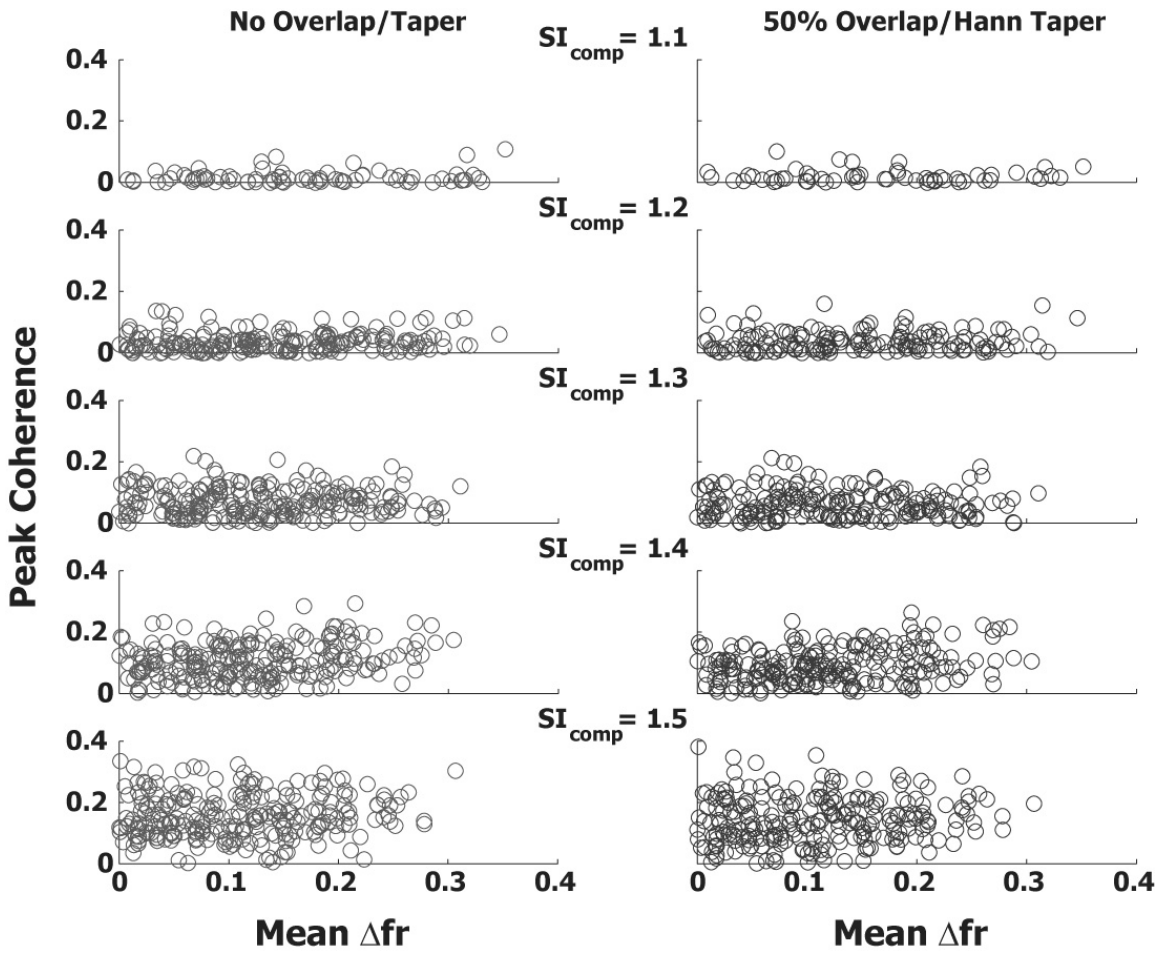

Figure 4-4. Peak coherence values plotted versus mean firing rate changes reveal no significant correlation at any synchronization level. Coherence calculated without segment overlap or taper are shown on the left, whereas coherence found with a 50% overlap and Hann taper are shown on the right. SI_{comp} varies from 1.1 to 1.5, representing very weak to very strong synchronization levels.

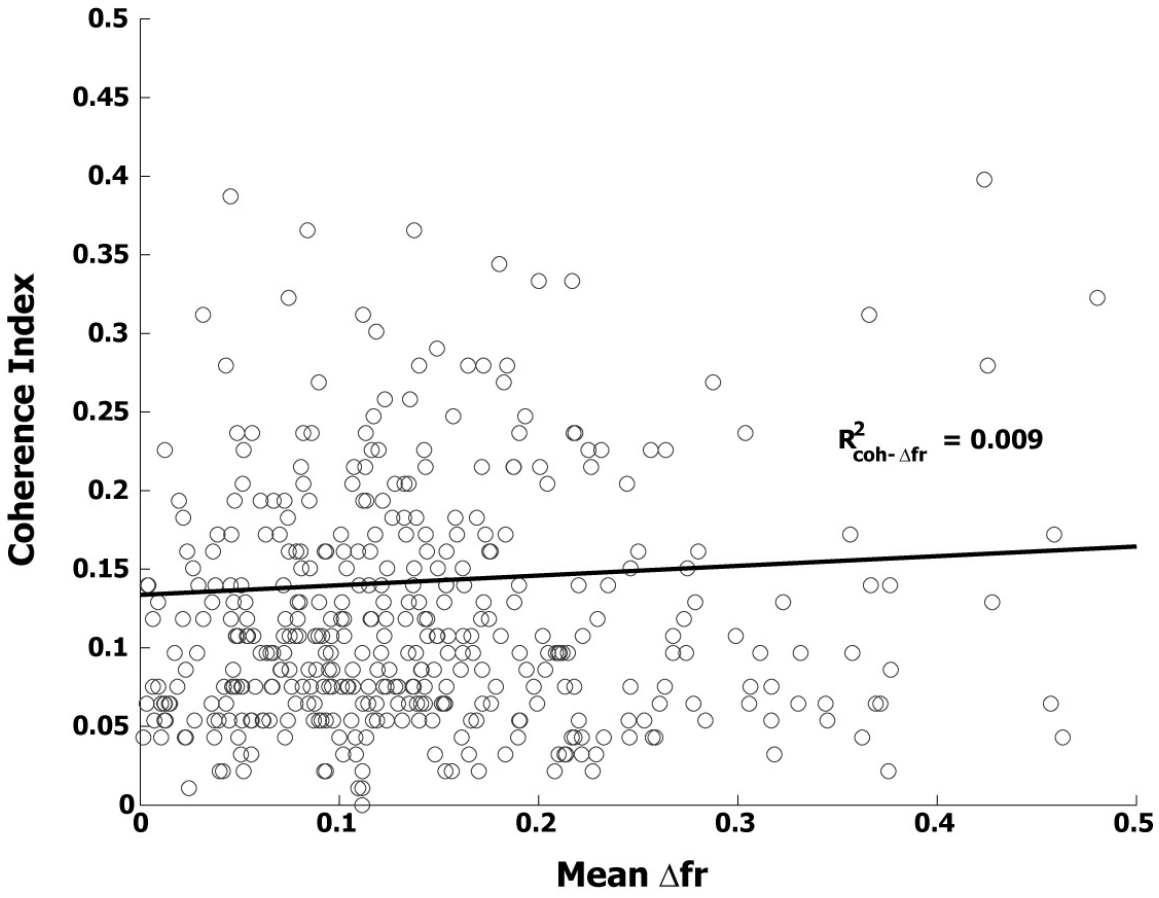

Figure 4-5. Peak coherence of physiological motor unit pairs from isometric pinch task experiment show no correlation to stationarity based on firing rate change during a trial.

Chapter 5: Summary

The relationship between force steadiness and motor unit synchronization has been investigated according to the specific aims outlined in Chapter 1. To identify which findings are associated with each aim, the study results are addressed accordingly.

SPECIFIC AIM #1

Develop a computational model to establish the best technique for computing coherence by using simulated motor unit firing events (spike trains) with varying firing frequency, common input frequency, noise (variability), and common input strength to find the method that produces the highest significant coherence value for a pool of synchronized motor unit pairs.

- Coherence incidence was significantly higher for tapered and overlapped segments, regardless of taper type.
- Coherence values decreased significantly as trial durations were shortened, especially for trial durations of 30 seconds.
- Increasing variability in the common input frequency decreased the coherence detection to levels that would make it undetectable even for high synchronization levels.
- Increasing variability in the firing rate decreased the coherence detection significantly, but not as dramatically as the variability of the common input frequency.

Using these findings, coherence was found using a 50% segment overlap and Hann taper. A minimum spike train overlap of 60 seconds was also established for coherence

measurements to improve the likelihood that coherence would be detected, if present. The last finding was particularly important for analysis considerations, because it demonstrated the sensitivity of coherence to common input frequency variability, which demonstrated that a strong common input with large frequency variance could go undetected by coherence measurement.

SPECIFIC AIM #2

Establish whether there exists a significant correlation between synchronization of adductor pollicis (AdP) and first dorsal interosseous (FDI) motor units and force steadiness during a steady submaximal pinch.

- A strong relationship between motor unit synchrony and force steadiness was not found.
- Pooled coherence revealed coherence primarily in the 0-10 Hz bandwidth, with a much smaller peak in the 16-34 Hz band for the 4, 8, and 12% MPF forces.
- Force spectral power was restricted to the 0-2 Hz range, corresponding to the frequency of adjustments attributable to proprioceptive and visual feedback.
- Across-muscle synchrony was consistently lower than that for within-muscle synchrony.

Based on this study's findings, motor unit synchrony and force steadiness during an isometric task are unrelated, regardless of how synchronization is measured. Motor unit coherence was predominantly in a bandwidth not associated with cortical activity during task performance (13-30 Hz), indicating that it was produced at subcortical or spinal levels. Force power in the 0-2 Hz range is consistent with that seen for proprioceptive and

visual responses. In spite of the multidigit nature of the performed task, there was no indication that coherence was involved in force coordination.

SPECIFIC AIM #3

Validate and refine the computational model using actual motor unit data including mean firing rate, firing rate variability, and synchronization levels.

- Data nonstationarity for physiological motor units is easily detectable as changes in mean firing rate and firing rate CV.
- Data nonstationarity increased with isometric force over a two-minute trial.
- Coherence was found to be insensitive to nonstationarity of the magnitude seen in the experimental data.

The work done to investigate this particular aim was modified somewhat because the range of parameters used for the simulation in Chapter 1 already encompassed those found in physiological motor units studied in Chapter 2. Instead of refining spike train parameters, the more pressing issue of nonstationarity was addressed. Coherence measurements are based on the premise of signal stationarity, i.e., stable mean, variance, and distribution, so it was critical to know if the amount of nonstationarity found in experimental spike trains would significantly affect coherence measurements. The coherence measurements proved to be insensitive to nonstationarity, most likely due the periodogram technique that establishes local stationarity for a group of short data segments. Although this technique had been originally developed for continuous signals, it appears to be just as effective for point process signals, such as spike train firing times.

DISCUSSION

This study established that coherence is best calculated using segment taper and overlap and is insensitive to data nonstationarity at the levels seen in motor unit experiments. Force unsteadiness did increase as force was reduced and significant motor unit coherence and short-term synchronization was found for the motor unit pairs in both hand muscles. However, we found no strong correlation between force steadiness and motor unit synchronization for a submaximal isometric pinch.

As discussed previously, it is likely that the force unsteadiness seen in these experiments is attributable to a decrease in twitch force tetanus as force is decreased. However, there remain many questions about the possible source of other types of force unsteadiness and their sources. Modeling and experimental results have shown that motor unit synchrony has some influence on force steadiness, but that correlation may only exist for certain conditions. For instance, there are the studies that found increased coherence for older adults (Semmler et al., 2003) and for force instruments with higher compliance (Kilner et al., 2002; Halliday, 1998). Additionally, Taylor et al., (2003) found that the connection between force fluctuation and motor unit synchronization was only detectable for simulated anisometric contractions.

Therefore, the logical next step for these experiments would be to repeat this experiment for a group of older adults or with a more compliant force measurement device. Older adults may have force unsteadiness that is driven by additional mechanisms that are correlated to motor unit coherence. A more compliant device will allow for the generation of additional unsteadiness by neurogenic and mechanical tremor, for which correlations to coherence have already been reported in single-digit experiments (Kilner et al., 2002).

However, before continuing to conduct studies regarding motor unit synchronization and, in particular, coherence measurements, there are several issues that need to be more carefully assessed. The findings of Chapter 1 raise issues with the practical use of coherence for motor unit studies, because its ability to detect branched common inputs is greatly diminished by trial length and input variability. Additionally, the use of a temporal index as an independent variable for measuring synchronization demonstrates that temporal measures will typically be far more sensitive than coherence. The advantages of temporal synchrony measurements over spectral measurements are that they are measured directly instead of estimated and that they are not reliant upon a constant input frequency. For instance, even if the common input frequency of the leaky integrator model changes, the synchronized spikes will still fire within a few milliseconds of each other. Therefore, cross-correlations will still produce the same lag time, but the common input frequency may change so much that its presence fails to produce a significant coherence measurement, due to the distribution of signal power over a broader bandwidth, instead of being isolated to a specific frequency. One final consideration with regard to coherence is the possibility that synchronization may not always be driven by a common source, negating the need for coherence measurements altogether.

This last point leads to broader, and possibly more important, questions that need to be more thoroughly addressed: Why does motor unit synchrony exist? Is it always driven by an periodic source or can it develop "spontaneously"? Is it a mechanism that conserves energy, a metabolic by-product, a higher form of communication, or simply a design idiosyncrasy? If it is a mechanism that conserves energy or a metabolic by-product, it should become more predominant as fatigue develops. On the other hand, if it is a higher form of communication, it should be more prevalent at task initiation and for

more complex tasks, just as the event-related desychronization (ERD) events seen in EEG seen at task initiation (Pfurtscheller, 1977).

Then again, neuromuscular synapses are far from precise in structure and the incidence of synchronization may be related to the arrangement, size, and biochemical reaction rates of muscle motor units. The repeated release of calcium and, subsequently, acetylcholine initiated by action potentials produced at a given firing rate could influence the firing of nearby motor units such that larger motor units or a group of motor units with similar firing rates may draw other motor unit firing rates into synchrony. With the advances in readily available computational power, the modeling of biological oscillators like the muscle motor unit has generated increasing interest. One of the first models, developed by Yoshiki Kuramoto, could produce "spontaneous" synchrony by simply allowing a group of linked oscillators with similar characteristics to fire on their own with their only common influence being their linkage to each other. Invariably, these oscillators would eventually oscillate in synchrony. The fact that motor units and cortical cells are physiologically linked and behave similarly suggests that they may also develop synchronized firing patterns spontaneously with no obvious purpose. It may be worthwhile to pursue more complex neuromuscular models to investigate this theoretical phenomenon.

It is also possible that coherence is a mechanism used to increase force economically. Keeping the model in mind, consider that for two motor units firing at a given rate, the addition of common input will cause both motor units to fire more frequently, because the input will serve to bring the membrane voltages to threshold more quickly. Therefore, by activating the common input, the body can produce higher forces with multiple motor units by increasing their firing rates without expending more energy to fire the individual motor units independently. This possibility may explain the

significant increase in coherence seen for the increase in force from 8% to 12% MPF for motor unit pairs in both muscles.

This study showed that even with the use of the most reliable coherence measurement technique, that motor unit coherence was not correlated to force steadiness, nor was motor unit synchronization measured in the temporal domain. It also showed that coherence measurements are insensitive to spike train nonstationarity, but that they are also less sensitive to synchronization than the time-domain short-term synchronization measurements. These findings should prove useful to improving the reliability and assessment of future motor unit synchronization studies and have provided additional experimental data for understanding of the nature of force steadiness and motor unit synchronization and the progression towards a better overall understanding of neuromuscular physiology.

References

Aboy M, Marquez OW, McNames J, Hornero R, Trong T, and Goldstein B. Adaptive modeling and spectral estimation of nonstationary biomedical signals based on Kalman filtering. IEEE Trans Biomed Eng 52:1485-1489, 2005.

Adrian ED and Bronk DW. The discharge of impulses in motor nerve fibres: Part II. The frequency of discharge in reflex and voluntary contractions. J Physiol 67:i3-151, 1929.

Allum JH, Dietz V, and Freund HJ. Neuronal mechanisms underlying physiological tremor. J Neurophysiol.,41:557–571, 1978.

Allum JH and Hulliger M. Presumed reflex responses of human first dorsal interosseus muscle to naturally occurring twitch contractions of physiological tremor. Neurosci Lett 28(3):309-14, 1982.

Amjad AM, Halliday DM, Rosenberg JR, and Conway BA. An extended difference of coherence test for comparing and combining several independent coherence estimates: theory and application to the study of motor units and physiological tremor. J Neurosci Methods 73:69-79, 1997.

Bendat JS and Peirsol AG. Random data-analysis and measurement procedures. John Wiley & Sons, Inc., New York, 2000.

Bremner FD, Baker JR, and Stephens JA. Effect of task on the degree of synchronization of intrinsic hand muscle motor units in man. J Neurophysiol 66:2072-2083, 1991a.

Bremner FD, Baker JR, and Stephens JA. Variation in the degree of synchronization exhibited by motor units lying in different finger muscles in man. J Physiol 432:381-399, 1991b.

Brillinger DR. Comparative aspects of the study of ordinary time series and point processes. In Developments in Statistics, Vol. 5 (ed. P. R. Krlshnaiah), pp. 33-133. Academic Press, New York, 1978.

Christakos CN, Papadimitriou NA, and Erimaki S. Parallel neuronal mechanisms underlying physiological force tremor in steady muscle contractions of humans. J Neurophysiol Vol. 95 (1):53-66, 2006.

Conway BA, Halliday DM, Farmer SF, Shahani U, Maas P, Weir AI, and Rosenberg JR. Synchronization between motor cortex and spinal motoneuronal pool during the performance of a maintained motor task in man. J Physiol 489 (Pt 3):917-924, 1995.

Cresswell AG and Loscher WN. Significance of peripheral afferent input to the alpha-motoneurone pool for enhancement of tremor during an isometric fatiguing contraction. Eur J Appl Physiol 82:129-136, 2000.

Datta AK and Stephens JA. Synchronization of motor unit activity during voluntary contraction in man. J Physiol 422:397-419, 1990.

DeLuca CJ. Physiology and mathematics of myoelectric signals. IEEE Trans Biomed Eng 26(6):313-325, 1979.

Dietz V, Hillesheimer W, and Freund HJ. Correlation between tremor, voluntary contraction, and firing pattern of motor units in Parkinson's disease. J Neurol Neurosurg Psychiatry 37:927-937, 1974.

Elble RJ and Randall JE. Motor-unit activity responsible for 8- to 12-Hz component of human physiological finger tremor. J Neurophysiol. 39 (2):370-83, 1976

Ellaway PH. Cumulative sum technique and its application to the analysis of peristimulus time histograms. Electroencephalogr. Clin. Neurophysiol. 45:302-304, 1978.

Ellaway PH and Murthy KS. The origins and characteristics of cross-correlated activity between gamma-motoneurones in the cat. Q J Exp Physiol 70:219-232, 1985.

Englehart KB and Parker PA. Single motor unit myoelectric signal analysis with nonstationary data. IEEE Trans Biomed Eng 41(2):168-180, 1994.

Enoka RM, Robinson GA, and Kossev AR. Task and fatigue effects on low-threshold motor units in human hand muscle. J Neurophysiol 62:1344-1359, 1989.

Enoka RM, Christou EA, Hunter SK, Kornatz KW, Semmler JG, Taylor AM, and Tracy BL. Mechanisms that contribute to differences in motor performance between young and old adults. J Electromyogr Kinesiol 13:1-12, 2003.

Farmer SF, Bremner FD, Halliday DM, Rosenberg JR, and Stephens JA. The frequency content of common synaptic inputs to motoneurones studied during voluntary isometric contraction in man. Journal of Physiology, 470, 125-155, 1993.

Freund HJ, Budingen HJ, and Dietz V. Activity of single motor units from human forearm muscles during voluntary isometric contractions. J Neurophysiol 38:933-946, 1975.

Galganski ME, Fuglevand AJ, and Enoka RM. Reduced control of motor output in a human hand muscle of elderly subjects during submaximal contractions. J. Neurophysiol. 69:2108-2115, 1993.

Halliday DM, Conway BA, Farmer SF, and Rosenberg JR; Using electroencephalography to study functional coupling between cortical activity and

electromyograms during voluntary contractions in humans. Neurosci. Lett. 241:1-4, 1998.

Halliday DM. Generation and characterization of correlated spike trains. Comput Biol Med 28:143-152, 1998.

Halliday DM, Conway BA, Farmer SF, and Rosenberg JR. Load-independent contributions from motor-unit synchronization to human physiological tremor. J Neurophysiol 82:664-675, 1999.

Halliday DM, Rosenberg JR, Breeze P, and Conway BA. Neural spike train synchronization indices: definitions, interpretations, and applications. IEEE Trans Biomed Eng. 53 (6):1056-66, 2006.

Hamilton AF, Jones KE, and Wolpert DM. The scaling of motor noise with muscle strength and motor unit number in humans. Exp Brain Res 157:417-430, 2004.

Hamm TM, Roscoe DD, Reinking RM, and Stuart DG. Detection of synchrony in the discharge of a population of neurons. I. Development of a synchronization index. J Neurosci Methods 13:37-50, 1985.

Harrison LM, Ironton R, and Stephens JA. Cross-correlation analysis of multi-unit EMG recordings in man. J Neurosci Methods 40:171-179, 1991.

Holdefer RN and Miller LE. Primary motor cortical neurons encode functional muscle synergies. Exp Brain Res. 146(2):233-43, 2002.

Huesler EJ, Maier MA, and Hepp-Reymond M-C. EMG activation patterns during force production in precision grip. III. Synchronisation of single motor units. Exp. Brain Res. 134:441-455, 2000.

Jensen BR, Pilegaard M, and Sjogaard G. Motor unit recruitment and rate coding in response to fatiguing shoulder abductions and subsequent recovery. Eur J Appl Physiol 83:190-199, 2000.

Johnson KV, Edwards SC, Van Tongeren C, and Bawa P. Properties of human motor units after prolonged activity at a constant firing rate. Exp Brain Res 154:479-487, 2004.

Jones KE, Hamilton AF, and Wolpert DM. Sources of signal-dependent noise during isometric force production. J Neurophysiol 88:1533-1544, 2002.

Kakuda N, Nagaoka M, and Wessberg J. Common modulation of motor unit pairs during slow wrist movement in man. J Physiol 520 Pt 3:929-940, 1999.

Keen DA, Yue G, and Enoka RM. Training related enhancement in the control of motor output in elderly humans. J Appl Physiol. 77:2648-58, 1994.

Kilner JM, Alonso-Alonso M, Fisher R, and Lemon RN. Modulation of synchrony between single motor units during precision grip tasks in humans. J Physiol 541:937-948, 2002.

Kukulka CG and Clanann HP. Comparison of the recruitment and discharge properties of motor units in human brachial biceps and adductor pollicis during isometric contractions. Brain Res 219:45-55, 1981.

Laidlaw DH, Bilodeau M, and Enoka RM. Steadiness is reduced and motor unit discharge is more variable in old adults. Muscle Nerve 23:600-612, 2000.

Logigian EL, Wierzbicka MM, Bruyninckx F, Wiegner AW, Shahahi BT, and Young RR. Motor unit synchronization in physiologic, enhanced physiologic, and voluntary tremor in man. Ann Neurol 23:242-250, 1988.

Lowery MM and Erim Z. A simulation study to examine the effect of common motoneuron inputs on correlated patterns of motor unit discharge. J Comput Neurosci 19 (2):107-24, 2005.

Macefield VG, Gandevia SC, Bigland-Ritchie B, Gorman RB, and Burke D. The firing rates of human motoneurones voluntarily activated in the absence of muscle afferent feedback. J Physiol (Lond) 471:429–443, 1993.

Maier MA and Hepp-Reymond MC. EMG activation patterns during force production in precision grip. II. Muscular synergies in the spatial and temporal domain. Exp Brain Res 103:123-136, 1995a.

Maier MA and Hepp-Reymond MC. EMG activation patterns during force production in precision grip. I. Contribution of 15 finger muscles to isometric force. Exp Brain Res 103:108-122, 1995b.

Makinen VT, May PJC, and Tiitinen H. The use of stationarity and nonstationarity in the detection and analysis of neural oscillations. NeuroImage 28:389-400, 2005.

Mananas MA, Fiz JA, Morera J, and Caminal P. Analyzing dynamic EMG and VMG signals of respiratory muscles. IEEE Eng Med Biol Mag 20:125-132, 2001.

Marsden CD, Meadows JC, and Merton PA. Isolated single motor units in human muscle and their rate of discharge during maximal voluntary effort. J Physiol (Lond) 217:12P–13P, 1971.

Marsden CD, Meadows JC, and Merton PA. "Muscular wisdom" that minimizes fatigue during prolonged effort in man: peak rates of motoneuron discharge and slowing of discharge during fatigue. Adv Neurol 39:169-211, 1983.

Masakado Y, Akaboshi K, Kimura A, and Chino N. Tonic and kinetic motor units revisited: does motor unit firing behavior differentiate motor units? Clin Neurophysiol 111:2196-2199, 2000.

Milner TE and Dahliwal SS. Activation of extrinsic and intrinsic finger muscles in relation to the fingertip force vector. Exp Brain Res 146:197-204, 2002.

Moritz CT, Barry BK, Pascoe MA, and Enoka RM. Discharge rate variability influences the variation in force fluctuations across the working range of a hand muscle. J Neurophysiol 93:2449-2459, 2005a.

Myers LJ, Erim Z, and Lowery MM. Time and frequency domain methods for quantifying common modulation of motor unit firing patterns. J Neuroengineering Rehabil 1:2, 2004.

Nordstrom MA, Fuglevand AJ, and Enoka RM. Estimating the strength of common input to human motoneurons from the cross-correlogram. J Physiol 453:547-574, 1992.

Nuttall AH. Some windows with very good sidelobe behavior. IEEE Trans. Acoustics Speech and Signal Proc ASSP-29:84-91, 1981.

Pfurtscheller G. Graphical display and statistical evaluation of event-related desynchronization (ERD). Electroenceph. clin. neurophysiol. 43:757-750, 1977.

Pincus SM, Cummins TR, and Haddad GG. Heart rate control in normal and aborted-SIDS infants. Am J Physiol 264:R638-646, 1993.

Pinna GD, Maestri R, and Di Cesare A. Application of time series spectral analysis theory: analysis of cardiovascular variability signals. Med Biol Eng Comput 34:142-148, 1996.

Rosenberg JR, Amjad AM, Breeze P, Brillinger DR, and Halliday DM. The Fourier approach to the identification of functional coupling between neuronal spike trains. Prog Biophys Mol Biol 53:1-31, 1989.

Salisbury JI and Sun Y. Assessment of chaotic parameters in nonstationary electrocardiograms by use of empirical mode decomposition. Annals of Biomedical Engineering, 32(10):1348–1354, 2004.

Santello M and Fuglevand AJ. Role of across-muscle motor unit synchrony for the coordination of forces. Exp Brain Res 159:501-508, 2004.

Sears TA and Stagg D. Short-term synchronization of intercostal motoneurone activity. J Physiol 263:357-381, 1976.

Semmler JG and Nordstrom MA. Motor unit discharge and force tremor in skill- and strength-trained individuals. Exp Brain Res 119:27-38, 1998.

Semmler JG, Steege JW, Kornatz KW, and Enoka RM. Motor unit synchronization is not responsible for larger motor unit forces in old adults. J. Neurophysiol. 84:358-366, 2000.

Semmler JG, Kornatz KW, and Enoka RM. Motor-unit coherence during isometric contractions is greater in a hand muscle of older adults. J, Neurophysiol, 90:1346-1349, 2003.

Semmler JG, Sale MV, Meyer FG, and Nordstrom MA. Motor-unit coherence and its relation with synchrony are influenced by training. J Neurophysiol 92:3320-3331, 2004.

Shelhamer M. On the correlation dimension of optokinetic nystagmus eye movements: computational parameters, filtering, nonstationarity, and surrogate data. Biol Cybern 76:237-250, 1997.

Sosnoff JJ and Newell KM. Are age-related increases in force variability due to decrements in strength? Exp Brain Res 174:86-94, 2006.

Spirduso WW, Francis K, Eakin T, and Stanford C. Quantification of manual force control and tremor. J Mot Behav 37:197-210, 2005.

Srinivas RM and Yeragani VK. A simple technique to quantify nonstationarity of heart rate time series: influence of autonomic nervous system. Cardiovascular Engineering 2(3):99-109, 2002.

Sutton GG and Sykes K. The variation of hand tremor with force in healthy subjects. J Physiol 191:699-711, 1967.

Taylor AM, Christou EA, and Enoka RM. Multiple features of motor-unit activity influence force fluctuations during isometric contractions. J Neurophysiol 90:1350-1361, 2003.

Thonet G and Vesin J-M. Stationarity assessment with time-varying autoregressive modeling. 1997 IEEE International Conference on Acoustics, Speech, and Signal Processing, 1997. ICASSP-97. 5:3721 - 3724, April 1997.

Tracy BL, Maluf KS, Stephenson JL, Hunter SK, and Enoka RM. Variability of motor unit discharge and force fluctuations across a range of muscle forces in older adults. Muscle Nerve 32:533-540, 2005.

Vaillancourt DE and Newell KM. The dynamics of resting and postural tremor in Parkinson's disease. Clin. Neurophysiol. 111:2046-2056, 2000.

Vaillancourt DE, Larsson L, and Newell KM. Time-dependent structure in the discharge rate of human motor units. Clin Neurophysiol 113:1325-1338, 2002.

Volkmann J, Joliot M, and Mogilner A. Central motor loop oscillations in Parkinsonian resting tremor revealed by magnetoencephalography. Neurology 46:1359–70, 1996.

Weber EJ, Molenaar PC, and van der Molen MW. A nonstationarity test for the spectral analysis of physiological time series with an application to respiratory sinus arrhythmia. Psychophysiology 29:55-65, 1992.

Welch, PD. The use of the fast fourier transform for the estimation of power spectra: a method based on time averaging over short modified periodograms. IEEE Trans. Audio and Electroacoust AU-15 2:70-73, 1967.

White LB and Boashash B. Cross spectral analysis of nonstationary processes. IEEE Trans Info Theory, 36(4):830-835, 1990.

Wiegner AW and Wierzbicka MM. A method for assessing significance of peaks in cross-correlation histograms. J Neurosci Methods 22:125-131, 1987.

Yao W, Fuglevand RJ, and Enoka RM. Motor-unit synchronization increases EMG amplitude and decreases force steadiness of simulated contractions. J Neurophysiol 83:441-452, 2000.

Vita

Charles Kevin Terry was born on July 30, 1961 in Tampa, Florida, to his parents, Joann Nell and Charles Ralph Terry. Kevin graduated from C. Leon King High School in Tampa in 1979 and then attended The University of Florida, where he received his B.S. degree in Aerospace Engineering. (He believes that the Gators winning two national championships and his graduation all in the same year are not at all a coincidence.) Kevin served as an officer in the United States Air Force for four years as a flight test engineer before being honorably discharged in 1988. After his military service, he worked at Pratt & Whitney Government Engines, testing components and subsystems of the Space Shuttle main engine and the F-15 and F-16 fighter jet engines. Following his work there, he returned to The University of Florida and earned his M.S. in Mechanical Engineering in 1994, before moving to Colorado. During his time in Colorado, Kevin competed in a number of triathlons, including a late-night finish in Ironman Canada in 2001. He finished his 7-year career at Ball Aerospace as an Integration and Test Manager and received an M.E. in Engineering Management from The University of Colorado at Boulder in 2002.

Permanent address: 7001 Reese Lane
Austin, TX 78757

This dissertation was typed by the author.